Faculty of Science

Analysis of nutrient content in rocks from New South Wales

A study of nutrient content in sedimentary and igneous rock samples within the wider Blue Mountains and Sydney Basin, New South Wales, Australia

Tibella Meytap

Degree of Bachelor of Science with a major in Earth Sciences
15 hec

Department of Earth Sciences
University of Gothenburg
2022 B-1204

UNIVERSITY OF GOTHENBURG

UNIVERSITY OF GOTHENBURG
Department of Earth Sciences
Geovetarcentrum/Earth Science Centre

Analysis of nutrient content in rocks from New South Wales

A study of nutrient content in sedimentary and igneous rock samples within the wider Blue Mountains and Sydney Basin, New South Wales, Australia

Tibella Meytap

ISSN 1400-3821

B1204
Bachelor of Science thesis
Göteborg 2022

Mailing address
Geovetarcentrum
S 405 30 Göteborg

Address
Geovetarcentrum
Guldhedsgatan 5A

Telephone
031-786 19 56

Geovetarcentrum
Göteborg University
S-405 30 Göteborg
SWEDEN

Abstract

Nitrogen, phosphorus and potassium are three of the main nutrients for the primary functioning of all biological life. These elemental nutrients are abundant in terrestrial systems and the lithosphere, where microbes and plants can access the nutrients in the rocks at the surface. This study focused on the nutrient content in sedimentary and igneous rock material from New South Wales, Australia, to locate the most nutrient rich areas based on their sedimentary environment. The methods that were used to analyze the total nutrient content of nitrogen (N), phosphorus (P) and potassium (K) were XRF and IRMS. The rock samples were collected from several areas spread out from Sydney Basin to the Blue Mountains. These areas encompass Narrabeen, Leumeah Road, Bradbury, Australian Botanical Garden, Mulgoa National Park, Bilpin, Kurrajong Heights, Mount Wilson, Mount Banks, as well as Lithgow and Sunny Corner. The results showed a high nutrient content in a specific shale called the Ashfield shale, which is the base formation of the Wianamatta shale. This shale was collected in the area of Leumeah Road and Bradbury in the southern part of New South Wales. The N/K correlation of the Ashfield shales gave a result of ~0,99, while the N/C correlation gave the result of 0,7. The analysis shows that the most nutrient rich rocks are based in the Triassic areas of New South Wales, where there used to be a shallow marine to brackish environment close to the Lachlan Fold Belt.

Sammanfattning

Kväve, fosfor och kalium är några av de mest viktiga näringsämnena för allt liv på jorden. Dessa tre element är rikliga i jorden, samt i litosfären, där mikrober och växter kan nyttja näringsämnena som finns på ytan av stenar och bergsmaterial. Denna studie fokuserade på näringsinnehållet i sedimentära och vulkaniska bergarter från New South Wales, Australien, för att kunna lokalisera näringsrika områden baserat på deras sedimentära miljö. I studien analyserades stenprovernas koncentrationshalt av näringsämnena kväve (N), fosfor (P) och kalium (K), med XRF (röntgenstrålning) och IRMS (Isotope Ratio Mass Spectrometry). Stenproverna samlades in från flera olika platser som sträckte sig från Sydney Basin till Blue Mountains. Dessa platser omfattar Narrabeen, Leumeah Road, Bradbury, Australian Botanical Garden, Mulgoa National Park, Bilpin, Kurrajong Heights, Mount Wilson, Mount Banks, samt Lithgow och Sunny Corner. Resultaten visade en högre koncentrationshalt i en specifik skiffer som kallas för Ashfield shale, vilken är basformationen av Wianamatta gruppen. Denna typ av skiffer hittades i Leumeah Road och Bradbury, som befinner sig på den södra delen av New South Wales. N/K korrelationen av Ashfield skiffern gav ett resultat på ~0,99, medan N/C korrelationen gav ett resultat på 0,7. Med dessa resultat noterades det att de mest näringsrika stenproverna är bundna till platser i New South Wales som är från Trias åldern, där den sedimentära miljön beskrivs vara en ytlig marin till bräcklig miljö nära Lachlan orogenen.

Table of Contents

1. Introduction

The cycle of mineral nutrients in the environment is a driving force for the growth and evolution of the biological ecosystem. Tectonic activity within the crustal Earth, as well as weathering and erosion processes of the outer crustal Earth are necessary for the content of plant nutrients in rock material to cycle. The general formation of rock is explained in Sedimentary Geology by Prothero & Schwab (2013) as first initiated by tectonic activity, which include processes that occur beneath the surface of the Earth´s crust. Igneous rocks are formed by either cooling of magma below the crust, or by eruption of lava that cools above the crust of the Earth. Types of igneous bedrock are volcanic basalts, gabbros and granites. Igneous rocks are the starting point for other types of bedrock, which are metamorphic (gneiss, schist, quartzite) and sedimentary (sandstones, conglomerate, shales, siltstones, claystones). Metamorphic rocks are created when preexisting rocks undergo transformation in their solid state by tectonic activity or intrusion of magma below the crust. These processes are initiated by the increased pressure and heat below the surface of the Earth. Sedimentary rocks are formed by a build-up of grains from weathered rocks that undergoes burial and lithification. Weathering and erosion are the two driving forces of the formation of sedimentary rocks, and this occurs at the surface of the Earth (Prothero & Schwab, 2013).

The state of the terrestrial ecosystem is both dependent on atmospherically and rock-derived elements. Atmospherically derived elements are nitrogen (N) and carbon (C), whereas rock-derived elements are phosphorus (P), potassium (K), magnesium (Mg) and calcium (Ca) (Chadwick et al., 1999). Rock-bound nutrients can be released by chemical or physical weathering, while atmospherically bound nutrients get fixated in the soil. Nutrient variation in rocks can alter through time by either depletion by weathering, or enrichment by tectonic activity. Depending on what type of rock the nutrient is hosted by, and the mineralogical constitution, the nutrients can vary significantly. Topics related to the total plant nutrient content in regards to soil chemistry, climate changes and the state of the biological ecosystem, are recently more of interest than before. Other studies of relevance similar to this topic have shown that the enrichment of bedrock nitrogen (N) can correlate to enhanced C storage and soil P retention, as well as the potential increase of free-living N

fixation in the ecosystems (Dynarski et al., 2019). This shows that the free-living N fixation can be controlled by bedrock N availability, climate and tectonics. Terrestrial nitrogen inputs to soil, depletion, global cycling and occurrence in the different layers of the Earth, are equally important to fully understand the global ecosystem biogeochemistry, ecology, soil science and global change (Dahlgren, 1994; Houlton & Morford, 2015). Elevated concentrations of N (> 0,01 %) have been found in most rock types (including igneous and metamorphic rock types), but are mostly found in sedimentary and metasedimentary rocks (Holloway et al., 2002). The increase of phosphorus during the Ediacaran period (635 - 541 Ma) is also correlated to the geochemical changes in the environment and the development of biological life (Reinhard et al., 2016; Laakso et al,. 2020).

1.1 Aim of study

In this study, raw rock material from the Blue Mountains and Sydney Basin, Australia, were analyzed to measure their nutrient content of nitrogen (N), phosphorus (P) and potassium (K), in correlation to their rock type and sedimentary environment. The collected rocks were analyzed by X-ray Fluorescence (XRF) and Isotope-Ratio Mass Spectrometry (IRMS) to determine their nutrient content.

1.2 Geology and formation of New South Wales

Sydney Basin and the Blue Mountains is located in New South Wales, which is the eastern part of Australia. New South Wales is based on the basement sediment of the Lachlan-, New England-, and Thomson Fold Belt, which are a part of the *Tasmanides* (O'Neill & Danis, 2013) and includes the Delamerian Orogen (see figure 1). This dates back to the Ordovician to Early Cretaceous and was formed by rifting and short interval deformation events.

The deformation events include cycles such as the Delamerian Cycle, Lachlan Super Cycle (Kanimblan, Tabberabberan, Benambran) and the Hunter-Bowen Super Cycle (1-4). The cycles are recorded since the Cambrian and into the Canozoic age (530 - 1 Ma) and involve tectonic processes such as subduction, convergence, rifting, contraction, shallow subduction, deformation uplift, faulting, compression, thrusting, collision, erosion and deposition (O'Neill & Danis 2013). During such processes, there has been numerous changes in the geochemical structure of the raw bedrocks.

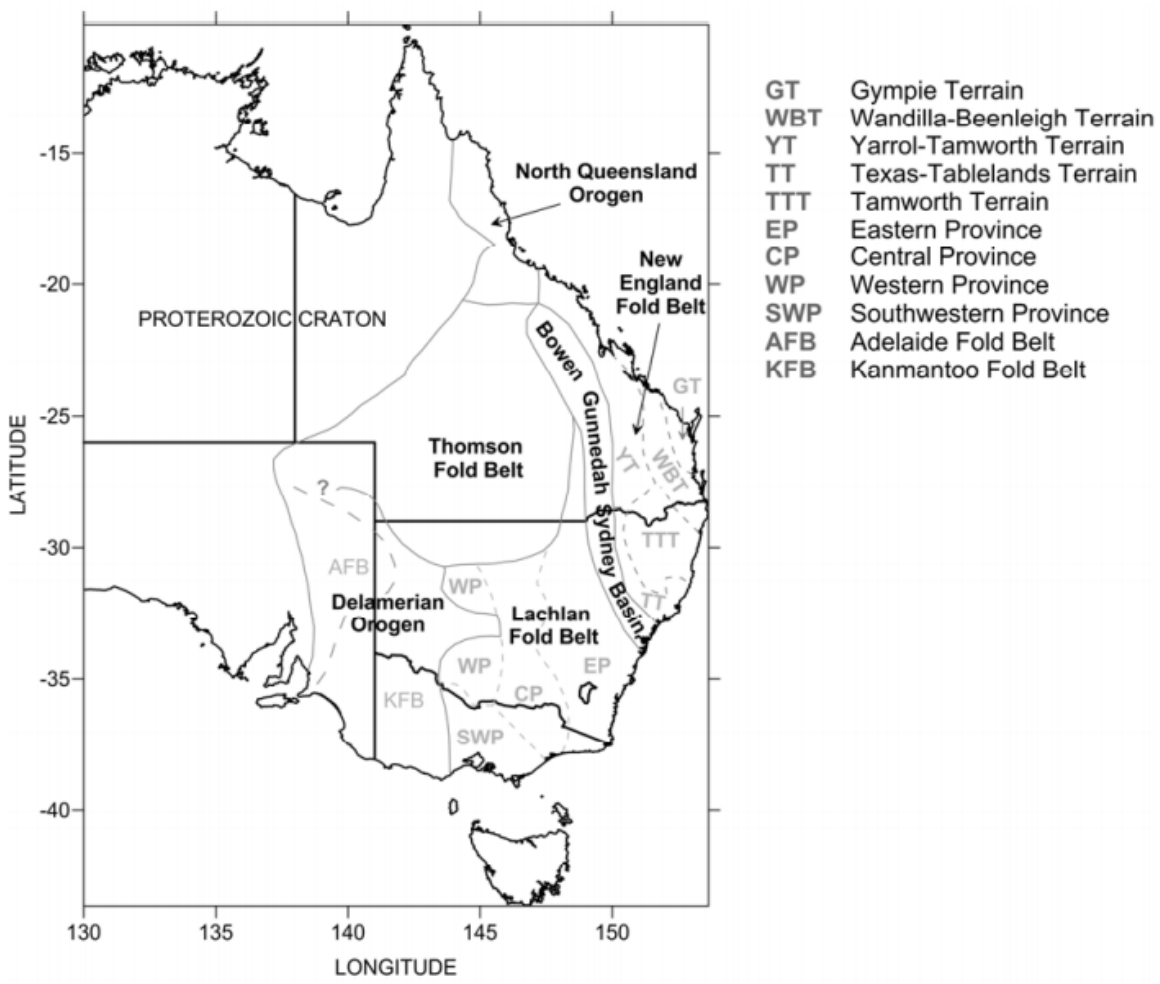

Figure 1. Location of the fold belts around the Tasmanides. The fold belts are the Lachlan Fold Belt, New England Fold Belt, Thomson Fold Belt and the Sydney Gunnedah Bowen Basin. Figure obtained from O'Neill & Danis 2013, *Geological characteristics and history of NSW with a focus on coal seam gas (CSG) resources.*

The Delamerian cycle is dated as the earliest in west Tasmania from 1270 - 1100 Ma. This relates to the tectonic significance at the time which was a amphibolite-grade metamorphism at circa 1270 Ma (Holm et al., 2003). Rocks of a basalt nature has been found in the Tasmanides between the west of Tasmania and the mainland, which is on King Island. The basalt rock is considered to be the oldest in the Tasmanides. Second oldest rock in this location is from circa 1100 Ma, and is a undeformed sandstone of shallow-water (Turner et al., 1992). Other significant ages that this cycle affected in the west of Tasmania is from >780 - 490 Ma. The Delamerian cycle is also connected to the mainland around the ages of 830 - 480 Ma, with extension and passive margin phase, as well as two main rift cycles. The first rift cycle is called the Adelaide Rift Complex (Cooper & Tuckwell 1971), while the second rift cycle is characterized by the formation of the Kanmantoo Trough. Rock types that are

significant to the Delamerian cycle are blue-schist metamorphosed mafic volcanic rocks that come from the allochthonous Bowry Formation (Holm et al., 2003). Other rock types of the younger ages are dolerites (725 Ma, Crook 1979), granites (760 Ma and 777 Ma, Turner et al., 1998), glacially-derived Sturtian conglomerates (700 Ma) and Marinoan conglomerates (~635 Ma) (Calver & Waiters 2000) and igneous rocks, such as tholeiites (600-580 Ma) (Crawford & Berry 1992; Direen & Crawford 2003; Crawford et al., 2003). Its development records supercontinent break-up in the Neoproterozoic, beginning at 827 Ma and continuing to the base of the Cambrian.

The Lachlan fold belt is dated from the basal Ordovician to the Carboniferous (~438 - 286 Ma) (Glen, R.A. 2005) and has an assumed substrate of continental, oceanic, as well as a mix of oceanic and continental material (Rutland 1976; Chappell & White 1974; Crook 1980; Scheibner 1973; Crawford et al. 1984). Cambrian rocks from the south coast of New South Wales, as well as numerous belts of Cambrian greenstone from central Victoria are overlapping from the Delamerian Orogen to the Lachlan Orogen. Other significant geological events the Lachlan Orogen was subjected to deformation events that resulted in fault systems divided into four subprovinces - Benambran Orogeny (Ordovician-Silurian boundary), Bindi deformation (Silurian-Devonian boundary), Tabberabberan Orogeny (late Early to Middle Devonian) and the Kanimblan Orogeny (Early Carboniferous). Rock types that are significant for the Lachlan Orogen are granites (Williams & Chappell 1998), volcanic and sedimentary rocks from the Cambrian, and turbidites from the Ordovician (Crawford et al. 1984; Gray & Willman 1991).

The New England fold belt has an old lithosphere of oceanic, continental and mixed continental and oceanic substrate. The orogen lies to the far east of the Tasmanides and has two structural subprovinces that were developed by a Late Devonian-Carboniferous convergent margin. These subdivisions has one external part and one internal part. The external part, that lies to the west, comprises a fold-thrust belt with granites; while the internal part comprises a multiply-deformed and metamorphosed accretionary complex with intruding granitoids (Leitch 1974). The majority of the Thomson fold belt is overlain by Mesozoic cover and is based in the central and western Queensland, and dated from the Precambrian to the Late Devonian (Murray 1994; Scheibner & Veevers 2000). The significant

rock types of this orogen are metasediments, phyllites, greenschist and amphibolite. The only age indicator in this area is biotite, which was K-Ar dated at 416 Ma (Murray 1994).

The Lachlan supercycle stretched from the Ordovician (ca. 490 Ma) to Carboniferous (320 Ma) and comprise of three cycles; the Benambran cycle (490-440 Ma), Tabberabberan cycle (430-380 Ma) and the Kanimblan cycle (380-320 Ma).

i. The Benambran cycle is characterized by rock types such as quartz-rich and craton-derived turbidites, black shales and tholeiitic basalt-chert with MORB-like chemistry. The turbidites of the Early and Middle Ordovician is described as *"...both thick and thin beds of sandstone grading up into siltstones and interbedded with multiply-cleaved slates."* (Glen, R.A. 2005). The sandstones contain mostly quartz, some detrital feldspars and white mica in the lower part of the sequence (VandenBerg et al., 2000).

ii. The second cycle of the Lachlan supercycle is the Tabberabberan cycle, which affected both the Lachlan and the North Queensland Orogen. This is identified by an intra-oceanic arc-subduction system from the New England Orogen (Glen, R.A. 2005). The Tabberabberan includes lithic basal sandstones and chert bands or lenses (Crawford 1988; Fergusson 1998; Stewart & Glen 1991; Colquhoun et al., 2004). There are also turbidites, contourites or siltstones (Jones et al., 1993; Glen 1994; Thomas et al., 2002) above chert that pass up into a 400 m thick sequence of black shale and siltstone (VandenBerg 1981; VandenBerg et al., 1992; VandenBerg & Stewart 1992; Glen 1992). Other rock types that come from this cycle are granites that have intruded the basement of the North Queensland and the Delamerian Orogen. There are also volcanic rocks of the Late Silurian to Middle Devonian age, and Middle to Late Devonian age. The older volcanic rocks was interpreted by Cawood & Flood (1989) and Offler & Gamble (2002) as an intra-oceanic arc with low K calc-alkaline signature. There are also findings of shallow-marine volcanoclastic sediments that come from this cycle in varying degrees of felsic and mafic nature. Other findings are basalt from the mid-Silurian, chert from the Late Silurian-Frasnian age, and siliceous chert from the Famennian age, which are indicated by Radiolaria (Ishiga et al., 1988; Aitchison et al., 1992).

iii. In the third cycle, referred to as the Kanimblan cycle, there were rifting and loading phases occurring in the Lachlan and Delamerian orogens. This was initiated by a rifting event in the Early-Middle Devonian, which produced A-type volcanics, granites and rift-related sediments (McIlveen 1974; Dadd 1992; Wyborn & Owen 1986; Raymond 1996; Collins 2002). Other rock types that were deposited in terrestrial basins during this time includes fluviatile sandstones, conglomerates, siltstones and mudstones. Here the quartz-rich Lambie group is introduced (Powell, 1984) and said to be a derivation of the Alice Springs Orogeny in central Australia caused by an uplift. The final deformation that this cycle underwent is dated at around 340 Ma, which is indicated in the Late Devonian Lambie facies rocks.

The Hunter-Bowen supercycle includes four cycles recorded from the Middle Devonian to the Triassic, where the first cycle began during the Late Devonian. The first cycle encompassed intermediate volcanism that dominated an east-facing continental or intra-continental arc, forearc basin bound by fault systems, and subduction complexes (Glen, R.A. 2005). Cycle 2 started during the Carboniferous and included an arc that was east-facing of the Andean type. The dominant rock type is felsic ignimbrites and granite to the west, where the cycle passes eastwards into the troughs of Yarrol and Tamsworth. Lastly it passed through the subduction complexes and accreted terranes. The third and forth cycles were connected with their occurrences. While the third cycle was initiated in the Early Permian, with association of crustal extension of Bowen-Gunnedah-Sydney basin and the first phase of the Hunter Bowen Orogeny; the fourth cycle had its development throughout the Permian to the Triassic. Throughout the fourth cycle, the basin system was affected by arc magmatism and terminated by the main phase of the Hunter-Bowen Orogeny.

1.3 Rock types of the Blue Mountains

The Blue Mountains is based on Permo-Triassic sediments that originates from the Permian, Narrabeen and Hawkesbury groups, and comprises 800 - 1000 m high flat terrains (van der Beek, 2001; Mclaren, n.d.). There are three sources of sediment in the Blue Mountains that have been identified; quartz-lithic debris from weathering mountains (the New England area), mature quartz (from the Upper Devonian quartzite in the Lachlan Fold Belt) and volcanoclastic sediment from the west (O'Neill & Danis 2013), with a mineralogical composition of alkali olivine (van der Beek, 2001).

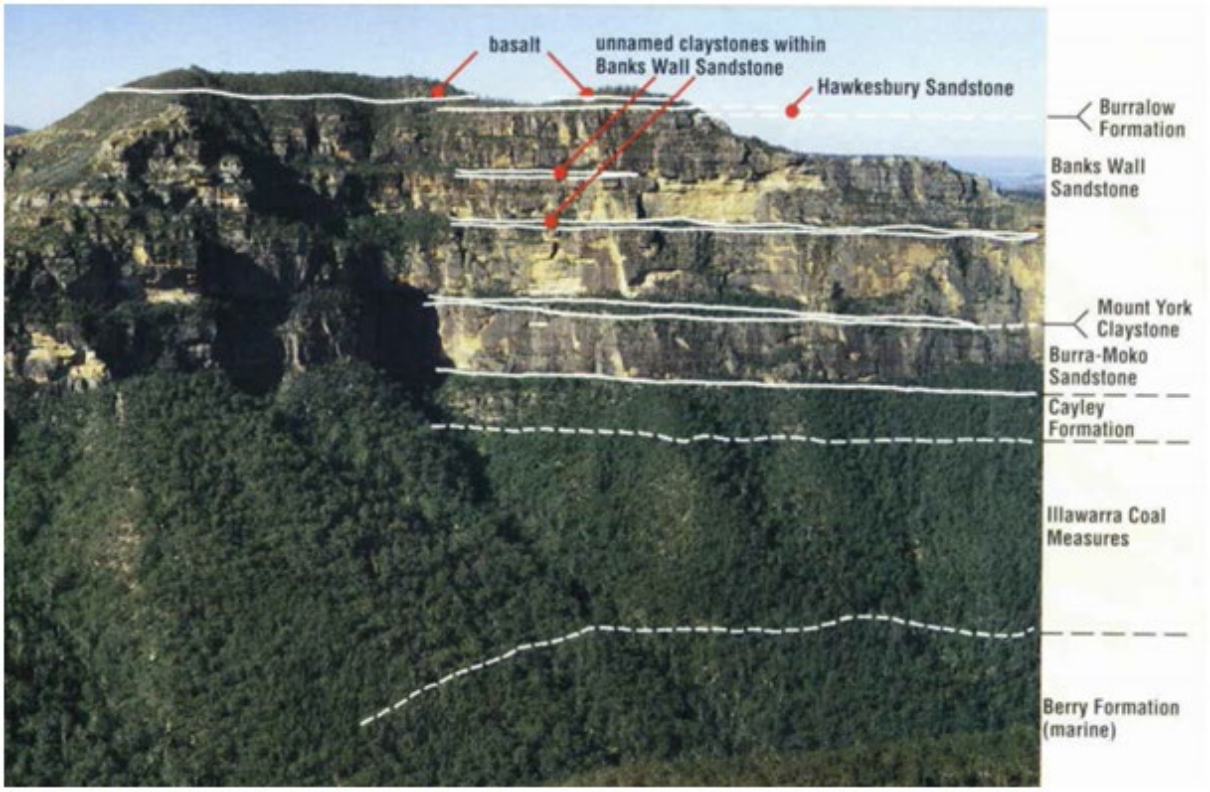

Figure 2. Stratigraphy and cross section of the Blue Mountain (Mclaren, n.d.; Pickett & Adler, 1997).

Sydney Basin consist mostly of sedimentary rocks from the Triassic (see figure 3, 4 and 5), both above and below sea-level. Further down there are older rocks dated back to Permian and Devonian - Ordovician. The cross section (figure 4) at the Blue Mountains side show rocks from the Triassic starting with a majority of rocks from the Narrabeen group at the top. Underneath the NB group (Narrabeen), there are Permian rock groups, such as the Illawarra Coal Measures (deltaic nature) and the Shoalhaven group (shallow-marine sediments) (van der Beek, et al., 2001).

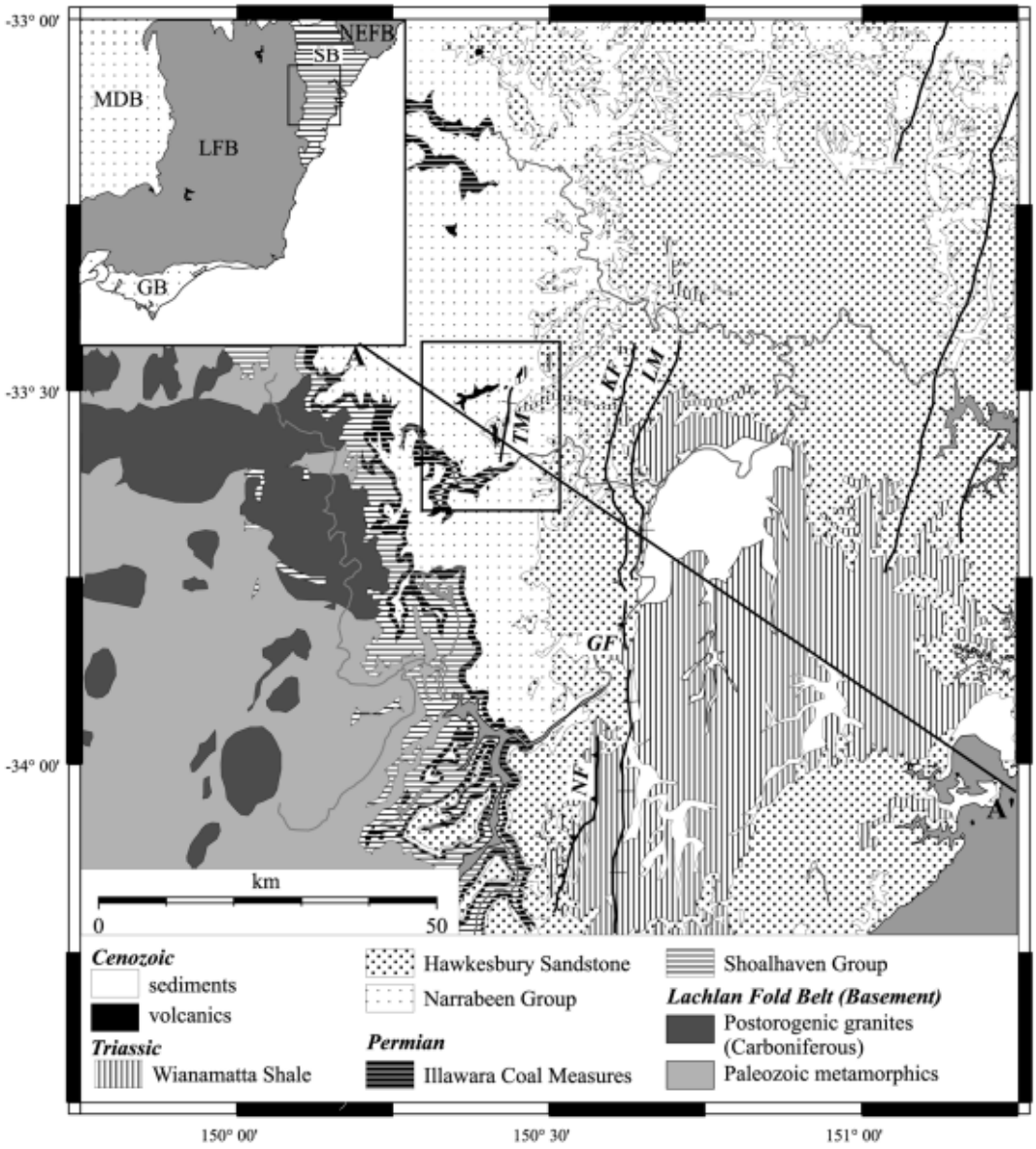

Figure 3. Geologic map showing the rock groups of Sydney Basin and the Lachlan Fold Belt, including a cross section, *see figure 4*. Map obtained from van der Beek, et al. (2001).

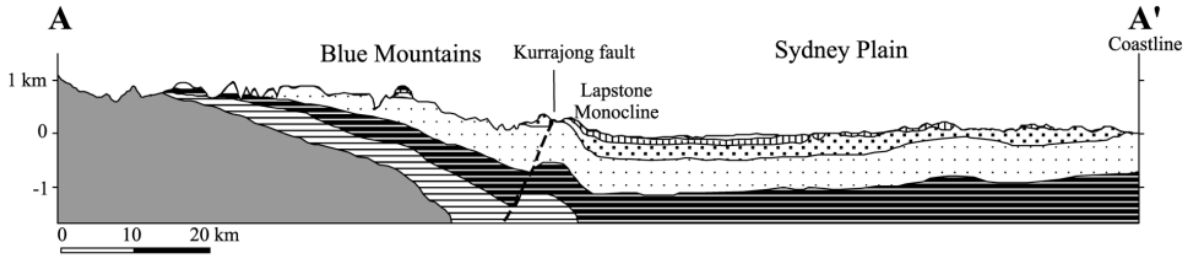

Figure 4. Cross section based on *figure 3*, with a focus on the Blue Mountains and Sydney Plain (van der Beek et al., 2001; modified from Bryan, 1966).

The basement of the Blue Mountains are Paleozoic metamorphics from the Lachlan Fold Belt. The topmost layer of the Sydney Plain is the Wianamatta Shale, followed by Hawkesbury Sandstone and the Narrabeen group. These are all rock groups from the Triassic age. Underneath the NB group, there is the Illawarra Coal Measures, as well as the Shoalhaven group, from the Permian age.

Another cross-section based on the Hunter-Mooki Fault line from the south-west to the north-east of Sydney Basin by Danis (2012) and Herbert & Helby (1980) (figure 5), shows a mixture of Triassic shales, sandstones and siltstones, claystones and laminites. The Narrabeen Group lies beneath the quartz rich Hawkesbury sandstone, following the Wianamatta Group at the top (McVicar et al., 2015; Mclaren, n.d.).

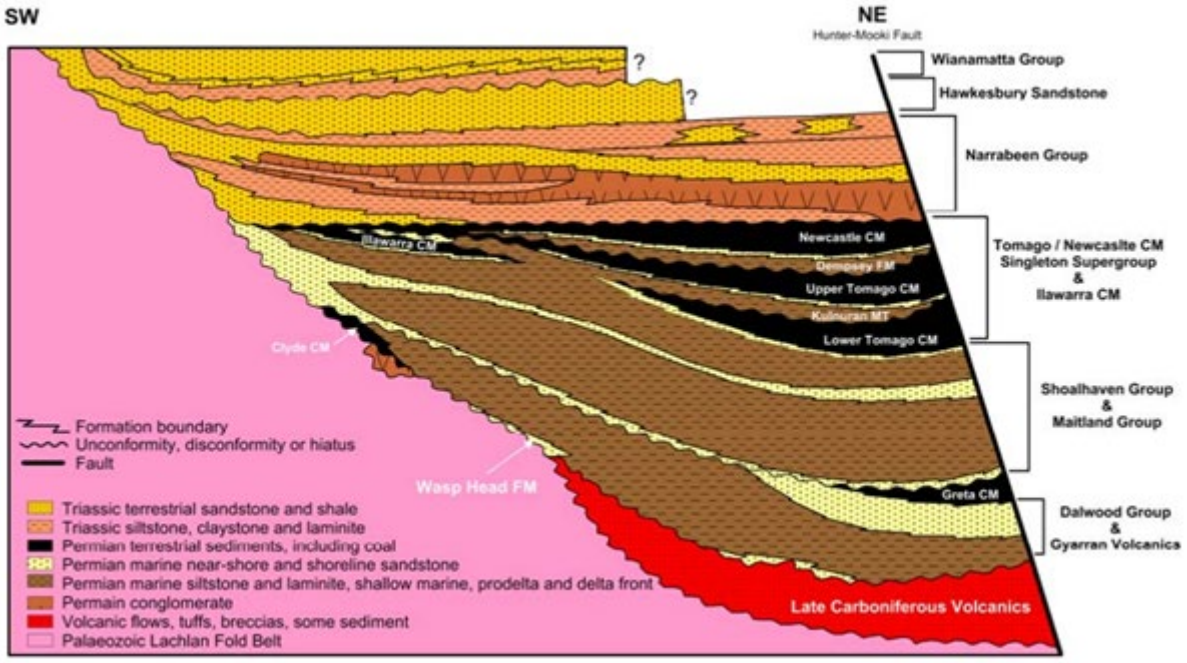

Figure 5. Cross-section of the rock types of Sydney Basin, including the fault line of Hunter-Mooki. Figure obtained from *The Geology of NSW - the geological characteristics and history of NSW with a focus on coal seam gas (CSG) resourcesreport*, by O'Neill & Danis (2013); adapted from Danis (2012) and Herbert & Helby (1980).

1.4 Rock groups of Sydney Basin

Sydney Basin is a Permo-Triassic foreland that was created when blocks from the New England and Lachlan orogen collided (Veevers et al., 1994; van der Beek, et al., 2001).

1.4.1 Narrabeen

The main rock group of Sydney Basin is the Narrabeen group which is based on the deposition of the New England Fold Belt (O'Neill & Danis, 2013). The bedrock of the Narrabeen group are dated from the early to the middle Triassic, around 250-200 Ma, where there was a change in the environment from lower to higher temperature in the climate conditions (McLaren, n.d.; *M.H. Monroe, 2011*). The sedimentary sequence of the Narrabeen group is varied vertically and has been studied many times. In Ben Spyrids *Narrabeen Field Report* (2016), they study the Narrabeen Headland sequence and the layers according to various geological events that may have occurred during its development. The Narrabeen group include rock types such as quartz lithic sandstone, Hawkesbury Sandstone (medium to coarse grained quartz rich fluvial sandstone (Mclaren, n.d.)), and lithic conglomerate. This group was formed by marine environments such as fluvial and fluvial-deltaic, as well as alluvial/estuarine (O'Neill & Danis, 2013; van der Beek, et al., 2001). The deposition of the Narrabeen sediment is based on the New England Fold Belt of 800 m lithic conglomerate.

As the Narrabeen Headland is a beach environment, the rocks are constantly affected by sea water and wind, as well as anthropogenic influence. The bedrock as a whole is described as a marine regression, signifying a stratigraphy of a younger environment of high energy rather than an older one. Spyrids (2016) also mentions that as the sea level regressed during the Triassic, and that the uplift of the New England Fold Belt may have been attributed at the same time (O'Neill & Danis, 2013). There has most likely been numerous depositional occurrences indicating the compositional mixture of sediments and texture throughout the bedrock wall. The bedrock stratigraphy show an increase of grain size the higher up it gets.

At the bottom of the sequence there is predominantly surface weathered shale that are combined with plant material, and also hinting other biological activity (Spyrids, 2016). Spyrids describes the bottom as a *Delta front* that is of fine grain sediments, with little to no sedimentary structures. There are a few indicators of river channel deposits that have been found in this section of the sequence that are filled with finer grained sediments. At the

middle section of the sequence there is mostly a mixture between siltstone and claystone, with some burrows and plant material. This part of the outcrop is described to have a *high degree of soft sediment deformation* (Spyrids, 2016). The cause of the deformation is because of *agitation prior to lithification*, which means that the sediment before turning into solid rock was influenced by some physical pressure and/or activity.

On the lower sections of the mid-section strata there can be found burrows and plant material in the shales and claystones, which can indicate the uplift during the Triassic, such as earthquakes, faulting, or glacial events. Other structures, such as concretions were also found, as well as *flaser bedding*. The structure of flaser bedding is described as an environment with low-medium energy fluctuation. Further analysis of the Narrabeen stratigraphy is explained as a heavily vegetated river delta front and plain. This is due to the regression of the sea. Spyrids (2016) describes the resulted vegetated area as indicative of a wetland or swampish environment, and not marine. The upper section of the stratigraphy is mostly sandstone of fine and medium grain size. Apparent weathering is present there as well, with some iron oxide hinting a reddish tone. Further up the sequence, McLaren, L (n.d.), describes the top unit of the Narrabeen as a Burralow member. The Burralow unit is based on lithic fragments to quartzose type and marks the boundary of Narrabeen and Hawkesbury (McVicar et al., 2015; Goldbery, 1969; McLaren, n.d.).

1.4.2 Wianamatta

The Wianamatta Group is another group of the Sydney Basin, and is a Mesozoic lacustrine unit based on three formations (van der Beek, et al., 2001), which are the Ashfield Shale, the Minchinbury Sandstones and the Bringelly Shale in the central part of Sydney Basin. This rock group consist of shales and sandstones and was deposited during a regression in the Mid-Triassic (Helby, 1973) and is described to be a "...*shaly formation and 304 m thick*" (Herbert, 1979). This group is based on the upmost unit of Sydney Basin, where sedimentation graded upward from subaqueous to shoreline to alluvial during a regression (Herbert & Helby, 1980). The Ashfield Shale is the base formation of the Wianamatta Group and was deposited in a shallow marine or brackish environment, where the main mineralogical constitution of the rock is dark-grey to black siderite. This shale is divided into four members which are the Rouse Hill Siltstone Member, the Kellyville Laminite Member, the Regentville Siltstone Member and the Mulgoa Laminite Member. The deposition of Minchinbury Sandstone was

deposited on top of the Ashfield Shale as a beach and barrier island complex and is a quartz-lithic sandstone with calcite as the dominant mineral, and the Bringelly Shale was deposited as a coastal plain environment on top of the Minchinbury Sandstone. The Bringelly Shale is the top and final formation of the Wianamatta Group and consist of fine-grained sediments, claystone, siltstone and laminite, with calcite as the major mineral as well (Herbert, 1979).

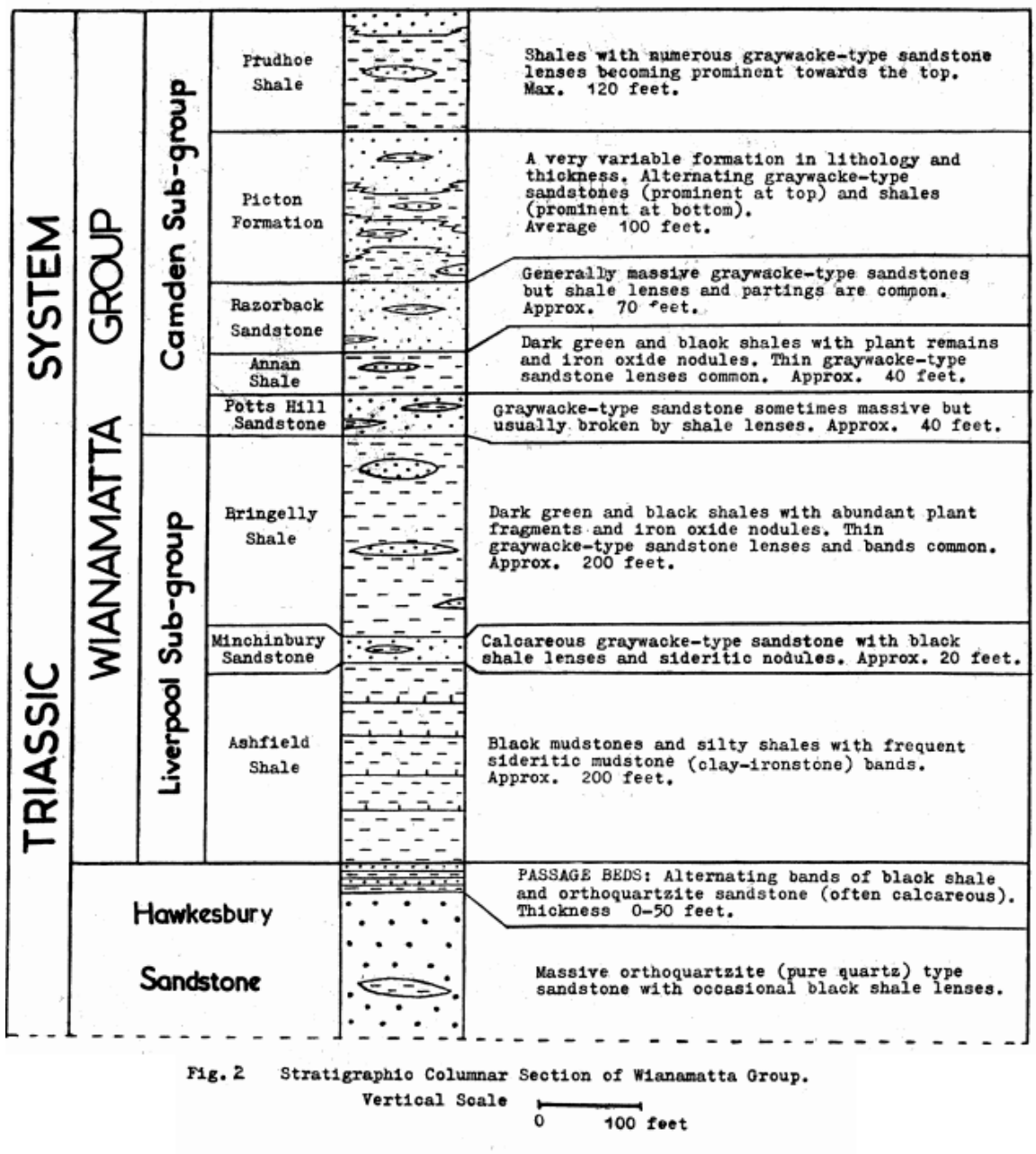

Figure 6. The stratigraphy of the Wianamatta Group (Lovering, J. F., 1954).

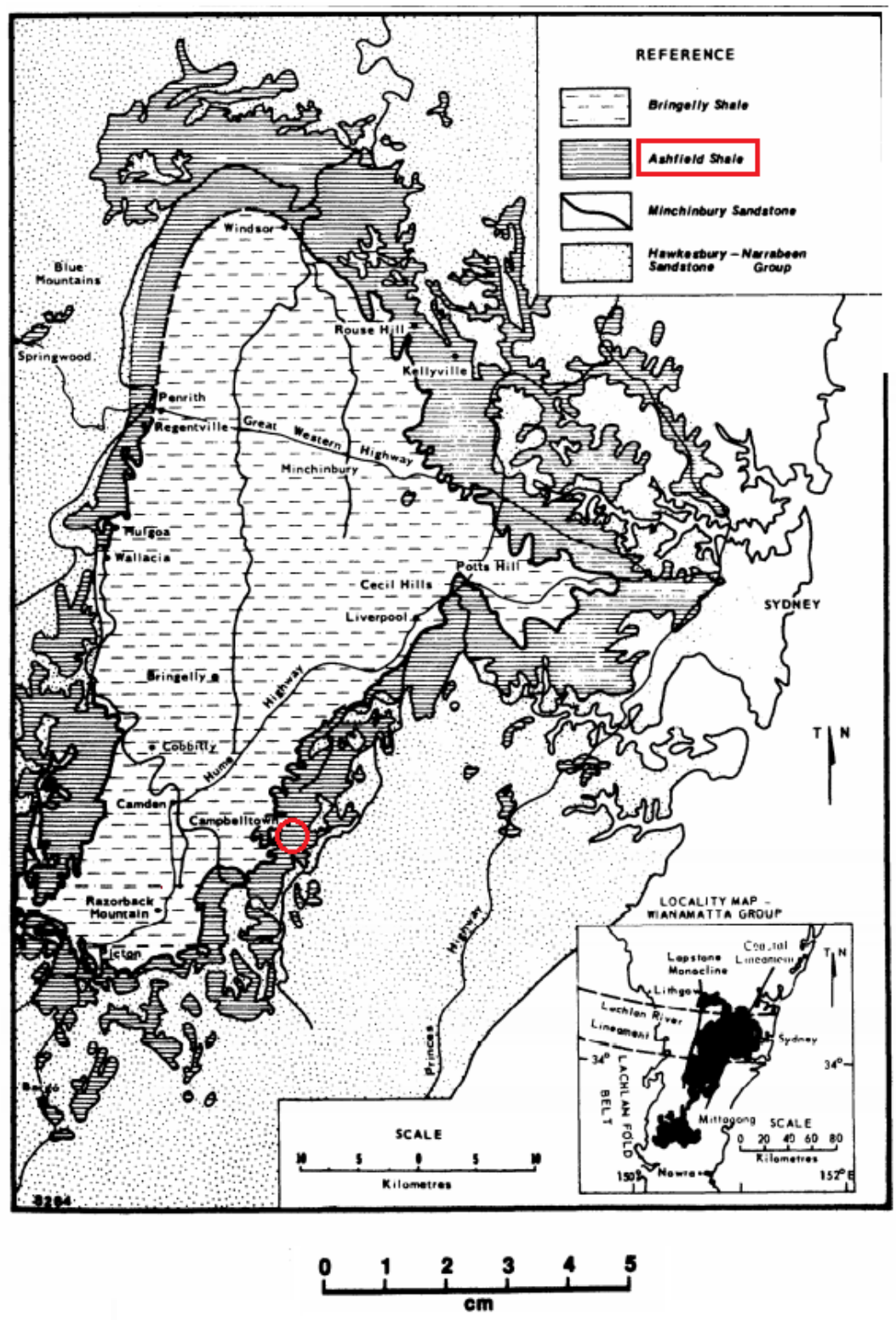

Figure 7. Map obtained from Herbert (1979). Edited to locate the sample area of Leumeah Road and Bradbury circled in red referencing the Ashfield Shale.

1.5 Nutrients

Nutrients that are essential for the growth and structure of plant material are nitrogen (N), phosphorus (P) and potassium (K). More specifically, the increase of nutrients such as phosphorus (P), which is a part of the energy molecule ATP, is essential for the continuation of biochemical reactions within cells and organisms that is obtained through photosynthesis (Misra, 2012). Nitrogen (N) is essential as it helps the cells, proteins, hormones and chlorophyll of the plants to synthesize (Follett, R. & Murphy, L. & Donahue, R.. (1981), whereas potassium (K) provides the plant enzyme activation. These elements can be derived from different sources such as the atmosphere, lithosphere and the mantle (Misra, 2012). The elements fluctuate in various rock types due to the mineral composition, geologic formation and where the rock material originates from. The major source of nitrogen is found in the atmosphere as N_2, and this is the primary source of nitrogen for plants. Phosphorus and potassium can mostly be found in the crust of the Earth (Misra, 2012). Nutrient cycling in the lithosphere occurs through weathering and erosion, upwelling, and tectonic activity such as subduction and eruption of the mantle.

1.5.1 The Nitrogen Cycle

Nitrogen, N, which is the main nutrient for the plants to produce cells, proteins, hormones and chlorophyll, has different ways of being fixated in the soil. The most common way is through the atmosphere, where the N_2 molecules gets converted into ecosystem-available N by microbes in the soil. The other is by weathering of nitrogen from its underlain bedrock (Houlton & Morford, 2015). For the N_2 molecule to be available for plants, microbes in the biomass must fixate the atmospheric nitrogen and convert it into ammonium ions (NH_4^+) and nitrate ions (NH_3^-). While nitrogen have three main forms in the soil; organic nitrogen, ammonium and nitrate ions (salts), and ammonium silicates − not all are ecologically available for uptake right away. Follet, R. et al., (1981) refers to the inorganic form of nitrogen, ammonium (NH_4^+), as the only ecologically available source for uptake. Since the ammonium ions have a positive charge, they can bind to the negatively charged soil by cation exchange complex (CEC). The negatively charged nitrate ions (NO_3^-) does not bind to the soil due to the same charge. Nitrate ions are most likely to be found dissolved in water or dried in the form of salts.

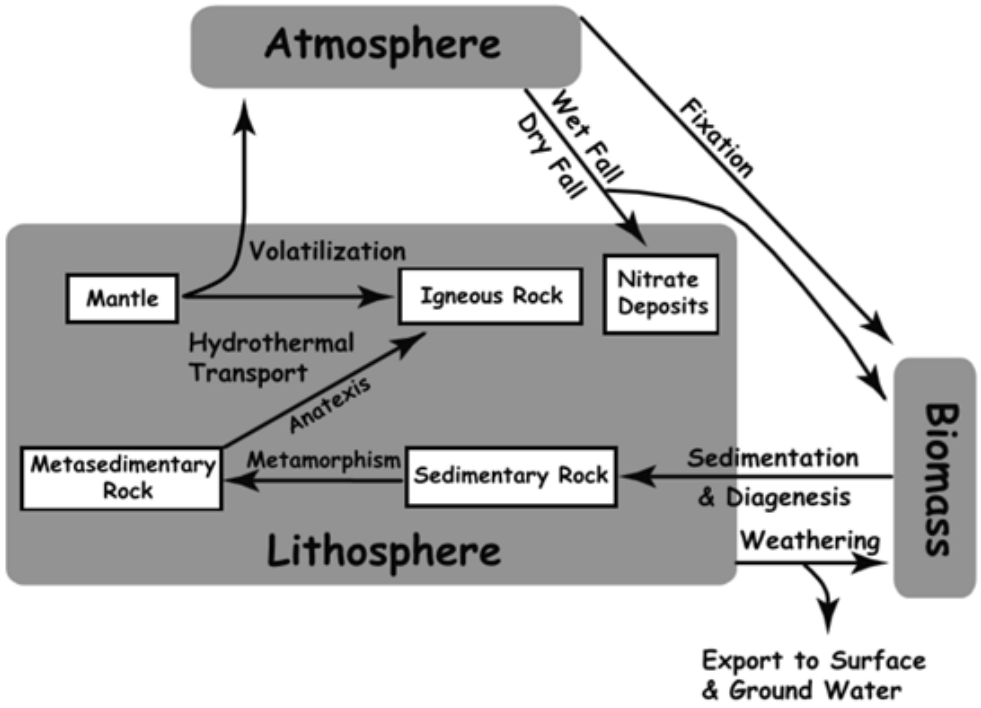

Figure 8. The nitrogen cycle through the atmosphere and lithosphere (Holloway, J. and Dahlgren, R., 2002).

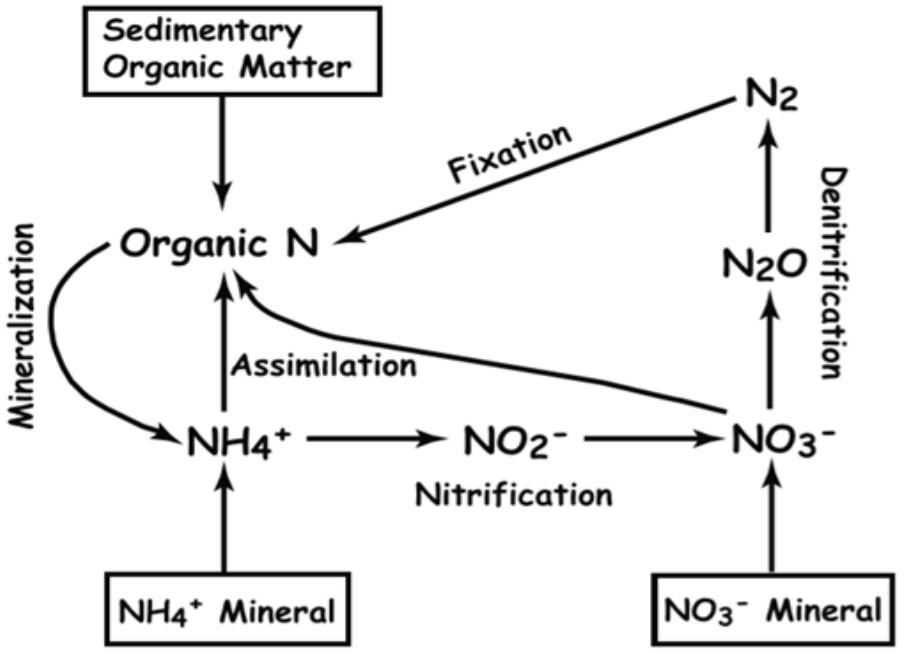

Figure 9. Schematic figure of geologic nitrogen input to terrestrial nitrogen through nitrogen cycling (Holloway, J. and Dahlgren, R., 2002).

The organic form of nitrogen must undergo a process of conversion to ammonium to be available. The process of converting organic nitrogen into available plant nutrients, ammonium, occurs when the rock is weathered and mineralized, if - however - said organic matter is associated with sedimentary and low-grade metasedimentary bedrock. This way the ammonium can enter the soil and be a part of the nitrogen cycling process, by either nitrification (ammonium oxidizes to nitrate, $NH_4^+ \rightarrow NO_3^-$) or digestion by biota (Holloway & Dahlgren, 2002).

For the mineral to be available for the plants in the soil, the bedrock needs to be decomposed, either by weathering or chemically by reaction. However, this is not considered to be as an efficient way for the nitrogen to be inserted into the soil, due to a slow decomposition rate (Holloway and Dahlgren, 2002).

1.5.2 The Phosphorus Cycle (and the Ediacaran influence)

Phosphorus, P, is another element that is classified as one of the most essential plant nutrients. The nutrient provides the plants with ATP (Adenosine Triphosphate; $C_{10}H_6N_5O_{13}P_3$) also known as the energy carrier. The ATP-molecule aid many biochemical reactions in organisms and is obtained through photosynthesis. Phosphorus is also a key point for the growth and structure of the plants. The phosphorus cycle has many aspects to it. Similar to nitrogen (N), phosphorus (P) must undergo molecular and chemical changes to be available for uptake as a nutrient (Misra, 2012).

Sedimentary rocks hold the major reservoir of phosphorus, therefore leading continental weathering of bedrock as a main supply of phosphorus. Orthophosphate (PO_4^{3-}) and apatite ($Ca_{10}(PO_4)_6(OH, F, Cl)_2$) are forms of the phosphorus mineral that organisms can digest and eventually excrete into soil or water (Misra, 2012). These forms of the phosphorus mineral can be bound to organic compounds which makes it easier for plants to absorb the phosphate ions, HPO_4^{2-} and HPO_4^-, from the soil (Stevenson & Cole 1999; Brady & Weil 2008). Phosphorus can also be found in marine sources, in the oceanic crust, where the phosphorus can undergo burial or remineralization through continental weathering (Laakso et al,. 2020).

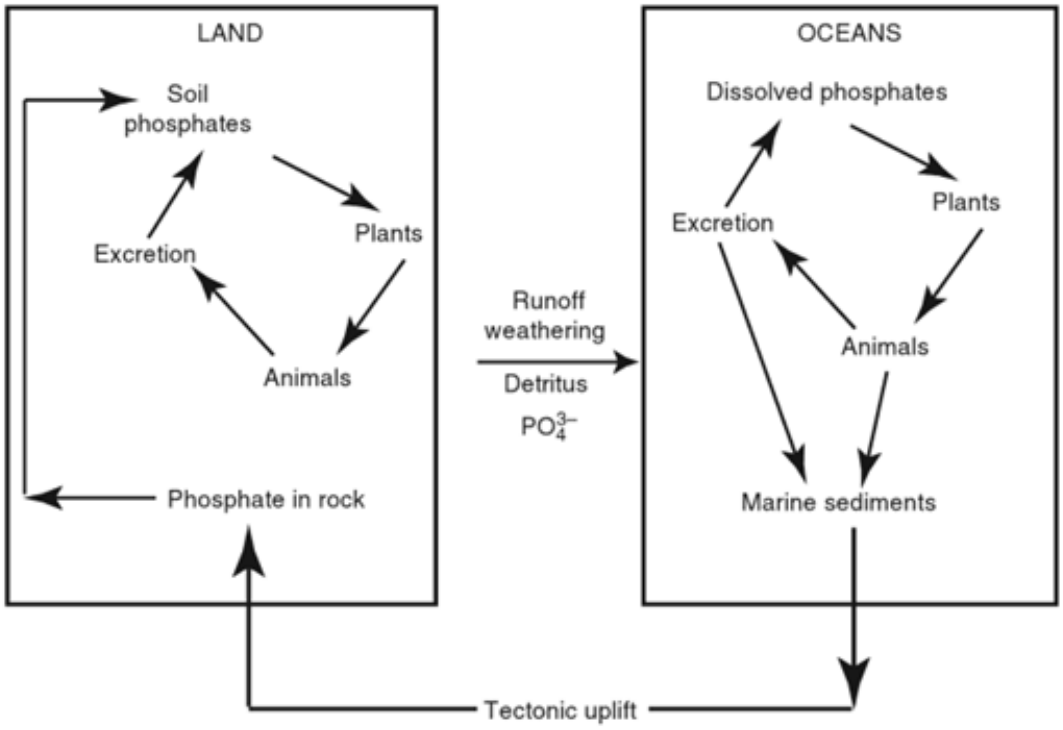

Figure 10. Schematic figure of the biogeochemical cycle of phosphorus (Misra, 2012).

The sources of phosphorus material in the oceanic crust are organic phosphorus compounds, calcium phosphates, phosphates absorbed on hydrous ferric oxides, as well as phosphates in $CaCO_3$. It is only through upwelling of the oceanic crust that the burial or mineralization of the phosphorus can reenter the surface waters and begin another cycle. The phosphorus in sedimentary bedrock are sheltered from cycling until physical or geochemical release, such as tectonic uplift or weathering (Misra, 2012).

Phosphorus does not only exist in the lithosphere, which is in the continental and oceanic crust, but also below it. *In Introduction to Geochemistry* by Misra (2012), they provide an estimation of the phosphorus element residing within the Earth. Phosphorus exist in most layers; inside the primitive mantle, which is based on analysis of mineral compositions such as komatiites, basalts and peridotite, as well as Cl carbonaceous chondrites. Phosphorus also exist within the Pyrolite, which is based on a hypothetical mixture of basalt (1) and dunite (3) in a 1:3 part relationship, otherwise known as pyroxene-olivine rock (Clark and Ringwood, 1964). However, most of the phosphorus is found within the oceanic crust (0,2 wt%), and followed by the continental crust at 0,11 wt%. See table 1 for further information.

Table 1. *List of major elements within the layers of the Earth (Misra, 2012).*

Oxide (wt%)	Primitive mantle† (1)	Primitive mantle (2)	Pyrolite (3)	Continental crust (4)	Oceanic crust (5)	"Normal" MORB (6)
SiO_2	45.0	49.9	45.16	59.7	49.4	50.45
TiO_2	0.20	0.16	0.71	0.68	1.4	1.61
Al_2O_3	4.45	3.65	3.54	15.7	15.4	15.25
Cr_2O_3	0.384	0.44	0.43			
MgO	37.8	35.15	37.47	4.3	7.6	7.58
FeO	8.05*	8.0*	8.04	6.5*	7.6	10.43*
Fe_2O_3			0.46		2.7	
CaO	3.55	2.90	3.08	6.0	12.5	11.30
MnO	0.135	0.13	0.14	0.09	0.3	
NiO	0.25	0.25	0.20			
CoO	0.013		0.01			
Na_2O	0.36	0.34	0.57	3.1	2.6	2.68
K_2O	0.029	0.022	0.13	1.8	0.3	0.09
P_2O_5	0.021	0.06	0.06	0.11	0.2	

(1) McDonough and Sun (1995), based on compositions of peridotite, komatiites, and basalts; (2) Taylor and McLennan (1985), based on CI carbonaceous chondrites; (3) Ringwood (1966); (4) Condie (1997); (5) Ronov and Yaroshevsky (1976); (6) Hofmann (1988).
*Total Fe as FeO.
†Primitive mantle (or bulk silicate Earth) = Earth's mantle immediately after the core formation (i.e., the present mantle plus crust).

1.5.3 The Potassium Cycle

Another important element for plant growth is potassium (K). Potassium as a plant nutrient helps to activate enzymes within the plants, which in turn aids the production of proteins, starches and ATP. Other important functions of potassium relates to the opening and closing of the stomata, and the exchange of water vapor (H_2O), oxygen (O_2) and carbon dioxide (CO_2). Potassium also helps with the growth of the plant, as well as the yield and health of its crops; however, it is not always available for plant uptake. There are different forms of potassium which determines the uptake availability - unavailable (mineral form), slowly available or fixed (trapped between clay layers), readily available (dissolved in water) and exchangeable. Unavailable potassium is mostly found in minerals such as feldspars and micas, and can only be available for plant uptake when the mineral undergoes weathering, erosion or dissolution (Kaiser & Rosen, 2018).

Weathering of potassium from the mica minerals is more beneficial as it is available for plants in unfertilized soils according to Singh, B. & Schulze, D. G. (2015). Other rock types that contain potassium is igneous rocks where there has been found evidence of higher K content. Granites and syenites contain up to 46 to 54 g K kg^{-1}, while in sedimentary rocks there is a decreased K content (Malavolta, 1985; Sparks 2001). The potassium can be dissolved from rocks in a series of chemical reactions, which involves the rapid exchange with hydrogen (H). The chemical process results in a layer of hydrolyzed aluminosilicates,

which can be dissolved. Similar to phosphorus, potassium can also be found in the primitive mantle and crust of the Earth. Another layer that potassium can be found is in the MORB, Mid-Ocean Ridge Basalt. However, the most potassium content can be found in the continental crust, with a content of 1,8 wt% (see table 1).

Sparks (2001), find that igneous rocks such as granites and syenites, as well as sedimentary rocks such as clayey shales, have higher K content than basalts. Rock material with higher content of potassium are mostly located in the upmost crust layers that are porous and permeable, which naturally makes rock areas with low permeability and porosity contain less potassium. While most basalts have low permeability and porosity due to their dense nature, there still are some basalts that are richer in potassium than other basalts (Jarrad, R., 2003; Hart, 1969; Hart et al., 1974). These K-rich basalts have undergone alteration by deep penetration of old oceanic crust (Jarrad, R., 2003; Donnelly et al., 1979a, 1979b). In the study of *K isotopes as a tracer for continental weathering and geological K cycling* by Li, S. et al., (2019), they propose that the driving force for potassium cycling is "*sediment diagenesis and low-temperature basalt alteration...*", which is also mentioned in the study of Jarrad, R. et al., (2003) of *Subduction Fluxes of Water, Carbon Dioxide, Chlorine, and Potassium.*

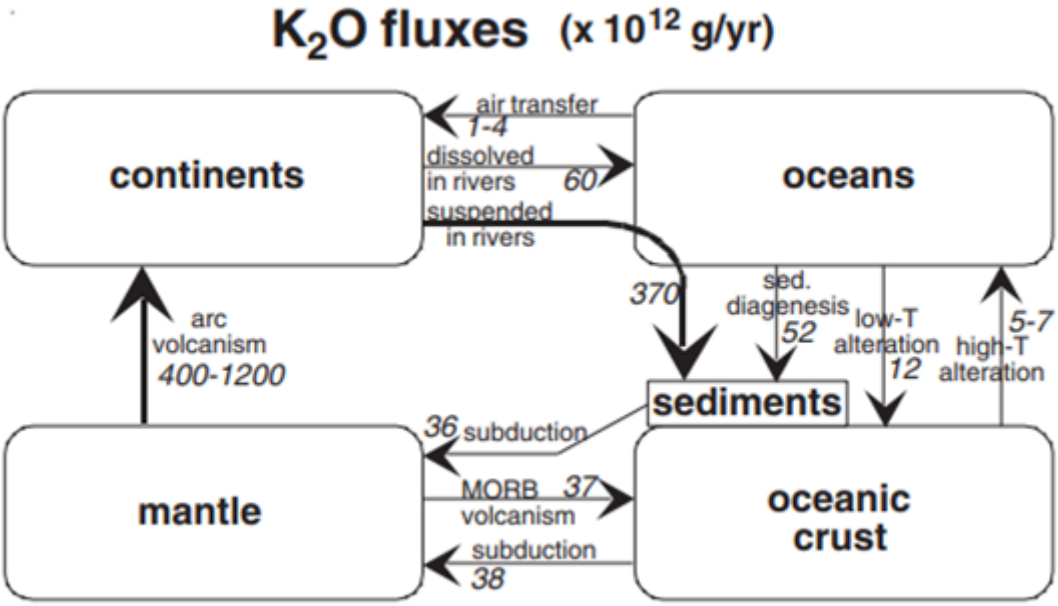

Figure 11. Schematic flowchart of global potassium fluxes, obtained from Jarrard (2003).

1.5.4 Significance of N/K ratio

The relationship between nitrogen (N) and potassium (K) is correlated through different means of interactions. Within plant material, there is a synergic interaction between the elements (Thummanatsakun, V. & Yampracha, S., 2018; Rietra et al., 2015), where low N content resulted in low K content, and high N content gave high K content (Baligar et al., 2001).

Other types of interactions occur within the lithosphere, in igneous and sedimentary rock material. Stevenson, F.J. (1962) explains the difference between how these two rock types, igneous and sedimentary, have their ammonium held within them. In igneous rock types, the majority of the ammonium can be found inside potassium-bearing minerals, such as feldspars; while in sedimentary rock types, the ammonium is found within secondary silicate minerals, micas. Most of the ammonium is fixed in igneous rock types; and only 1/10 and 2/3 in shales (sedimentary rock type) (Karro, E., 1999).

2. Method

From October to December of 2018, rock samples from different locations within the Blue Mountains and Sydney Basin, Australia, were collected and shipped to the GVC institute for analysis of their total nutrient content (see table 3 for their characteristics in appendix B). Any sample of impractical size, excessive weathering, fractures and contamination were discarded from further analysis. The samples that were chosen for analysis were sawed with Profi 2000, and cleaned with distilled water wash or hydrogen-peroxide boiling to eliminate the weathered and contaminated surfaces (see table 4, appendix C). Quantifying the total nutrient content of the rock samples were divided into two analysis methods; *X-Ray Fluorescence* (XRF) for the quantification of phosphorus (P) and potassium (K) (whole rock with flat surface), and *Isotope-Ratio Mass Spectrometry* (IRMS) for the quantification of nitrogen (N) (pulverized rock).

2.1 XRF Analysis

A handheld XRF analyser (Olympus Delta X) was used to measure the wt% of phosphorus (P) and potassium (K) on each rock sample. For this specific XRF-analyser, the detection-limit goes from magnesium (Mg) to uranium (U). XRF is a method that uses X-Ray wavelength to distinguish between different elemental atoms in a sample or an object by emitting high-energy photons from the X-ray source, resulting in electron jumping within the electron orbitals (K, L and M lines) that surrounds the atom nucleus. When this happens, a secondary X-ray photon is produced, which is called fluorescence (Olympus NDT, 2012).

Before analyzing the rock samples, standard samples were analyzed beforehand. The used standards were *Mica Fe A2*, *NIST 610*, *JWRW 2* and *OREAS 24* from GeoReM (Jochum K.P., et al., 2007). Each sample was analyzed 3 times at minimum (see tables 5, 6, 7 and 8, appendix D and E) with a tripod setup. There were two beams that were shot. The first beam was 60 seconds and the second beam was 80 seconds. The results were plotted in a diagram and calibrated to find the linear equation to use for the calculated ppm values of the rock samples (see figures 39-42, appendix D and E). The average value of the rocks in each location was then calculated to correlate the rock type and geologic age to the P and K content.

2.2 IRMS Analysis

Before the IRMS analysis for the measurement of the total nitrogen content (N), the rocks were crushed into a powder using an iron mortar. For a homogeneous size of each sample, the rock powders were sieved to a size equal to - or - less than 600 µm. The iron mortar and sieve were cleaned with distilled water and 99,5 % ethanol after each crushing and sieving.

Preparation for IRMS -

Each rock powder were measured to (~50 mg) and enclosed with a tin capsule. The standard used was *Low Organic Content Soil*, with a weight of 40 mg. In addition to the standards and samples, there were 10 empty tin capsules included. Each sample had three replicates; the total amount of standards were 26, and the rock samples were 84. Analyzing the N content of the samples, the Isotope-Ratio Mass spectrometer had a furnace temperature of 1000°C. In combination with the tin capsules, the thermal energy rose to 1400°C. No program was used on this analysis. The content of nitrogen (N) in % was correlated to the K, P and C content in the samples, and to the locations in which the samples were collected.

2.3 GIS - Locating the areas on a GIS map.

A base map of New South Wales was downloaded from *https://search.geoscience.nsw.gov.au/product/9232* (2019-06-14) and opened in ArcMap (GIS). Each location was mapped out with coordinates (see appendix A) before creating shapefiles (points) to show where the samples were collected (figures 12-19). Although each point in the map contained information of the geological settings, no further analysis was pursued to create detailed shapefiles of the locations. The detailed information was instead taken directly from the data source to be informed alongside map figures 12-19.

2.4 Location Overview

The following maps are based on a geologic data source map of New South Wales from geoscience.nsw.gov.au (Colquhoun, G.P., et al., 2018) and were created using ArcGIS.

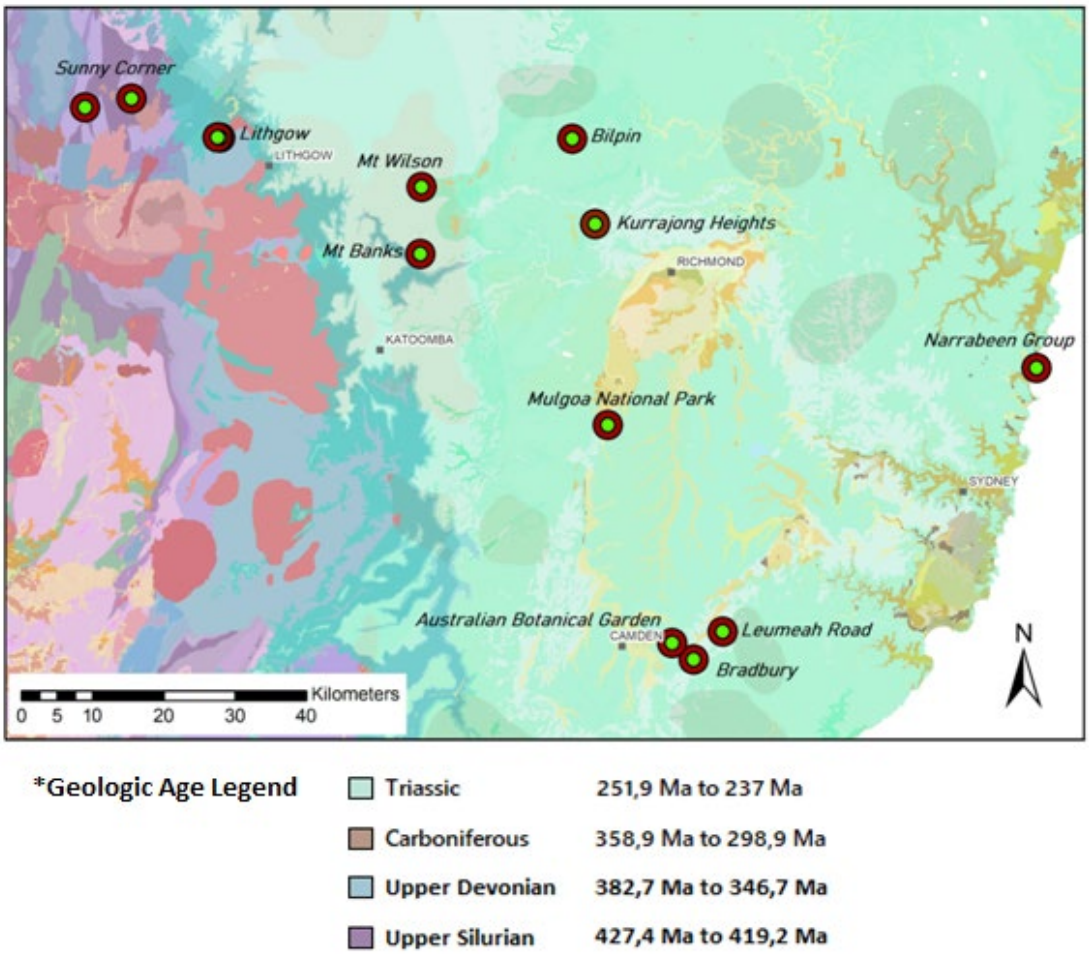

Figure 12. Locations of where the rock samples were collected in New South Wales. The colors indicate specific rock types and geological ages in the area. See figures 13-19 for a closer look at each site. Map was created with ArcGIS. *Geologic Age Legend refers to the GIS data source of the New South Wales map (Colquhoun, G.P., et al., 2018).

This color-based map shows the approximate ages of the terrestrial environment based on the locations. The locations stretches from Sunny Corner to Sydney Basin of New South Wales, where the bedrocks closest to the basin have a range of different sedimentary rocks such as sandstone, shale, siltstone, mudstone and claystone. Rocks that were collected further into the continent are of igneous nature, such as volcanic basalt, or metamorphic rocks like schists, quartzites or slates (see table 3, appendix B, for detailed characteristics).

2.4.1 Rocks from the Triassic 251,9 Ma to 237 Ma

Narrabeen

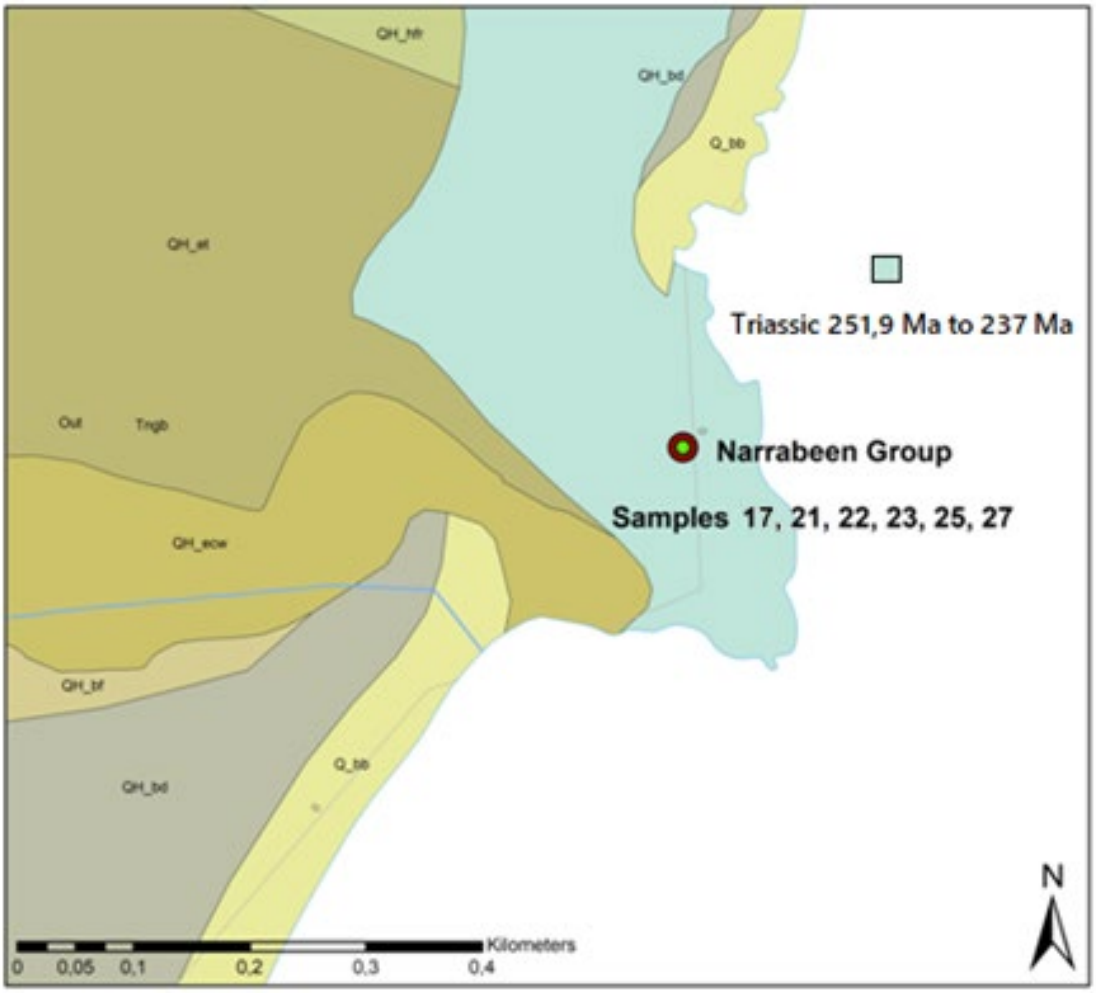

Figure 13. Narrabeen group samples (17, 21, 22, 23, 25, 27). The located area for the collected samples are taken from the same bedrock wall, but from different heights, as well as fallen rocks and rocks found on the ground. Rock types are shales, sandstones and siltstones (see figure 24 and table 3, appendix B). Map was created with ArcGIS.

Leumeah Road, Bradbury, Australian Botanical Garden

The rocks that were found and collected on Bradbury and Leumeah Road were the Ashfield Shale types from the Mid-Triassic (Helby, 1973), which is a dark-grey to black siderite. From the location of Australian Botanical Garden, a claystone was collected.

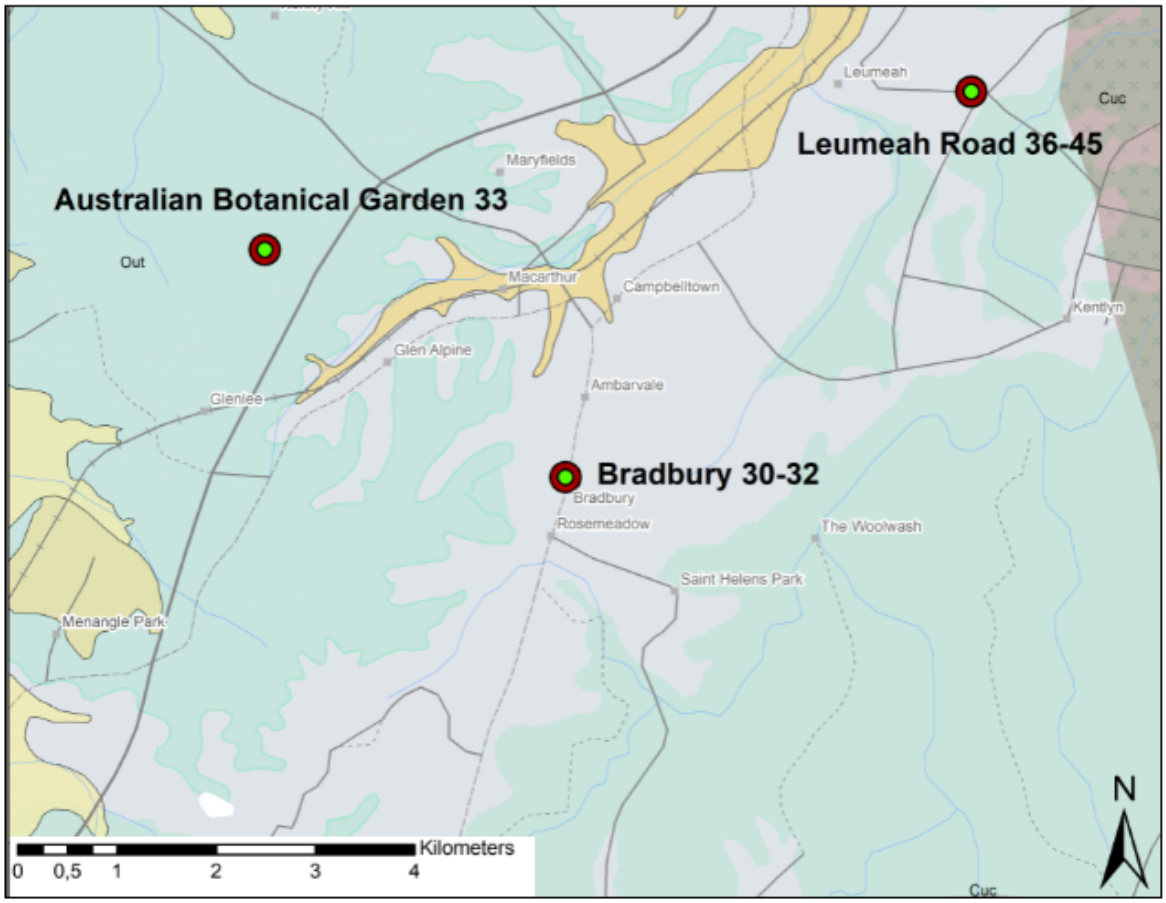

Figure 14. Sampling locations of Leumeah Road (samples 36-45), Bradbury (samples 30-32) and Australian Botanical Garden (sample 33). Rock types are shales, siltstones and claystones (see table 3, appendix B). Map was created with ArcGIS.

Mulgoa National Park

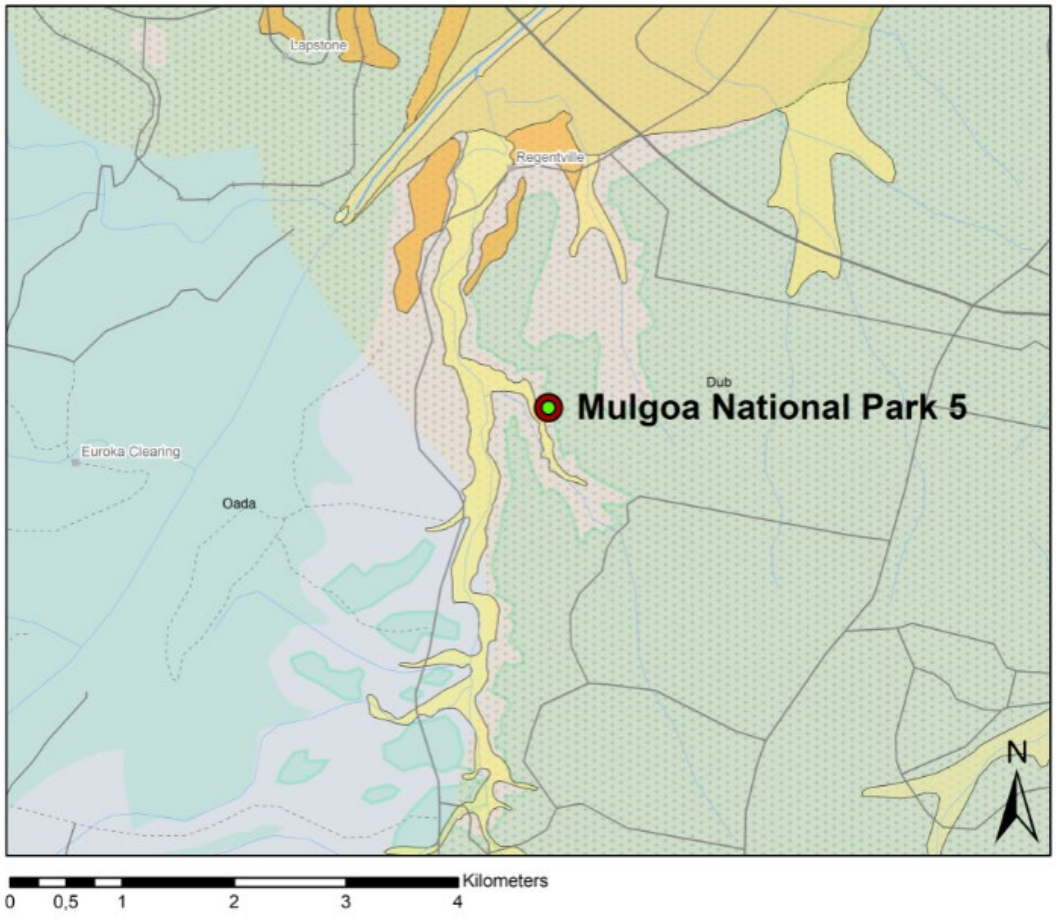

Figure 15. A schist was collected from Mulgoa National Park (sample 5). This location lies to the north from the Ashfield Shales of Bradbury and Leumeah Road (see table 3, appendix B). Map was created with ArcGIS.

Kurrajong Heights, Bilpin

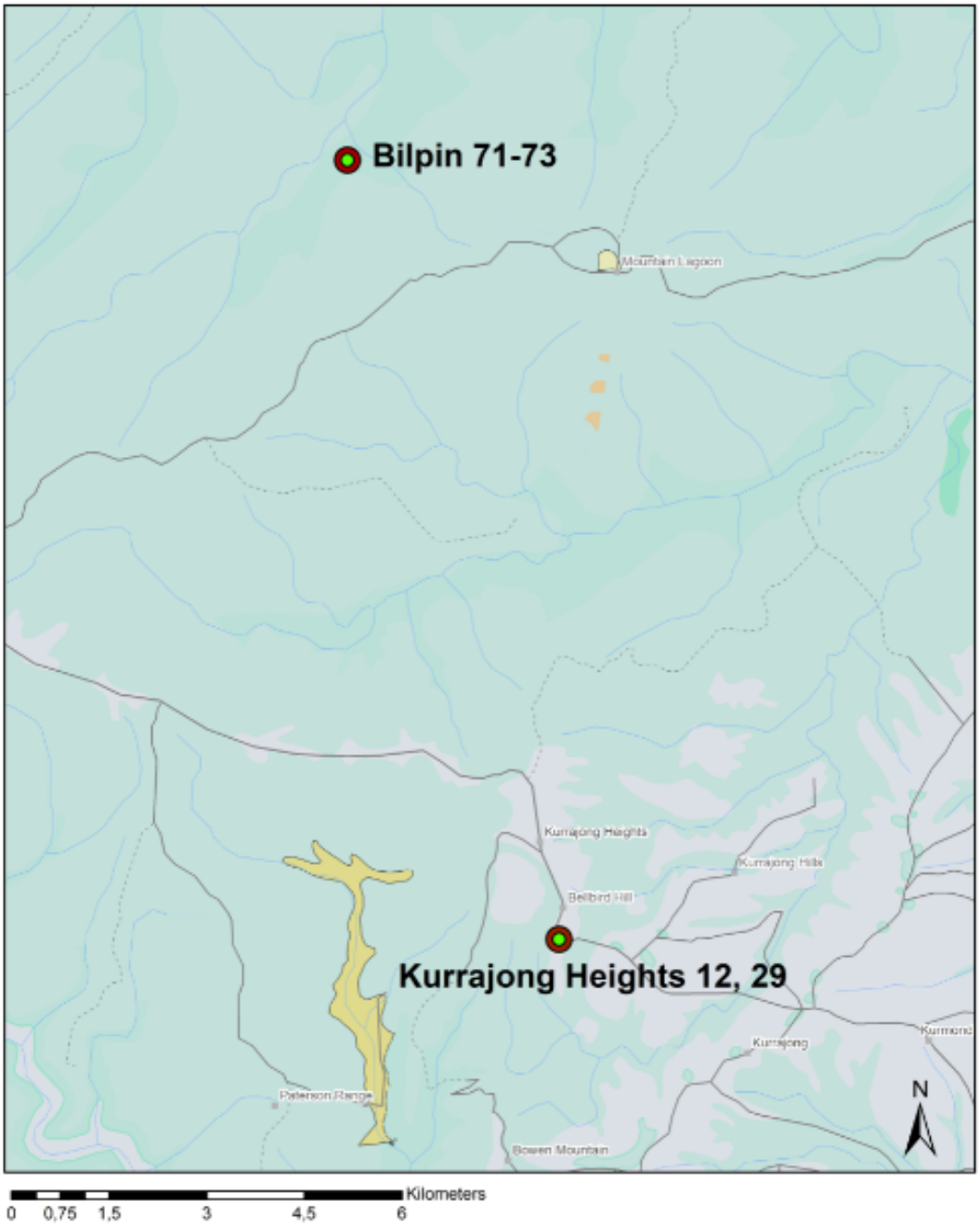

Figure 16. Locations of Kurrajong Heights and Bilpin. Hawkesbury Sandstone was collected from Kurrajong Heights (sample 12, 29), and Triassic shale from Bilpin (sample 71-73) (see table 3, appendix B). Map was created with ArcGIS.

2.4.2 Rocks from the Carboniferous 358,9 Ma to 298,9 Ma

Mount Wilson, Mount Banks

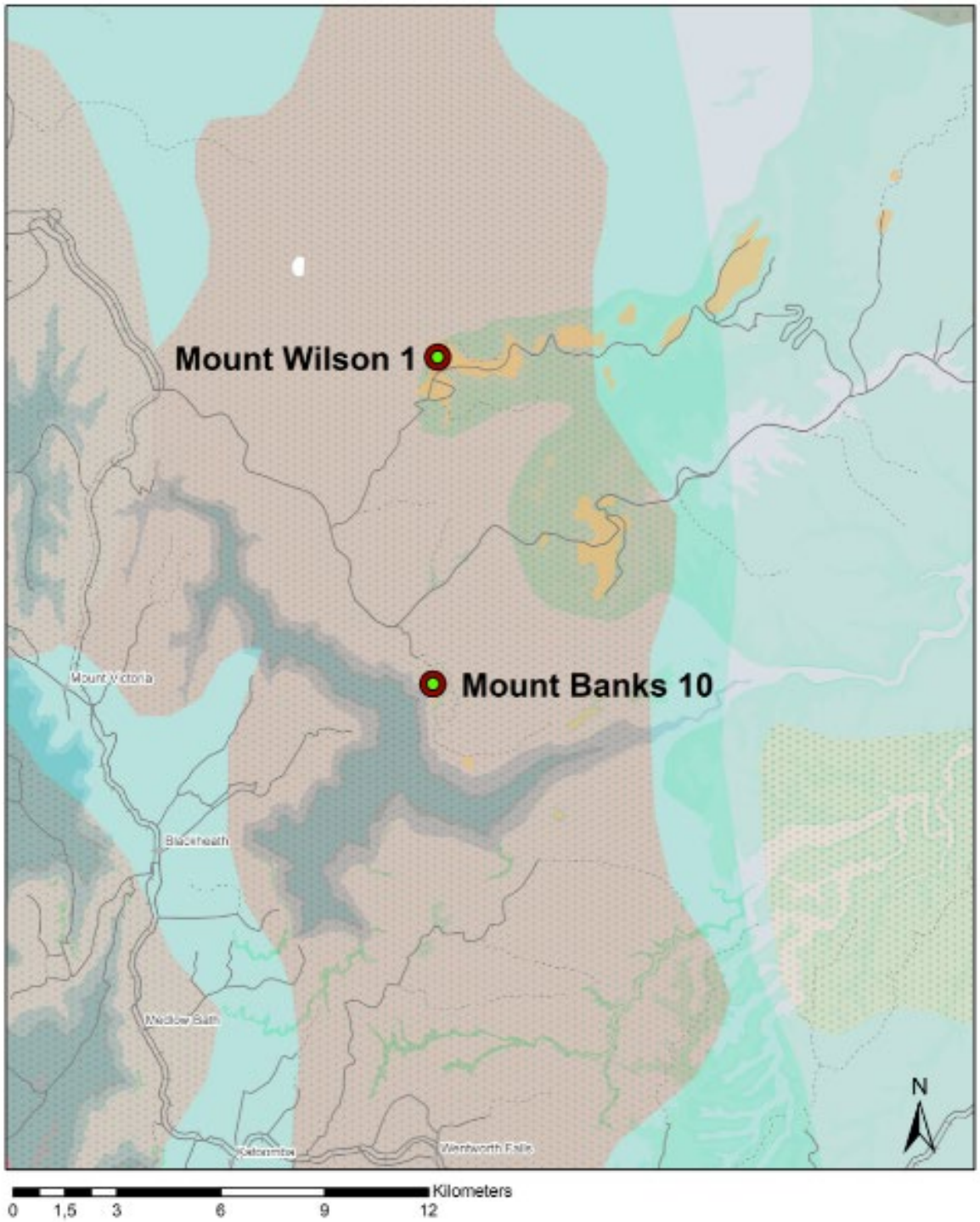

Figure 17. Volcanic rocks was collected from Mount Wilson (sample 1) and Mount Banks (sample 10) (see table 3, appendix B). Map was created with ArcGIS.

2.4.3 Rocks from the Upper Devonian 382,7 Ma to 346,7 Ma

Lithgow

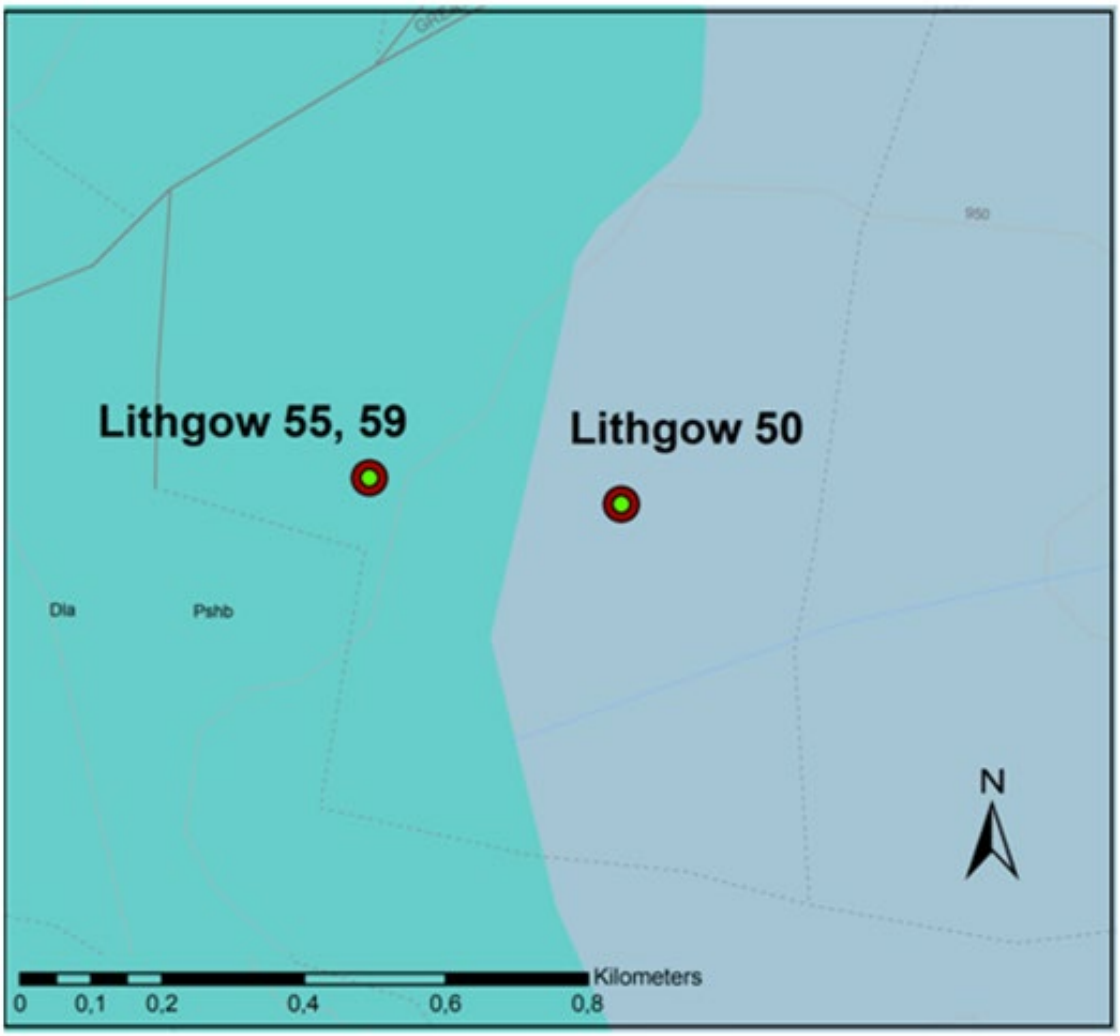

Figure 18. Devonian Shales were collected from Lithgow (sample 50, 55, 59) (see table 3, appendix B). Map was created with ArcGIS.

2.4.4 Rocks from the Upper Silurian 427,4 Ma to 419,2 Ma

Sunny Corner

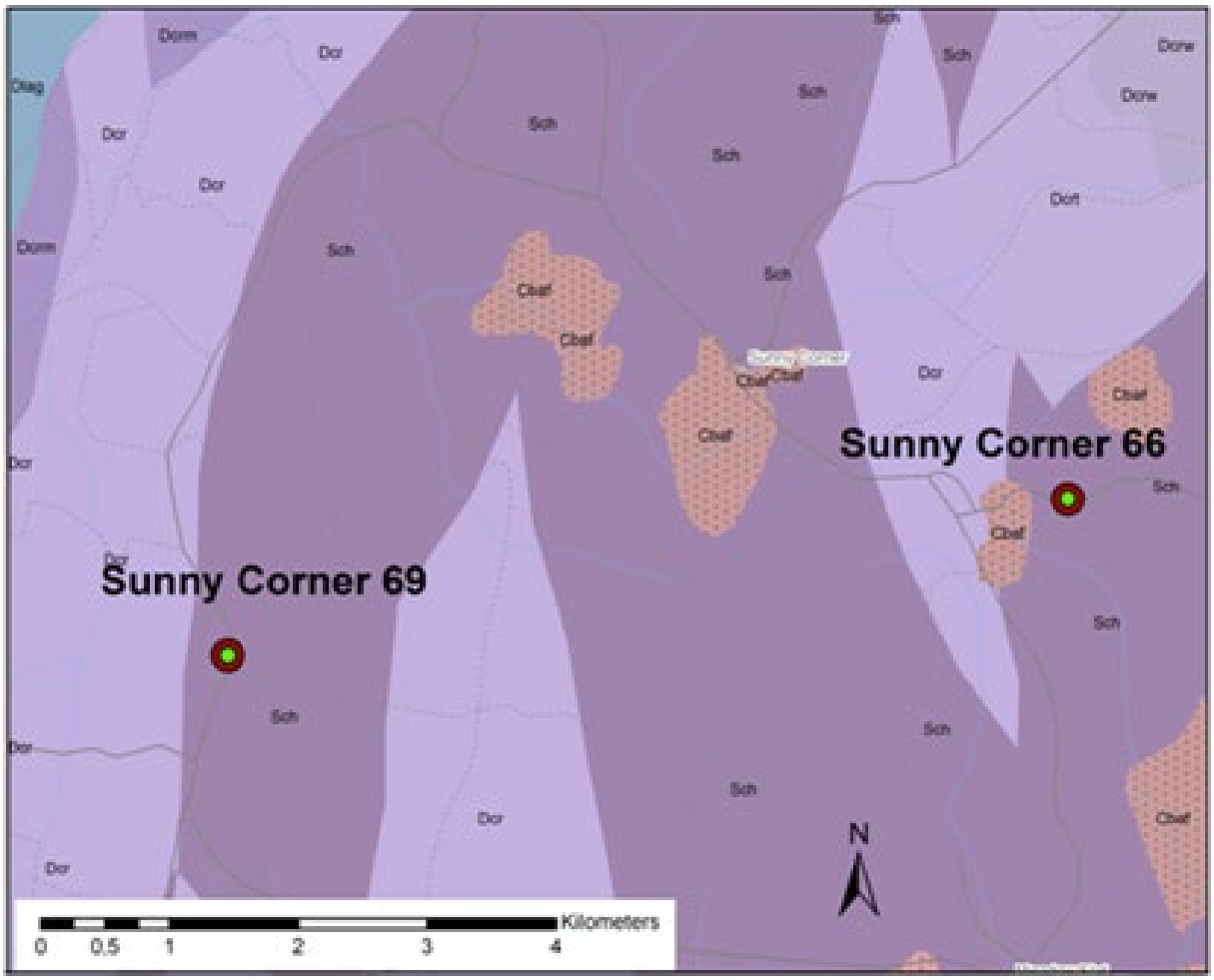

Figure 19. Silurian shale, quartzite and sandstone was collected from Sunny Corner (sample 66, 69) (see table 3, appendix B). Map was created with ArcGIS.

3. Results

The following information presents the results of the analysed raw rock material; rock type, nutrient content and correlation results of N/K and N/C.

Map overview

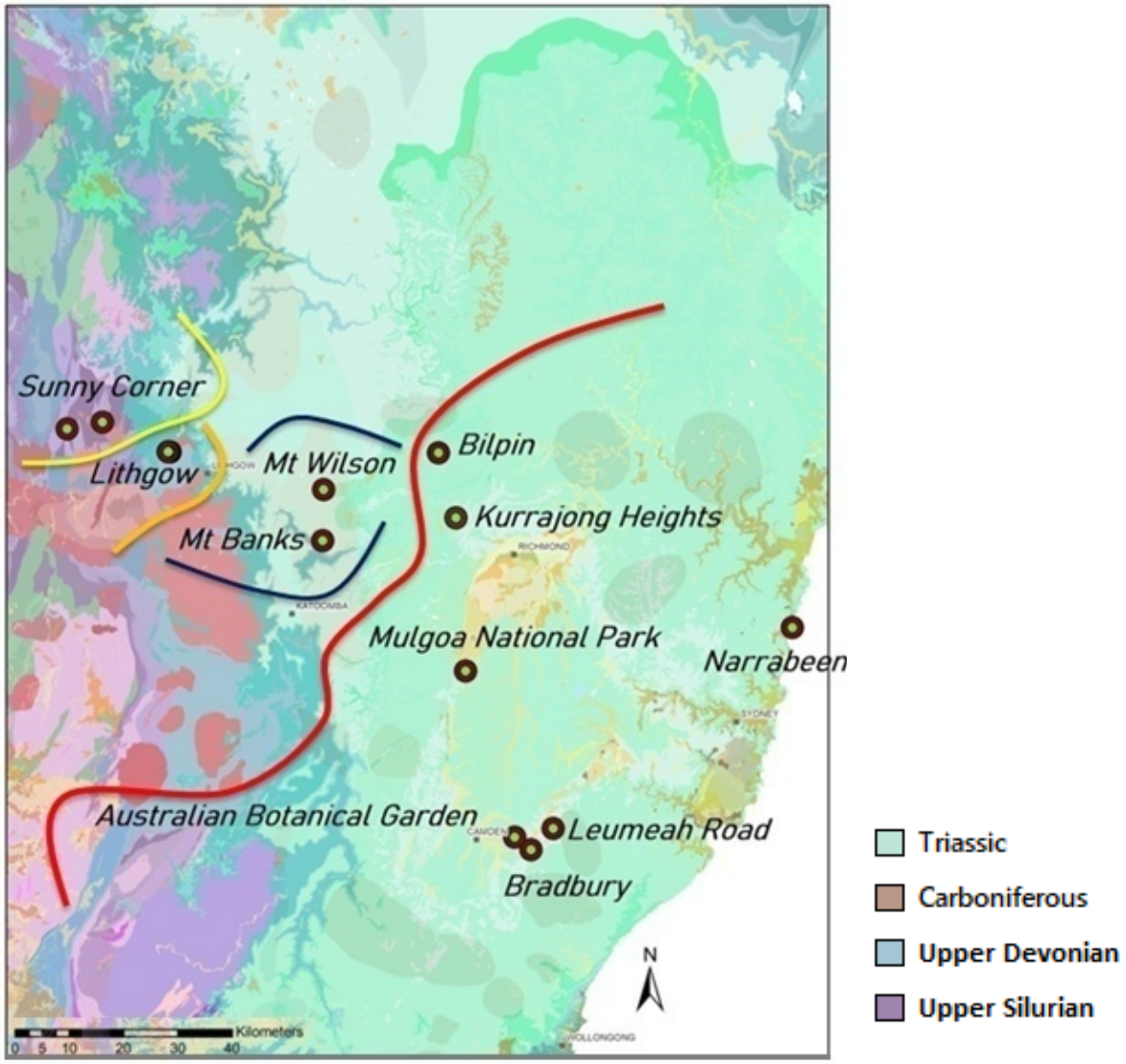

Figure 20. Map divided in sections of approximate geological ages, dating from Silurian to Triassic, for simple categorization. Color markings (yellow, orange, blue, red) indicate an estimated divide in bedrock and geological ages. Data from: https://search.geoscience.nsw.gov.au/product/9232 (2019-06-14). Map was created with ArcGIS.

Locations and geological ages of collected rock samples:

- Upper Silurian (427,4 - 419,2 Ma) — Sunny Corner
- Upper Devonian (382,7 - 346,7 Ma) — Lithgow
- Carboniferous (358,9 - 298,9 Ma) — Mt Wilson, Mt Banks
- Lower/ Middle Triassic (251,9 - 237 Ma) — Kurrajong Heights, Narrabeen, Leumeah Road, Bradbury, Bilpin, Australian Botanical Garden, Mulgoa National Park

Table 2. *Location of samples and rock types (location is shown in figure 20).*

Location	**Rock type(-s)**
Australian Botanical Garden	Claystone, shale
Bilpin	Triassic Shale
Bradbury	Ashfield Shale
Kurrajong Heights	Hawkesbury Sandstone
Leumeah Road	Ashfield Shale
Mulgoa National Park	Schist
Narrabeen	Siltstone, shale, sandstone
Mt Banks	Basalt
Mt Wilson	Basalt
Lithgow	Devonian Shale
Sunny Corner	Silurian Shale, sandstone

List of sample names in alphabetical order, excluding Narrabeen*:

Australian Botanical Garden (Claystone)	ABG-Clay
Bilpin (Triassic Shale)	BPTri-Sh
Bradbury (Ashfield Shale)	BB-Ash
Kurrajong Heights (Hawkesbury Sandstone)	KJHSa
Leumeah Road (Black Ashfield Shale)	LMR-AshBl
Leumeah Road (Brown Ashfield Shale)	LMR-AshR
Lithgow (Devonian Shale)	LG-DevSh
Mount Banks (Basalt)	MtB-Ba
Mount Wilson (Basalt)	MtW-Ba
Mulgoa National Park (Schist)	MNP-Sch
*Narrabeen (Sandstone 7-8 m)	NBSa7-8
*Narrabeen (Siltstone 6 m)	NBSi-6
*Narrabeen (Shale 3 m)	NBSh3
*Narrabeen (Shale 1-2 m)	NBSh1-2
*Narrabeen (Shale 0,4 m, sample 22)	NB22
Sunny Corner (Silurian Shale)	SC-Sh

*Narrabeen is following its height sequence from highest to lowest (m).

3.1 Nitrogen content (N %)

The following figures show the nutrient content in each specific location, starting with nitrogen (N). As shown in the figure below (figure 21), the highest N content is found within the Ashfield shales of Leumeah Road (0,072 N%) and Bradbury (0,068 N%), as well as the claystone from Australian Botanical Garden (0,065 N%); followed by some shales, siltstones and sandstones from the Narrabeen area, ranging from the lowest of 0,002 N% in the Narrabeen sandstone (NBSa7-8) to the highest of 0,048 N% in the Narrabeen shale (NBSh1-2). The basaltic rocks (Mt. Wilson and Mt. Banks) gave a result of 0,002 N%, while sedimentary rocks from Sunny Corner and Lithgow gave results ranging between ~0,005 - 0,007 N% (see table 9, appendix F).

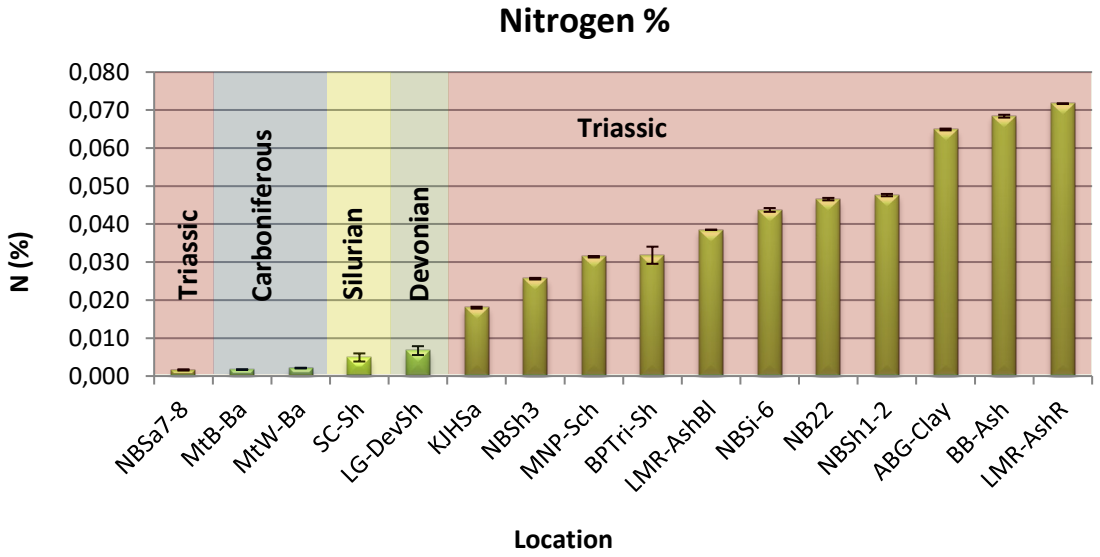

Figure 21. Results of the nitrogen content of the samples. Most of the samples show a significant N value ranging from 0,002 - 0,072 %. The geological ages are included with selected background colors to show the age trend of the nitrogen content. Triassic (red), Carboniferous (blue), Devonian (green), Silurian (yellow). Graph was created with Microsoft Excel.

3.2 Phosphorus content (P ppm)

The highest phosphorus content (29195 ppm) belongs to the Leumeah Road's Ashfield shale (LMR-AshBl). Other phosphorus contents are detected from 89 ppm to 7948 ppm (see details on figure 22 and table 9, appendix F).

The samples that showed no phosphorus content are the sandstones of Kurrajong Heights and Narrabeen; the Devonian shales of Lithgow and the Silurian shales of Sunny Corner. The higher levels of the Narrabeen sequence at 3-8 m height did not show any phosphorus content either. The rock types were sandstones, siltstones and shales.

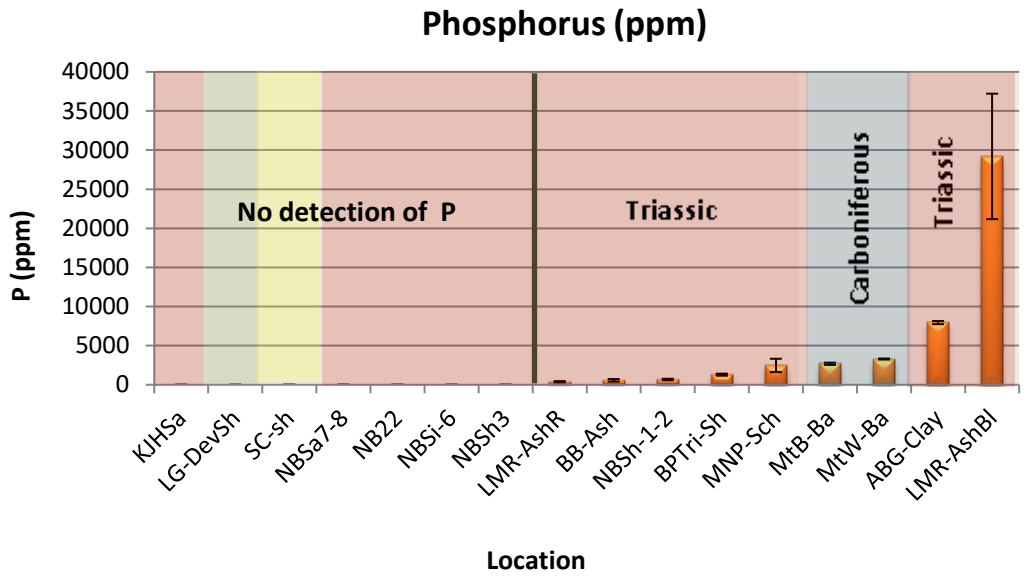

Figure 22. The mean results of phosphorus in each site shows P content ranging from 0 ppm to 29195 ppm. The geological ages are included with selected background colors to show the age trend of the nitrogen content. Triassic (red), Carboniferous (blue), Devonian (green), Silurian (yellow). Graph was created with Microsoft Excel.

3.3 Potassium content (K ppm)

Potassium content ranges from 0 - 21707 ppm, where the highest content belongs to the Narrabeen shale at 1,2 m height (NBSh1-2) (see figure 23 below; and table 9, appendix F). The results range from 9000 to 22000, except for one sandstone sample from Narrabeen that has a content of 1848 K ppm (NBSa7-8).

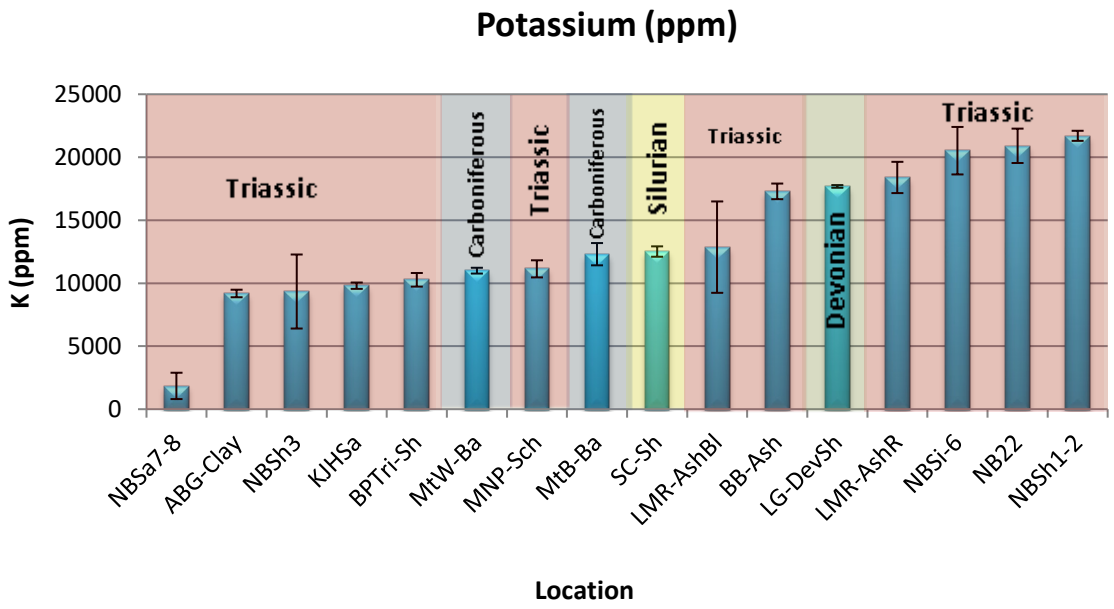

Figure 23. The results show an even variation of the potassium content ranging from 0 ppm to 21707 ppm, where the highest K content belongs to the Narrabeen shales. The geological ages are included with selected background colors to show the age trend of the nitrogen content. Triassic (red), Carboniferous (blue), Devonian (green), Silurian (yellow). Graph was created with Microsoft Excel.

3.4 Narrabeen group focus:

The following graphs show the nutrient content based on height (from 0 to 8 meters) of where the samples were collected from the Narrabeen wall stratigraphy. The zero point marks the bottom of the cliff.

Figure 24. Photograph of the Narrabeen stratigraphy. Edited to show height sequence (m) of where the rock samples were collected from (2018-11-03).

3.4.1 Nitrogen, Phosphorus and Potassium content:

In most heights, the N content is between 0,044 to 0,049 %, but drops down to 0,002 N % at 7-8 m height. This is also the lowest measured N content. At the lowest section of the stratigraphy (30-40 cm), the N value is at 0,047 %. From 1,2 - 1,7 m, the N content stays around 0,047-0,049 %. Further up the wall (~3 m) the N content is measured to be 0,026 %, and at 6 m it increases to 0,044 % (see graph 25A, figure 25).

The first and only detected section of phosphorus (P) in the Narrabeen group lies in the 1-2 m height. This content is detected in 3 shale samples (NBSh1-2) that lies in the height of 1,2 m and 1,7 m. The content is measured to be between 907 - 1247 P ppm. No phosphorus is detected at 30-40 cm group (it was below detection limit of the XRF), and no detection from 3 - 8 m (see graph 25B, figure 25).

The potassium (K) content is detected at 30-40 cm (31196 ppm), which is the lowest level of the stratigraphy. Further up the sequence at 1,2 m the detected K gives a value of 34080

ppm, which is also the highest potassium content of the Narrabeen sequence. At 1,7 m - 8 m, the detected K content ranges from 14424 ppm to 30677 ppm (see graph 25C, figure 25).

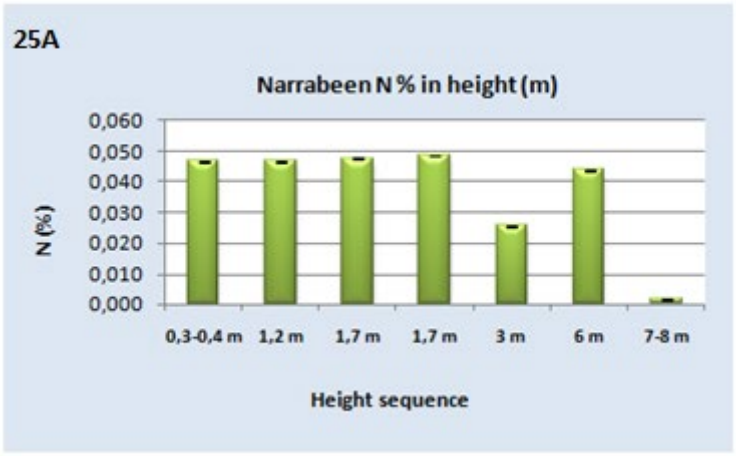

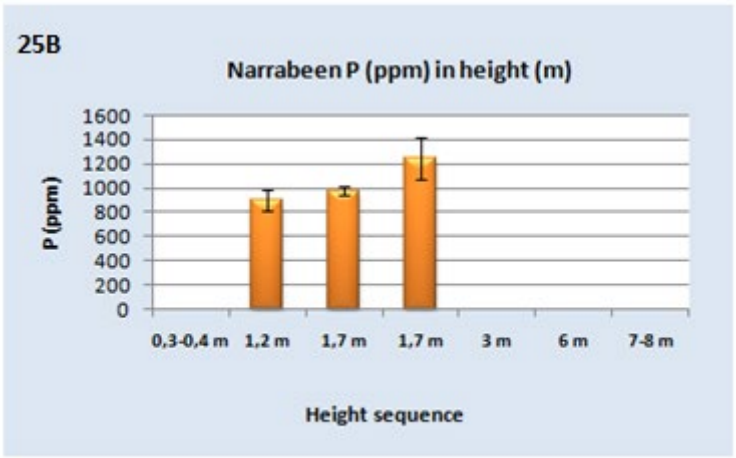

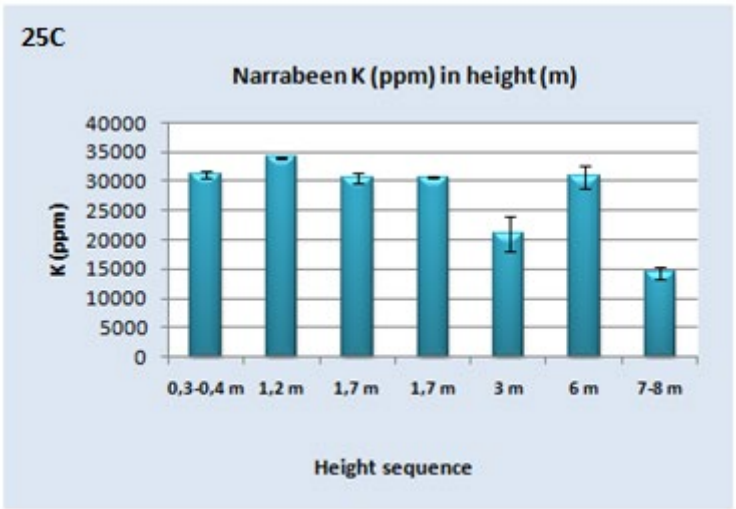

Figure 25. Graph 25A shows the Nitrogen content. Graph 25B shows the Phosphorus content. Graph 25C shows the Potassium content. Graphs created with Microsoft Excel.

3.5 Correlation of N/K and N/C

The correlations of the element contents (nitrogen, potassium and carbon) of the samples are grouped according to their location (see figure 20). The correlation of nitrogen (N) and potassium (K), or carbon (C), contents in the Narrabeen stratigraphy (top row - graphs 26A and 26B, figure 26); and in Leumeah Road and Bradbury, where both locations have the rock type of Ashfield Shale and are in proximity to each other (bottom row - graphs 26C and 26D, figure 26). The N/K contents correlation of Narrabeen group has a high R^2 value of ~0,97, and the N/C contents correlation an R^2 value of 0,64. The correlation between the Ashfield shales are ~0,99 for N/K and 0,7 for N/C.

This section give results for the correlation between the samples according to their sedimentary environment and location; the correlation is between N/K and N/C.

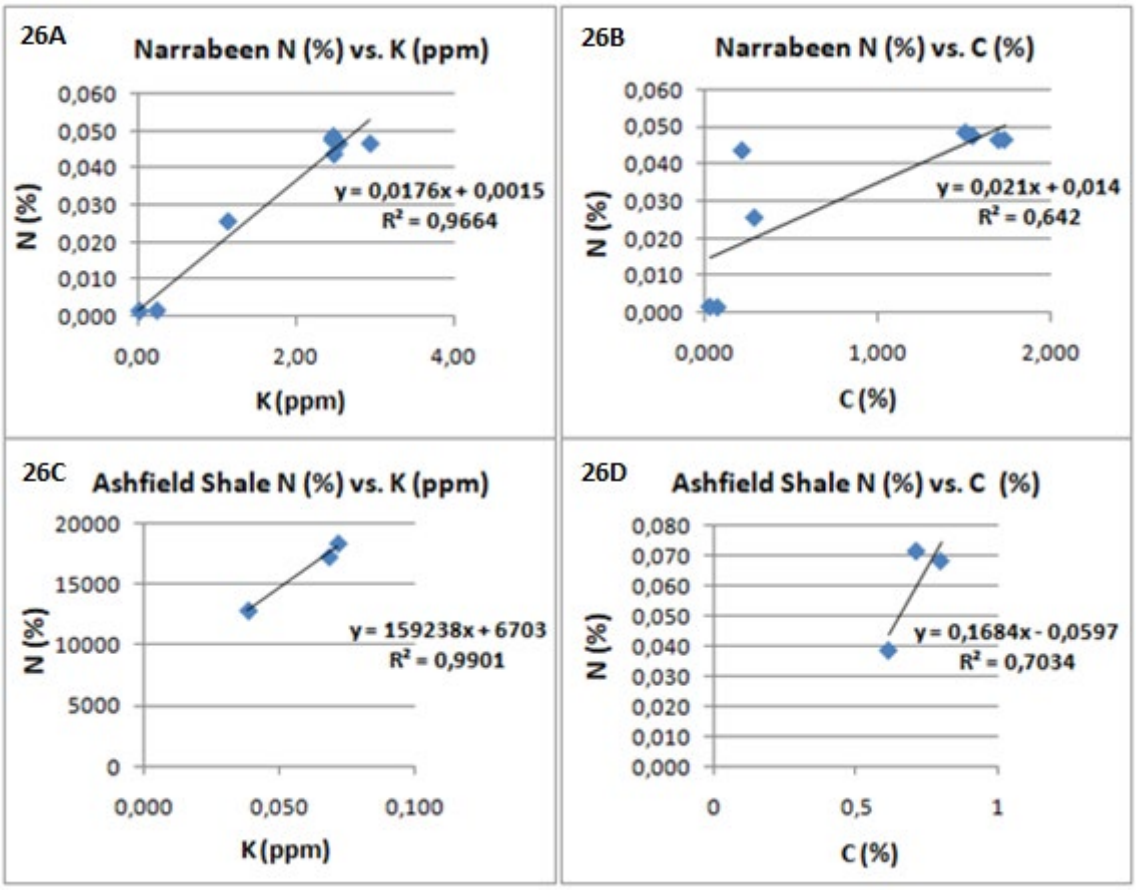

Figure 26. Samples have been selected based on their location proximity and their rock type. The N/K correlation of the Narrabeen group gives a close correlation of ~ 0,96 (26A), while the N/C gives a lower value (~0,64) (26B). The Ashfield shales from Leumeah Road (2 samples) and Bradbury (1 sample) also give a close correlation of the N/K (~0,99) (26C), with a N/C value of ~0,7 (26D). Graphs were created with Microsoft Excel.

N/K correlation of the Triassic rocks (Ashfield shales of Bradbury and Leumeah Road, Triassic shale from Bilpin, sandstone from Kurrajong Heights and the schist from Mulgoa National Park; claystone of Australian Botanical Garden excluded) gave a result of ~0,97 (see figure graph 27A), while the Silurian-Devon-Carbon rocks (Mt Banks, Mt Wilson, Lithgow and Sunny Corner) give a correlation result of 0,72 (see figure graph 27C). Results of the N/C for the Triassic rock shows a correlation of 0,83 (see graph figure 27B), while N/C for Silurian-Devon-Carbon group gives a correlation of 0,86 (see graph figure 27D).

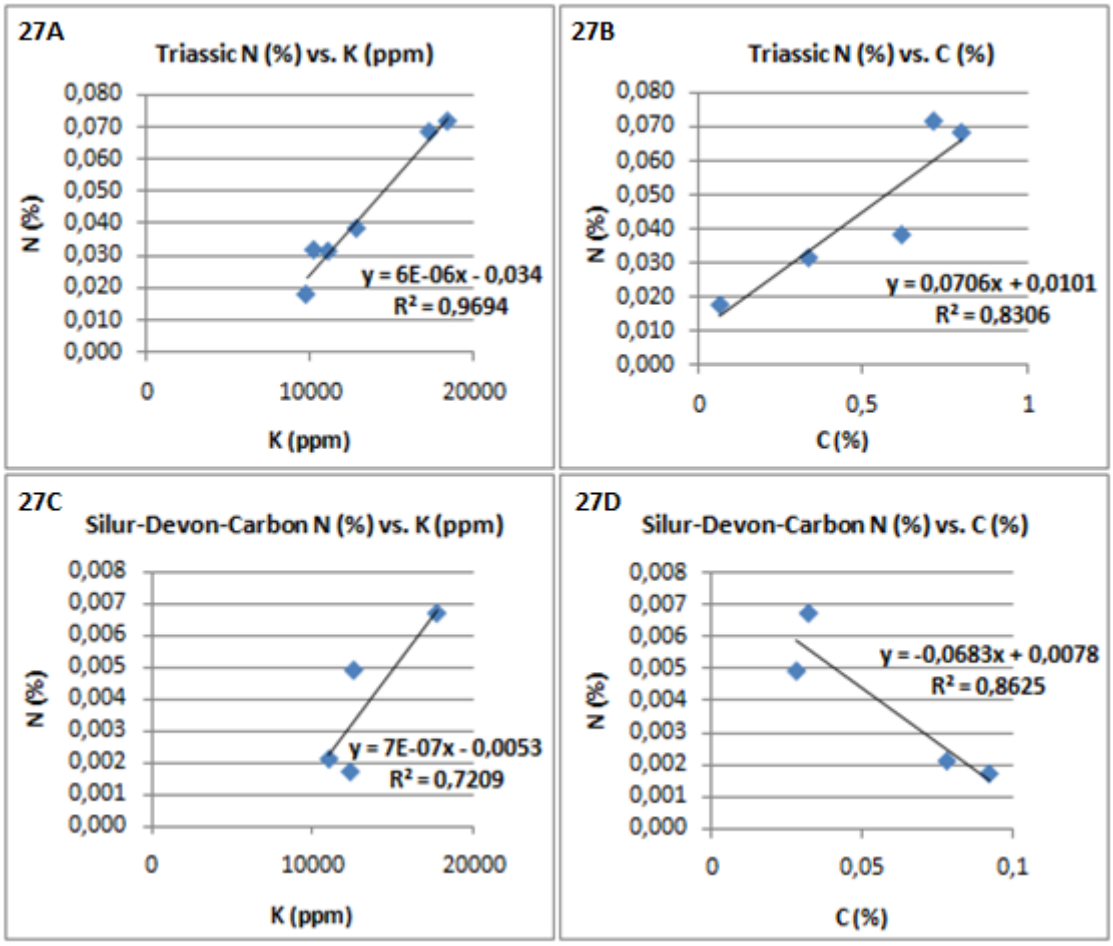

Figure 27. Correlation results of N/K values; Triassic group (27A and 27B) and Silur-Devon-Carbon group (27C and 27D). Samples have been selected based on their proximity in location and age grouping (see figure 20). Graph 27D is showing a negative value, which is further explained in the discussion. Graphs were created with Microsoft Excel.

3.6 Correlation of N plant and N rock

The correlation result of the nitrogen concentration in plants and rocks showed a R^2 value of ~0,43. The sites of the plant sampling was in Mount Banks, Kurrajong Heights, Narrabeen Headland, Leumeah Road, Australian Botanical Garden and Bradbury.

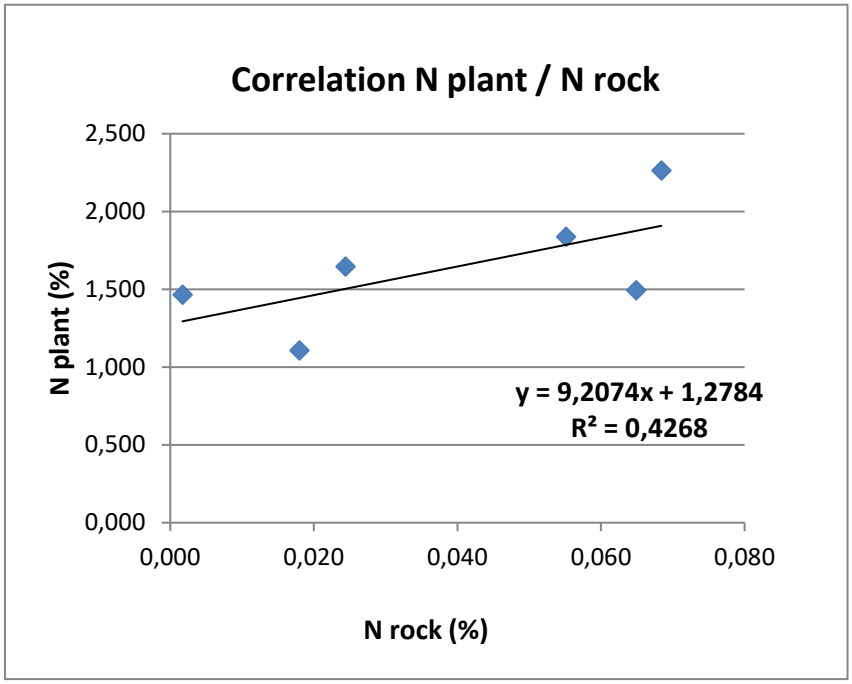

Figure 28. Correlation of N in plant vs. N in rock material. Graph was created with Microsoft Excel.

4. Discussion

The nutrient content is higher within certain rock types (see figure 29), such as shales and siltstones and mudstones. A general description of each rock can give clues as to how and why they might give these results.

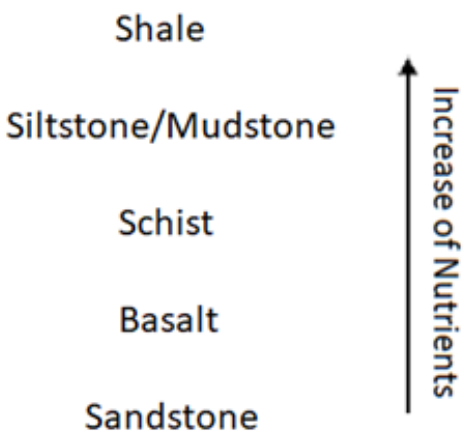

Figure 29. Schematic figure of N content according to the rock types.

Shales, mudstones and siltstones are all fine-grained particles of silt and/or clay (Hobart, 2005a; 2005b). Shales and mudstones are very similar except that shales show lamination and/or fissility, which mudstones do not. Mineral clays that are common in shales are illite, kaolinite and smectite. Siltstones are composed of mostly silt-particles which are between 0,0625-0,0039 mm in diameter. The common denominator for nutrient-rich rocks are that they have smaller particle sizes that bind the minerals closer together.

Shales that undergo high pressure, chemical reactions and heat within the Earth's crust, eventually turn into schists (Hobart, 2005c). Schists have minerals that are plate-formed, such as muscovite, biotite and chlorite. The transition from shale to schist is the following; shale/mudstone - slate - phyllite - schist. Further metamorphosis of schist creates a gneiss. This specific rock has been altered and changed from chemical reactions, high pressure and heat, which have affected the mineralogical structure, as well as the nutrient content.

Basalts are igneous rock types that are composed of fine-grained particles and prominent minerals such as plagioclase and pyroxene (Hobart, 2005d). This rock type forms by eruption

of lava onto the surface which makes them crystallize their minerals in a faster rate. Nutrients such as nitrogen is not common or exist below the Earth's crust (see table 1, section **1.5.2**).

Sandstones are mostly composed of "sand-grained" quartz particles, that are around 0,0625-2 mm. The spaces between the sand particles can be filled in with smaller grains that bind the sand together, such as clay and silt (Hobart, 2005e). This rock type erodes easily, which makes it more difficult for smaller elements/nutrients to bind into its matrix.

4.1 Gradient in Nitrogen (N) content of different rock types:

Increased nitrogen (N) content can mostly be found in shales and mudstone (Durr et al., 2005; Goldblatt et al., 2009; Houlton & Morford, 2015). Porous rocks such as sandstones are more prone to weathering, while shales, siltstones, mudstones and claystones are more resistant to weathering due to the grain size, mineralogical composition and chemical bonding within the mineral. Chemical and physical weathering mechanisms on the rock releases mineral bound nutrients.

According to the study *The durability of Ashfield Shale*, by Ghafoori, et al. (1994), they study the weathering processes in the Ashfield shale specifically, and discuss the difference between cycles of weathering - both chemical and physical. The initiation of physical weathering is the starting point for chemical weathering processes in shales. Weathering is evident in rocks as they begin to show discoloration. Most weathering in occur in clay dominant shales, with 45-60% clays, such as kaolin and illite (Loughnan, 1960; Dolanski, 1971; Slansky, 1973, as cited in Gahfoori, 1994). There is an increase in porosity with clay minerals that makes the rock less dense. Water is also a factor that increases weathering of shales. Shales that have an increased quartz content are less prone to weathering.

Other studies show that different temperatures of the rock can alter the total N concentrations and be released from sediments (Bebout and Fogel, 1992; Bebout et al., 1999; Williams et al., 1992). Rocks that exceed the temperature of 300°C are depleted in N, while temperatures of 50-150°C can free some nitrogen in the form of ammonium, NH_4^+, and be fixed and stable in silicate minerals or mobilized in pore fluids (Boudou et al., 2008; Compton et al., 1992; Sadofsky and Bebout, 2003; Williams et al., 1992).

There are three groups of nitrogen in organic and silicate reservoirs that suggest thermal framework when it comes to the nutrient stability in the various temperatures. The groups are listed as: **1.** Shallow burial diagenesis (temperatures are lower than 80°C) of organic-rich rocks, where the highest N content is found to be exceeding 2000 mg N kg^{-1}. **2.** Rocks from greater burial depths that includes prograde diagenesis and metamorphism (temperature exceeds 80°C) with N concentrations that falls below 2000 mg kg^{-1}. These are related to sedimentary and low-grade metasedimentary rocks (Boudou et al., 2008; Busigny and Bebout, 2013). **3.** Rocks at metamorphic temperatures of higher than 450°C, where the total N concentration is decreased to below 400 mg kg^{-1}, in minerals such as micas and feldspars (Bebout and Fogel, 1992; Bebout et al., 1999).

4.2 Gradient in Phosphorus (P) content of different rock types:

For the analysis of phosphorus content, there was no regulation set to one significant type of rock, nor sedimentary environment. The phosphorus content shows an increase in one shale sample in particular (see figure 22). This sample was from Leumeah Road, an Ashfield shale from the Triassic age (251,9 - 237 Ma). There were, however, other samples of Ashfield shales that showed much less P content (Leumeah Road and Bradbury). In terms of appearance (color of rock and surface weathering) the Ashfield shale with an increase of P content did not share the same characteristics as the other Ashfield shales with less P content (see appendix F, table 9; appendix E, table 7 and 8, figures 41 and 42). The Ashfield shale sample *LMR-AshBl,* had a hard surface and little to no weathering, while the other Ashfield shales were less dense and showed more surface weathering, including some minor cracks. The second highest P content belongs to the claystone of Australian Botanical Garden. This rock had no specific orientation in its structure and was a mixture of clay-, silt- and mudstone.

The increase of phosphorus was likely enriched during the Ediacaran period of 635-541 Ma by the initiation of the thermal Proterozoic orogenesis. During the orogenesis, sulfide weathering and erosion were increased in sedimentary rocks (Laakso, et al., 2020). This event caused phosphorus to remineralize and oxidant supply to increase. Further discussed by Herbert, C., (1979) is the phosphate mineral present in the Ashfield Shale as phosphatic nodules from apatite, with a concentration up to 20 %. Concentrations of P_2O_5 was also first

discovered by Lassack and Golding (1967) in Sydney Basin, in the Newport Formation of the Narrabeen Group. The concentration was measured to be 18,9 %. Another study have shown higher phosphate concentration in the center of the Ashfield Shale (Pacminex Pty Ltd, 1969), which is supported by several samples that were analysed of the dark-grey siltstones of the Kellyville Siltstone Member that had a value of 0,9 % P_2O_5.

An additional member that shows higher concentrations of phosphate is the Rouse Hill Siltstone Member, which is also based in the center of the Ashfield Shales. Most of the phosphate concentration is centered in the phosphatic nodules as carbonate apatite (Byrnes, 1975) with a composition of more than 60% phosphate mineral in the form of carbonate apatite, alongside with siderite at 5-20 % and other minerals such as diagenetic quartz, kaolin and pyrite.

Although no phosphorus (P) was detected within the collected rock samples from the Silurian shales of Sunny Corner in this study; Offler, R. (1984), presented in his study of mineral analysis '*Geology and ore genesis of silver-lead-zinc-copper sulphide deposits, Sunny Corner, NSW*', concentration results of ~0,02-0,16 P_2O_5% within silicic volcanic rocks from the north of Sunny Corner. Comparing the P results of the volcanic rocks from Sunny Corner (Offler, R., 1984) to the P results obtained in this study from Mt Banks and Mt Wilson (see figure 22), we can see a higher nutrient content within the basalts from Mt Banks and Mt Wilson. A possible indication of the nutrient difference can be due to the changes within the environment, such as weathering and difference in sedimentary environment.

4.3 Gradient in Potassium (K) content of different rock types:

Potassium is detected in all samples (however excluded from one sample based in Lithgow, sample no. 59). The most K content is detected in the Narrabeen shale that is on the 1-2 m height in the Narrabeen stratigraphy (NBSh1-2) (see graph 25C, figure 25).

In the study of *Dynamics of K in Soils and Their Role in Management of K Nutrition* (Sparks, D. L., 2001), the abundance of potassium in soils and minerals, as well as where the K content is more increased, is discussed. Igneous rocks have most K in comparison to sedimentary rocks according to Sparks (2001) - however, there is a significant difference within the types of igneous rocks and sedimentary rocks that can help determine the abundance of K. For

igneous rock types - granites, syenites, basalts and peridotites are listed. As cited in Jarrard's *Subduction Fluxes of Water, Carbon Dioxide, Chlorine, and Potassium* (2003), the most K enrichment is evident in old oceanic crusts, which reside in the upper crusts in porous and permeable zones (Donnelly et al., 1979a, 1979b). Potassium enrichment is found also in altered basalts (Hart, 1969; Hart et al., 1974). The K content is increased in granites and syenites with a value of 46 to 54 g K kg^{-1}, whereas in basalts there is a K content of 7 g K kg^{-1} and in peridotites there is 2,0 g K kg^{-1}. For sedimentary rock types, clayey shales gives a K content of 30 g K kg^{-1}, and for limestones the K content is 6 g K kg^{-1} (Sparks, 2001; Malavolta, 1985). In this instance, the two most abundant rock types are granites and syenites, and clayey shales. For potassium abundance in mineral form, there is muscovite, biotite and feldspars.

4.4 Relationship between N and K within the analyzed rocks

As seen in figure 26A, 26C, 27A and 27C (section **3.5**), the N/K ratio gave a higher correlation value for rock that were of the same or similar type, which was the Ashfield shales of Bradbury and Leumeah Road (see figure 26C). The Narrabeen wall had a correlation value of ~0,97 (see figure 26A). Within the Narrabeen wall (see figure 21, section **3.4**) there is diversity in rock type and general grain size. The formation of each rock section within the wall were created on different times and different external environments, which can be one of the reasons why the Ashfield shale have higher correlation. However, the difference is small.

For the rocks within the same geological age group, Triassic (see figure 12, 20), the N/K correlation was ~0,97. These are the rock samples from Bradbury and Leumeah Road (Ashfield shales), Triassic shale from Bilpin, sandstone from Kurrajong Heights and the schist from Mulgoa National Park. Older rock groups of the Silurian-Devon-Carbon ages gave the results of 0,72 (see figure 27C). These were the rock samples from Mt Banks, Mt Wilson, Lithgow and Sunny Corner. There is an apparent difference between rocks that are closer in time, as well as closer in sedimentary environment, which is seen in the Ashfield shales (see figure 26C) vs. the older rock group of the Silurian-Devon-Carbon ages (see figure 27C).

4.5 Negative correlation of N/C

The N/C of Silurian-Devon-Carbon gave a negative correlation. A negative correlation is indicative of one element increasing, and the other one decreasing. The R^2 value shows a high correlation of 0,86, where the nitrogen (N) decreases as carbon (C) increases.

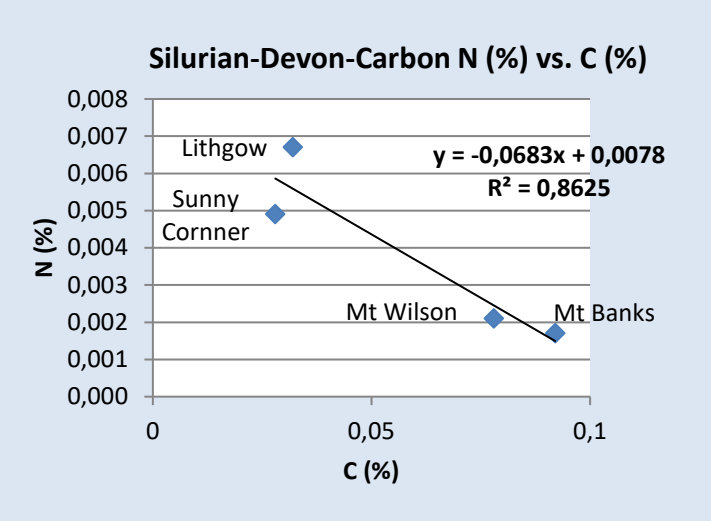

Figure 30. Initial correlation for Silurian-Devon-Carbon C/N, where nitrogen (N) decreases as carbon (C) increases. Samples involved are from Lithgow, Sunny Corner, Mt Banks and Mt Wilson. Mean value from Lithgow is based on samples 50, 55, and 59; and samples from Lithgow are based on the mean value of rock samples 66 and 69. Graph was created with Microsoft Excel.

There was a total of 3 samples from Lithgow (sample 50, 55 and 59), and 2 samples from Sunny Corner (66 and 69). While the rocks came from the same locations, there was a distinct difference in their appearance and colors (see table 3). The data was calculated based on mean value of all the rock samples, which in turn gave a negative correlation. These rocks have different origin; basalt/volcanic rock from Mt Banks and Mt Wilson; Devonian shales from Lithgow; and Silurian shales from Sunny Corner.

In the example below (see figure 31), the correlation is lower than the previous one. However, we can notice a trend above the red line (a) where Lithgow (50, 55) and Sunny Corner (69) seem to give a positive correlation; whereas Lithgow (59), Sunny Corner (66), Mt Wilson and Mt Banks, under the red line (b), give a negative correlation. Further study of the rock samples can give clues to this occurrence.

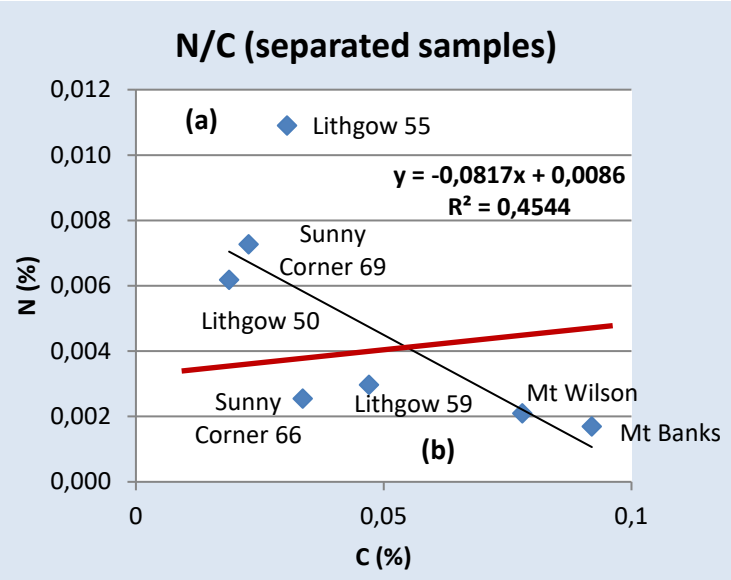

Figure 31. Negative correlation of all samples from Lithgow (50, 55, 59), Sunny Corner (66, 69), Mt Wilson and Mt Banks. This R^2 value is significantly lower at 0,45 in comparison to figure 30. The red line is included to show a possible correlation between Lithgow (50, 55) and Sunny Corner (69). Graph was created with Microsoft Excel.

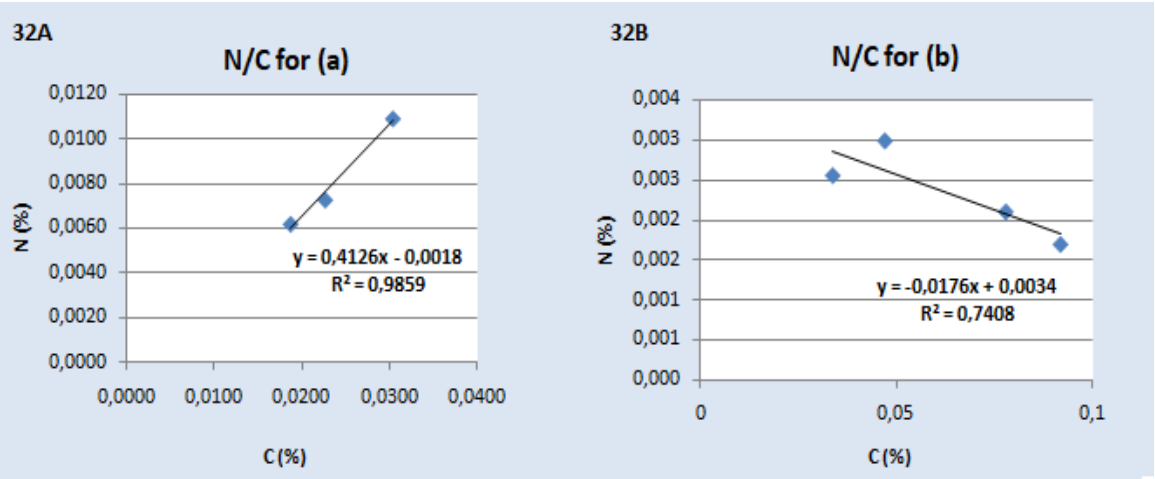

Figure 32. The N/C correlation for group (a) (graph 32A), with samples Lithgow (50, 55) and Sunny Corner (69), give a positive correlation and an R^2 value of 0,98. This indicates a high correlation between these rocks in terms of their N/C content. The N/C correlation for group (b) (graph 32B), with samples Lithgow (59), Sunny Corner (66), Mt Banks and Mt Wilson, give a negative correlation with a R^2 value of 0,74. Graphs were created with Microsoft Excel.

4.6 How does quartz affect the nutrient availability?

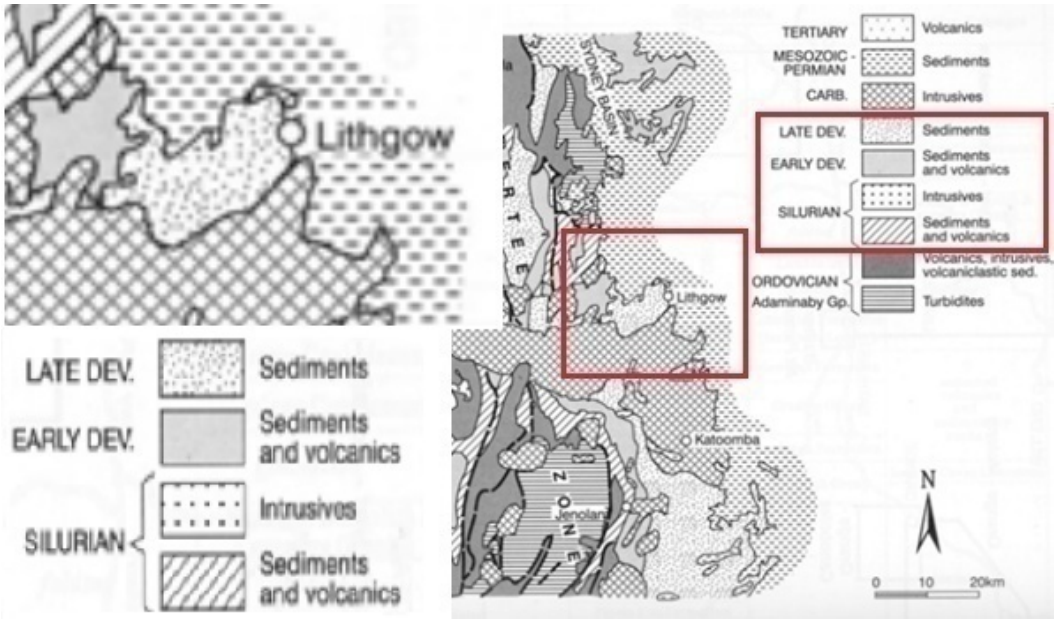

Figure 33. Geological map of the Lachlan Orogen in New South Wales (Downes et al., 2004; Branagan & Packham 2000). Edited version; focused on Lithgow and Sunny Corner.

Another factor that can be discussed is the quartz-rich shales from the Silurian age, from Sunny Corner. According to the study of Offler, R (1984) "*Geology and ore genesis of silver-lead-copper sulphide deposits, Sunny Corner, NSW*..", he describes the sedimentary texture as "*interbedded fawn to yellow, poorly sorted quartz wackes and siltstones...", "...The siltstones are even-grained and consists of quartz clasts and oriented white mica in a chlorite and iron oxide cement."* Samples from Lithgow and Sunny Corner are directly affected by the Lachlan Orogen. Many quartz-rich sediments, as well as some cherts and black shales, were created during the development of the Lachlan Orogen in the early Ordovician through tectonic activity such as subduction, back arc extension, uplift, rifting, volcanism, deformation and intrusion (Downes et al., 2004).

Quartz has the mineral formula of SiO_2, and hardness of 7 in the Mohs hardness scale, which is considered very hard and resistant to chemical weathering. The bonds between the silica and the oxygen atoms are strong, and bonded by a polar covalent bond. Other elements cannot come between and interact within the atomic layers of the SiO_2 molecule. Based on the mineralogical characteristics of quartz as a sedimentary rock mineral, other elements might have already dissolved or weathered, especially for sand and gravel sized quartz

minerals (Richardson, 2018). Quartz does not affect the nutrient availability, it only acts as a system for nutrients to filter through into the soils. Nutrients are obtained from the surrounding area; nitrogen (N) from the atmosphere, phosphorus (P) and potassium (K) through other sources of rock material that are capable of weathering.

4.7 Is there a trend from older to younger bedrock material that decide the concentration of nutrient availability?

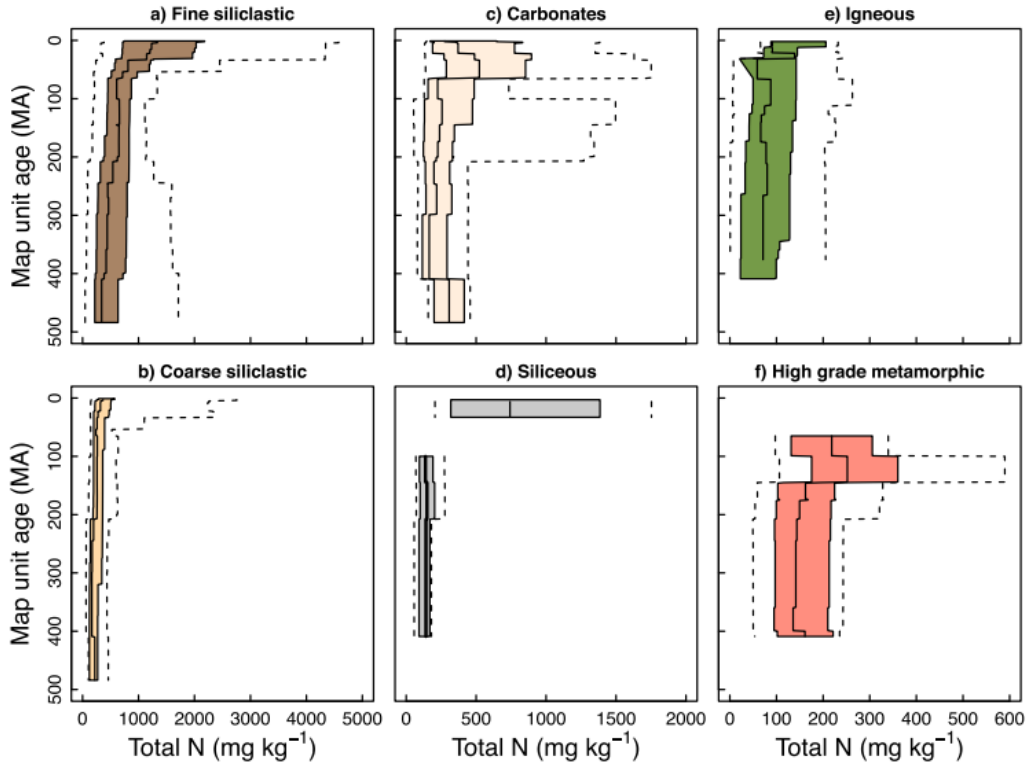

Figure 34. Graphs of different rock types and their total N availability in relation to geologic age. Figure obtained from Morford et al., (2016).

In the study of Morford et. al., (2016) *Geochemical and tectonic uplift controls on rock nitrogen inputs across terrestrial ecosystems*; there is a given geological timeframe of increased nutrient availability that supports the younger geological ages - Paleozoic to Late Jurassic (542 - 145 Ma), as shown in figure 34. Total N increases for rocks that are from younger geological ages, regardless of sedimentary lithology as the figure shows. However, the fine-grained siliciclastic rocks were measured to have the highest median nitrogen content (Morford et al., 2016).

4.8 Comparison of nutrient content in New South Wales, AUS vs. California, USA

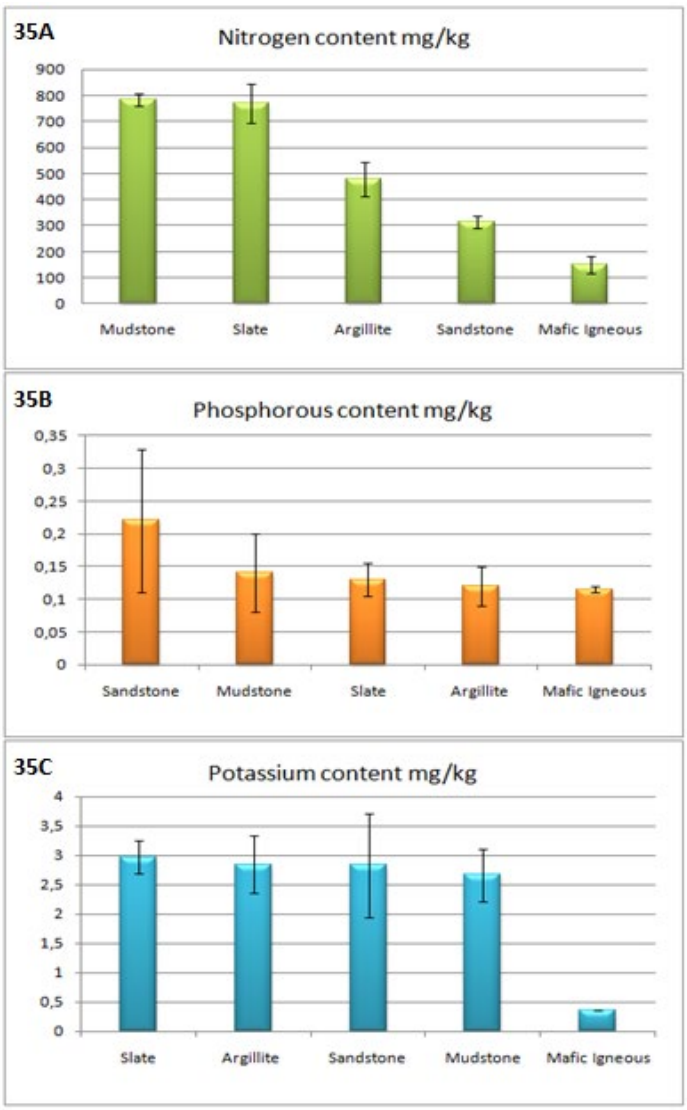

Figure 35. The data for the total nitrogen is taken from the data base of Morford et al., (2016). Graphs of nutrient availability were calculated with standard error bars. Geological timeframe is from 542-145 Ma. Graph 35A shows the nitrogen content, where mudstone has the highest N content. Graph 35B shows the phosphorus content, with sandstone as the most P rich rock. Graph 35C shows the potassium results where slate is the most K rich rock. Graphs were created with Microsoft Excel.

These results show some similarity to this analysis of the N, P, K content of the rocks from New South Wales. The potassium (K) content is even through the sedimentary rocks, except the igneous rocks (basalts). Taking the standard error into consideration for the data base of the Morford phosphorus content with the sandstone as the most P-rich rock, there is most likely an apparent difference between each rock for itself (see table 14, appendix H).

However, not all samples that were analyzed in their study were equal to the samples used for this analysis. The data chosen from the study of Morford et al., (2016) are equal or similar to the ages and rock material that were analyzed in this study.

4.9 Correlation N/K

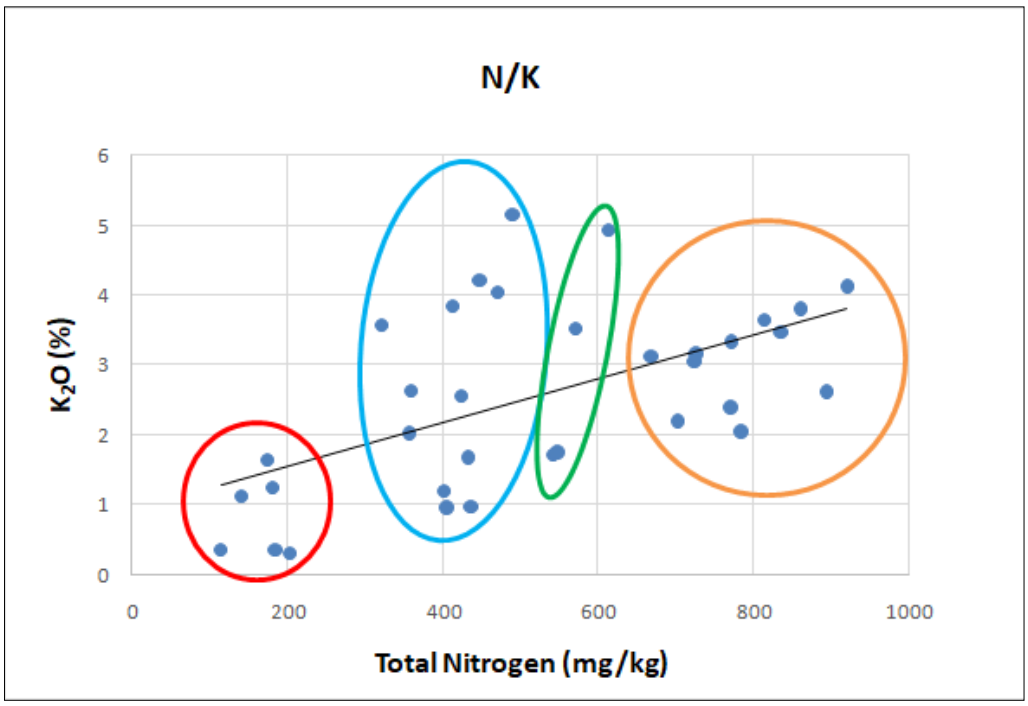

Figure 36. The graph is a new data analysis of the data base from the Morford et al., 2016. Correlation of nitrogen and potassium of the analyzed samples from the study of Morford et al., (2016). The chosen rock samples were of the similar geological ages (from the oldest 2500, to the youngest 65,5 Ma). The red color indicates ages from 2500 - 65,5 Ma. Blue color has the geological ages of 542 - 145 Ma. The green color indicates the geological ages of 488 - 145 Ma; while the geological ages of the orange group of rocks are 298,9 - 145 Ma). Graph was created with Microsoft Excel.

In figure 36 we see that the selected rock samples of the study (Morford et al., 2016) appear to be grouped. The colored circles are indicators of estimated ages of the rocks, which are based on the supplementary document of the analyzed samples (see table 14, appendix H). There is a prominent trend with the groups that are significant factors supporting the high nutrient availability of rock samples that belong to younger geological ages. Red circle group indicate ages from 2500 - 65,5 Ma; blue circle group are ages from 542 - 145 Ma; green circle group have ages from 488 - 145 Ma; and for the orange circle group, the ages are from 298,9 - 145 Ma. The older the sedimentary rocks are, the lesser nutrients they contain due to different kinds of weathering.

4.10 Correlation of geologic age

Seen in figure 37 below, the rocks belonging to the 2500 - 65,5 Ma have the lowest R^2 value, while the rocks from 488 - 145 Ma (37C) has the highest correlation value of ~0,97. Looking at the correlation graph of 37D dating from 298,9 - 145 Ma, there is a separation of two groups (one circled in orange and one in green). Separating the groups, there is an increase in correlation. The samples in the orange circle gives the R^2 value of ~0,5, while the samples within the green one gives an R^2 value of ~0,89.

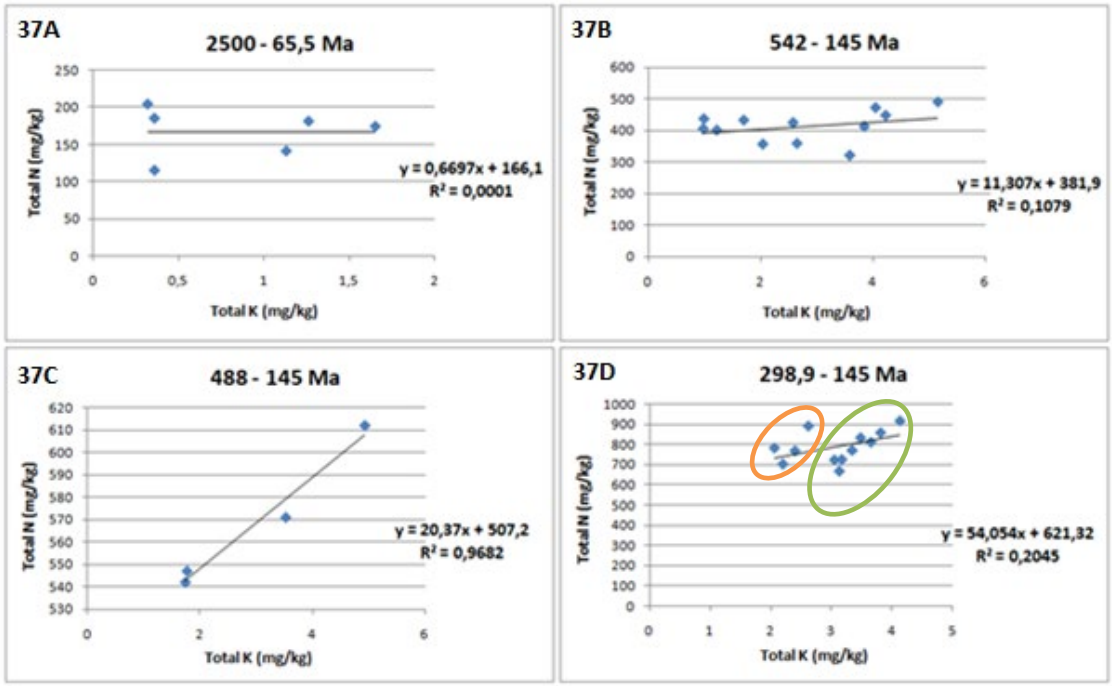

Figure 37. Correlation of geological ages of the data base from the Morford et al., (2016). Graph 37A shows the ages between 2500 - 65,5 Ma; Graph 37B shows the ages from 542 - 145 Ma; Graph 37C shows the ages of 488 - 145 Ma; and graph 37D shows the ages from 298,9 - 145 Ma. Graphs were created with Microsoft Excel.

For each group there is a mixture of different rock types, which might describe the correlation results. Graph 37A have rock types of mafic igneous, sandstone, argillite and silicaceous; graph 37B include rocks such as argillite, slate and sandstone; graph 37C have argillite, slate and mudstone; and graph 37D have argillite, slate, mudstone and shale.

Due to the different types of rock material and that the samples (a few of them) come from different locations around in California, USA, correlation results are somewhat expected.

4.11 Correlation of rock type (N/K)

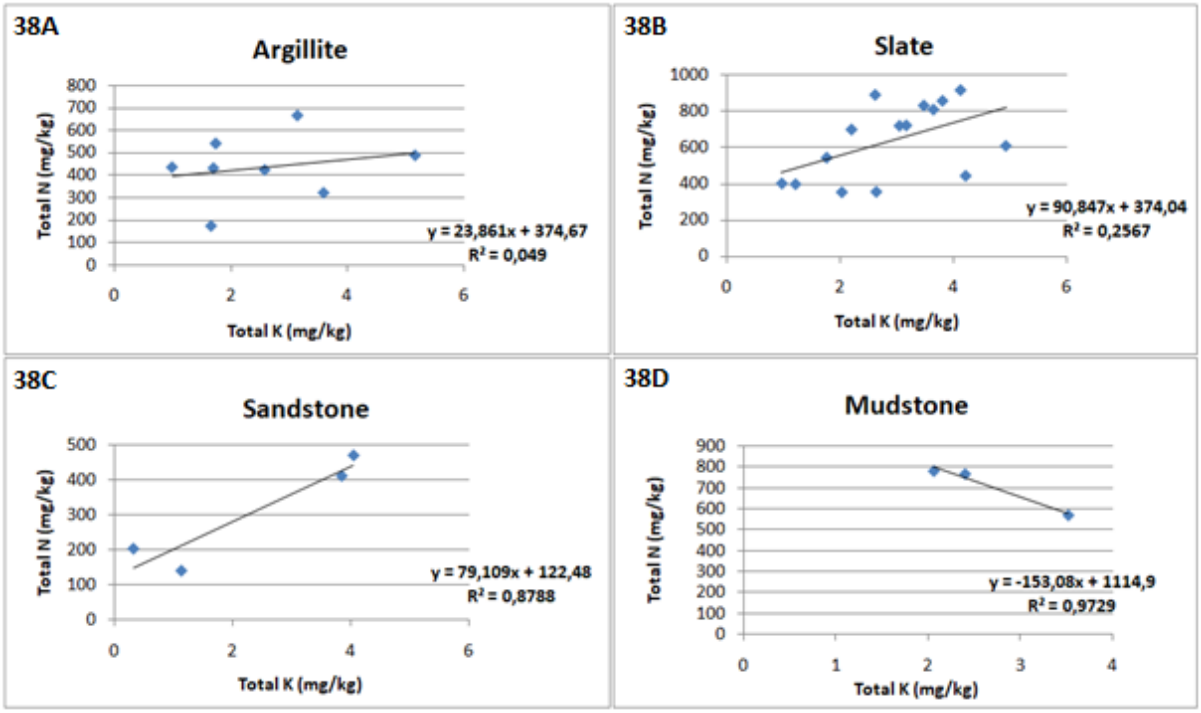

Figure 38. Correlation of rock type of the data base from the Morford et al., (2016). Graph 38A shows argillite; graph 38B shows slate; graph 38C shows sandstone; and graph 38D shows correlations of mudstone. Graphs were created with Microsoft Excel.

The results for the correlation of rock types from California, USA, gives somewhat more scattered results. Looking at graph 38A (argillite) and 38B (slate), the correlation results give less significance than graph 38C (sandstone) and graph 38D (mudstone). This is also due to the fact that there are less sandstone and mudstone samples to compare. Another factor for the correlation results might be that the rocks for each graph only follow 'rock type' and not similar or same sedimentary environment.

Here we also see an example of a negative correlation (graph 38D - mudstone), where the total nitrogen (N) content decreases as the total potassium (K) content increases. In previous discussion about negative correlation (**section 4.5**), the characteristics of the rock and its sedimentary environment was taken into consideration.

5. Conclusion

The results show that sedimentary rocks, more specifically the Ashfield shales, a subgroup of the Wianamatta Shale from Bradbury and Leumeah Road, contain higher nutrient content for all analyzed nutrients; nitrogen, phosphorus and potassium. The phosphorus (P) content was 29195 ppm and nitrogen (N) concentrations varied from 0,068 - 0,07 N%. These locations are of transitional deltaic environments.

Rock samples from Mt Wilson and Mt Banks; Lithgow and Sunny Corner, contain less nutrients, although have a mineral composition of mostly quartz. These sites are of deep marine to terrigenous, to shallow marine environments. Potassium (K) content in these rock samples varied from 12000 - 18000 ppm.

Nitrogen content that exceeds the value of 0,01% is considered to be of ecological importance, which mostly have been found in sedimentary and metasedimentary rocks (Holloway and Dahlgren, 2002). There were many samples that showed significance to this matter that ranged from 0,018 - 0,072 N %. From the highest to the lowest nitrogen content; Ashfield Shale from Leumeah Road (0,072 N %) and Bradbury (0,068 N %) > Claystone from Australian Botanical Garden (0,065 N %) > Shale from Narrabeen (0,047 N %) > Triassic shale from Bilpin (0,032 N %) > Schist from Mulgoa National Park (0,031 N %) > Shale from Narrabeen (0,026 N %) > Sandstone from Kurrajong Heights (0,018 N %).

Samples that lacked significant nitrogen content came from the basalts of Mount Wilson and Mount Banks, some sedimentary samples of the Narrabeen group, as well as the shales of Sunny Corner and Lithgow. These values ranged from ~0,002 - 0,007 N %.

The phosphorus content ranged from 0 - 29195 ppm, where the highest phosphorus value belonged to one of the Ashfield Shales from Leumeah Road with a P content of 29195 ppm. The other values are (from highest to the lowest P content); Claystone from Australian Botanical Garden (7948 P ppm) > Basalt from Mt Wilson (3294 P ppm) > Basalt from Mt Banks (2681 P ppm) > Schist from Mulgoa National Park (2469 P ppm) > Triassic shales from Bilpin (1290 P ppm) > Shale from Narrabeen (667 P ppm) > Ashfield Shale from Bradbury (556 P ppm) > Ashfield Shale from Leumeah Road (385 P ppm). Shales and sandstones of Kurrajong Heights, Lithgow, Sunny Corner and Narrabeen showed no phosphorus detection.

Correlations of N/K and N/C show significant R^2 values (from 0,7 - 0,99) that strongly indicate that the samples are related to the location they are set on and their rock type. Samples with the significant correlations are the Ashfield shales (Bradbury and Leumeah Road), combined with the sandstones of Kurrajong Heights, the schist from Mulgoa National Park and the Triassic shale from Bilpin. Their N/K correlation showed the R^2 value of 0,97. However, dividing the groups to only the Ashfield shales, the R^2 value would be 0,99. The N/C correlation of these values (Ashfield combined with the samples mentioned above) would show less significance in this case. The Narrabeen group had a N/K correlation value of 0,97, and N/C value of 0,85. The mountains (Banks and Wilson) combined with Lithgow and Sunny Corner gave the N/K correlation = 0,72 and N/C = 0,86. In conclusion, the more similar and closer in sedimentary environment the rock groups are, the higher the N/K correlation.

There was however no significant N/N correlation between rocks and plants (analysis of plant leaves) that came from the same source in theory, and was therefore excluded from further investigation.

6. Acknowledgement

Thank you to Johanna Pihlblad, Western Sydney University and John Turner, Forsci Pty. Ltd for assistance in the field; to Elena Belousova, Macquaire University for advice on the geological locations; and thank you to Louise C. Andresen for the continuous support and patience from start to finish.

7. References

Aitchison, J.C., Flood, P.G. & Spiller, F.C.P. (1992). *Tectonic setting and palaeoenvironment of terranes in the southern New England Orogen, eastern Australia as constrained by radiolarian biostratigraphy.* Palaeogeography, Palaeoclimatology, Palaeoecology, 94, 31-54.

Baligar, V.C., Fageria, N.K. & He, Z.L. (2001). *Nutrient use efficiency in plants*. Communications in Soil Science and Plant Analysis. 32:921-950.

Bebout, G.E. & Fogel, M.L. (1992). *Nitrogen-isotope compositions of metasedimentary rocks in the Catalina Schist, California: Implications for metamorphic devolatilization history.* Geochim. Cosmochim. Acta, 56(7), 2839-2849.

Bebout, G.E., Cooper, D.C., Bradley, A.D. & Sadofsky, S.J. (1999). *Nitrogen-isotope record of fluid-rock interactions in the Skiddaw Aureole and granite.* English Lake District, Am. Mineral., 84(10), 1495-1505.

Boudou, J.P., Schimmelmann, A., Ader, M., Mastalerz, M., Sebilo, M. & Gengembre, L. (2008). *Organic nitrogen chemistry during low-grade metamorphism.* Geochim. Cosmochim. Acta, 72(4), 1199-1221.

Brady, N.C. & Weil, R.R. (2008). *The nature and properties of soil, 14 ed*. Prentice-Hall, Upper Saddle River, New Jersey.

Branagan, D.F. & Packham, G.H. (2000). *Field geology of New South Wales (3rd edition).* Department of Mineral Resources, Sydney, 418 pp.

Bryan, J.H., ed. (1966). *Geological map of Australia, sheet 56-5 (Sydney).* N.S.W. Geol. Surv., scale 1 : 250.000.

Busigny, V. & Bebout, G.E. (2003). *Nitrogen in the silicate Earth: Speciation and isotopic behavior during mineral-fluid interactions.* Elements, 9(5), 353-358.

Byrnes, J.G. (1973). *Phosphate in the Ashfield Shale.* Rep. geol. Surv. N.S.W., GS 1975/319 (unpubl.).

Calver, C.R. & Walters, M.R. (2000). *The Late Neoproterozoic Grassy Group of King Island, Tasmania: correlation and palaeogeographic significance.* Precambrian Research, 100, 299-312.

Cawood, P.A. & Flood, R.H. (1989). *Geochemical character and tectonic significance of Early Devonian keratophyres in the New England Fold Belt, eastern Australia.* Australian Journal of Earth Sciences, 36, 297-311.

Chadwick, O.A., Derry, L.A., Vitousek, P.M., Huebert, B.J. & Hedin, L.O. (1999). *Changing sources of nutrients during four million years of ecosystem development.* Nature **397**, 491-497. https://doi.org/10.1038/17276.

Chappell, B.W. & White, A.J.R. (1974). *Two contrasting granite types.* Pacific Geology, 8, 173-174.

Collins, W.J. (2002). *Nature of extensional accretionary orogens.* Tectonics, 21, 10.1029/ 2000TC001272 001276.001271-001276.001279.

Colquhoun, G., Cameron, R., Meakin S., Hendrickx, M. & Vassallo, J. (2004). *Stratigraphy and structure of the Cargelligo region, central Lachlan Orogen, NSW*. Abstracts of the Geological Society of Australia, 73, 150.

Colquhoun, G.P., Hughes K.S., Deyssing, L., Ballard J.C., Phillips G., Troedson A.L., Folkes C.B. & Fitzherbert J.A. (2018). *New South Wales Seamless Geology dataset*, version 1 [Digital Dataset]. Geological Survey of New South Wales, NSW Department of Planning and Environment, Maitland. Accessed 14 June 2019, from https://search.geoscience.nsw.gov.au/product/9232.

Compton, J.S., Williams, L.B. & Ferrell, R.E. (1992). *Mineralization of organogenic ammonium in the Monterey Formation, Santa-Maria basin and San-Joaquin basin, California, USA.* Geochim, Cosmochim, Acta, 56(5), 1979-1991.

Cooper, RF. & Tuckwell, K.D. (1971). *The Upper PreCambrian Adelaidean of the Broken Hill area - a new subdivision.* Quarterly Notes of the Geological Survey of New South Wales, 3, 8-16.

Crawford, A.J., Cameron, W.E. & Keays, R.R. (1984). *The association boninite low-Ti andesitetholeiite in the Heathcote greenstone belt, Victoria; ensimatic setting for the early Lachlan Fold Belt*. Australian Journal of Earth Sciences, 31, 161-174.

Crawford, A.J. (1988). *Cambrian*. In: Douglas, J.G. & Ferguson, J.A. (eds) *Geology of Victoria*, 2nd edition. Geological Society of Australia, Victorian Division, Melbourne, 37--62.

Crawford, A.J. & Berry, R.F. (1992). *Tectonic implications of Late Proterozoic-early Palaeozoic igneous rock associations in western Tasmania*. Tectonophysics, 214, 37-56.

Crawford, A.J., Meffre, S. & Symonds, P.A. (2003). *120 to 0 Ma tectonic evolution of the southwest Pacific and analogous geological evolution of the 600 to 220 Ma Tasman Fold Belt System.* In: HILLIS, R.R. & MOLLER, R.D. (eds) Evolution and Dynamics of the Australian Plate. Geological Society of Australia, Special Publications, 22 and Geological Society of America Special Paper, 372, 383-4O3.

Crook, K.A.W. (1979). *Tectonic implications of some field relationships of the Adelaidean Cooee Dolerite, Tasmania.* Journal of the Geological Society of Australia, 26, 353-361.

Crook, K.A.W. (1980). *Fore-arc evolution in the Tasman Geosyncline: the origin of southeast Australian continental crust.* Journal of the Geological Society of Australia, 27, 215-232.

Dadd, K.A. (1992). *The Middle to Late Devonian Eden-Comerong-Yalwal Volcanic Zone of southeastern Australia: an ancient analogue of the Yellowstone-Snake River Plain region of the USA.* Tectonophysics, 214, 277-291.

Dahlgren, R. (1994). Soil *Acidification and Nitrogen Saturation from Weathering of Ammonium-bearing Rock*. Nature. 368. 838-841. 10.1038/368838a0.

Danis, C. (2012). *The Thermal Structure of The Sydney Gunnedah Bowen Basin Eastern Australia*. Unpublished Phd Thesis, Macquarie University.

Direen, N.G. & Crawford, A.J. (2003). *Fossil seaward dipping reflector sequences preserved in southeastern Australia.* Journal of the Geological Society, London, 160, 985-990.

Dolanski, J. (1973). *X-ray identification of clay mounts from Wianamatta shale core.* Rep. Geol. Surv, New South Wales, GS 1971/757 (unpubl.).

Donnelly, T.W., Pritchard, R.A., Emmermann, R. & Puchelt, H. (1979a). *The aging of oceanic crust: synthesis of the mineralogical and chemical results of Deep Sea Drilling Project, Legs 51 through 53, Initial Rep*. Deep Sea Drill. Proj., 51 – 53, 1563 – 1577.

Donnelly, T.W., Thompson, G. & Robinson, P.T. (1979b). *Very-lowtemperature hydrothermal alteration of the oceanic crust and the problem of fluxes of potassium and magnesium, in Deep Drilling Results in the Atlantic Ocean: Ocean Crust, Maurice Ewing Ser.,* vol. 2, edited by M. Talwani, C. G. A. Harrison, and D. E. Hayes, pp. 369 – 382, AGU, Washington, D.C.

Downes, Peter & Pogson, Denis & Nix, L & Robson, David & Sherwin, Lawrence. (2004). *World-class mineral deposits of the Lachlan Orogen, New South Wales — Australia.* ASEG2004 Excursion Guide. 10.13140/RG.2.1.2892.9368.

Durr, H.H., Meybeck, M. & Durr, S.H. (2005). *Lithologic composition of the Earth's continental surfaces derived from a new digital map emphasizing riverine material transfer.* Global Biogeochem. Cycles, 19, GB4S10, doi:10.1029/2005GB002515.

Dynarski, Katherine & Morford, Scott & Mitchell, Scott & Houlton, Benjamin. (2019). *Bedrock Nitrogen Weathering Stimulates Biological Nitrogen Fixation*. The Bulletin of the Ecological Society of America. 100. e01562. 10.1002/bes2.1562.

Fergusson, C.L. (1998). *Cambrian-Silurian oceanic rocks, upper Howqua River, eastern Victoria: tectonic implications.* Australian Journal of Earth Sciences, 45, 633-644.

Follett, R. & Murphy, L. & Donahue, R.. (1981). *Fertilizers and Soil Amendments*.

Ghafoori, M., Airey, D. & Carter, J. (1994). *The Durability of Ashfield Shale.* 3315-3321.

Glen, R.A. (1992). *Thrust, extensional and strike-slip tectonics in an evolving Palaeozoic orogen - a structural synthesis of the Lachlan Orogen of southeastern Australia.* Tectonophysics, 214, 341-380.

Glen, R.A.. (2004). *Plate tectonics of the Lachlan Orogen: a framework for understanding its metallogenesis*. Abstracts of the Geological Society of Australia, 74, 33-36.

Glen, R.A.. (2005). The Tasmanides of eastern Australia. Geological Society, London, Special Publications. 246. 23-96. 10.1144/GSL.SP.2005.246.01.02.

Goldbery, R. (1969). *Geology of the Western Blue Mountains.* 20 ed. Sydney: Geological Survey of New South Wales.

Goldblatt, C.M., Claire, W., Lenton, T.M., Matthews, A.J., Watson, A.J. & Zahnle, K.J. (2009). *Nitrogen-enhanced greenhouse warming on early Earth.* Nat. Geosci., 2(12), 891-896.

Gray, D.R. & Willman, C.E. (1991). *Deformation in the Ballarat Slate Belt, central Victoria, and implications for crustal structure across southeast Australia*. Australian Journal of Earth Sciences, 38, 171-201.

Hart, S.R. (1969). *K, Rb, Cs contents, and K/Rb, K/Cs ratios of fresh and altered submarine basalts*. Earth Planet. Sci. Lett., 6, 295 – 303.

Hart, S.R., Erlank, A.J. & Kable, E.J.D. (1974). *Sea floor basalt alteration: some chemical and Sr isotopic effects.* Contrib. Mineral. Petrol., 44, 219 – 230.

Helby, R. (1973). *Review of Late Permian and Triassic palynology of New South Wales*. Geol. Soc. Aust., Spec. Publ., 4, 141-155.

Herbert, C. (1979). *The geology and resource potential of the Wianamatta Group.* Bull. geol. Surv. NSW., 25, 203 pp.

Herbert, C. & Helby, R. (Editors). (1980). *A guide to the Sydney Basin. Geological Survey of New South Wales Bulletin 26*, Bulletin No. 26. Department of Mineral Resources, New South Wales.

Hobart, M.K., PhD. (2005a). *Shale is the most abundant sedimentary rock and is in sedimentary basins worldwide*. Geology and Earth Science News and Information. Retrieved June 24, 2022, from https://geology.com/rocks/shale.shtml

Hobart, M.K., PhD. (2005b). *A clastic sedimentary rock composed of silt-sized grains*. Geology and Earth Science News and Information. Retrieved June 24, 2022, from https://geology.com/rocks/siltstone.shtml

Hobart, M.K., PhD. (2005c). *A foliated metamorphic rock that contains abundant platy mineral grains*. Geology and Earth Science News and Information. Retrieved June 24, 2022, from https://geology.com/rocks/schist.shtml

Hobart, M.K., PhD. (2005d). *What Is Basalt, How does It Form, and How Is It Used?* Geology and Earth Science News and Information. Retrieved June 24, 2022, from https://geology.com/rocks/basalt.shtml

Hobart, M.K., PhD. (2005e). *A clastic sedimentary rock composed of sand-sized grains of mineral, rock, or organic material.* Geology and Earth Science News and Information. Retrieved June 24, 2022, from https://geology.com/rocks/sandstone.shtml

Holloway, J. & Dahlgren R. (2002). Nitrogen in rock: Occurrences and biogeochemical implications. Global Biogeochemical Cycles. 16. 65-1.

Holm, O.H., Crawford, AJ. & Berry R.F. (2003). *Geochemistry and tectonic setting of rectaigneous rocks in the Arthur Lineament and surrounding area, northwest Tasmania.* Australian Journal of Earth Sciences, 50, 903-918.

Houlton, B. & Morford, S.. (2015). *A new synthesis for terrestrial nitrogen inputs*. SOIL. 1. 381-397. 10.5194/soil-1-381-2015.

li, Shilei & Beard, Brian & Raymo, Maureen & Wang, Xiaomin & Chen, Yang & Chen, Jun. (2019). *K isotopes as a tracer for continental weathering and geological K cycling*. Proceedings of the National Academy of Sciences. 116. 10.1073/pnas.1811282116.

Ishiga, H., Leitch, E.C., Watanabe, Z., Naka, T. & Iwasaki, M. (1988). *Radiolarian and conodont biostratigraphy of siliceous rocks from the New England Fold Belt.* Australian Journal of Earth Sciences, 35, 73-80.

Jarrard, Richard. (2003). *Subduction Fluxes of Water, Carbon Dioxide, Chlorine, and Potassium.* Geochemistry Geophysics Geosystems - GEOCHEM GEOPHYS GEOSYST. 4. 10.1029/2002GC000392.

Jochum, K. P., Nohl, U., Herwig, K., Lammel, E., Stoll, B. & Hofmann, A. W. (2007). *GeoReM: A New Geochemical Database for Reference Materials and Isotopic Standards.* https://doi.org/10.1111/j.1751-908X.2005.tb00904.x

Jones, B.G., Fergusson, C.L. & Zambelli, P.F. (1993). *Ordovician contourites in the Lachlan Fold Belt, eastern Australia.* Sedimentary Geology, 82, 257-270.

Kaiser & Rosen. (2018). *Potassium for crop production*. University of Minnesota Extension, retrieved 24 August 2020, from https://extension.umn.edu/phosphorus-and-potassium/potassium-crop-production.

Karro, E. (1999). *Quality of bedrock groundwater in western Finland, with special reference to nitrogen compounds*. Bulletin of the Geological Society of Finland. 71. 243-251. 10.17741/bgsf/71.2.003.

Laakso, Thomas & Sperling, Erik & Johnston, David & Knoll, Andrew. (2020). *Ediacaran reorganization of the marine phosphorus cycle.* Proceedings of the National Academy of Sciences. 117. 201916738. 10.1073/pnas.1916738117.

Lassack, E.V. & Golding, H.G. (1967). *Phosphatic bands in Narrabeen sediments.* Aust. J. Sci., 29(7), 223-224.

Leitch, E.C. (1974). *The geological development of the southern part of the New England Fold Belt.* Journal of the Geological Society of Australia, 21, 133-156.

Loughnan, F.C. (1960). *The origin, mineralogy and some physical properties of the commercial clays of New South Wales.* University of New South Wales, Geological Series, 2, 348 p.

Lovering, J.F. (1954). *The stratigraphy of the Wianamatta Group Triassic System, Sydney Basin.* Records of the Australian Museum 23(4): 169–210, plate xii. [25 June 1954].

Malavolta, E. (1985). *Potassium status of tropical and subtropical region soils. p. 163-200*. In R.D. Munson (ed.) *Potassium in agriculture*. American Society of Agronomy, Madison, WI.

McIlveen, G.R. (1974). *The Eden-Comerong-Yalwal Rift zone and the contained gold mineralisation*. Geological Survey of New South Wales Bulletin, 16, 245-277.

Mclaren, L. (n.d.). *Geology of the Blue Mountains*. GEOS 272 - Research Report.

McVicar TR, Pinetown KL, Hodgkinson JH, Barrow OV, Rachakonda PK, Zhang YQ, Dawers WR, Macfarlane C, Holland KL, Marvanek SP, Wilkes PG, Li LT & Van Niel TG. (2015). *Context statement for the Hunter subregion. Product 1.1 for the Hunter subregion from the Northern Sydney Basin Bioregional Assessment.* Department of the Environment, Bureau of Meteorology, CSIRO and Geoscience Australia, Australia.

Misra, K. C. (2012). *Introduction to geochemistry.* John Wiley & Sons.

Monroe, M.H. (2011). *Australia: The Land Where Time Began. [Accessed 01-09-2016, by Mclaren, L. (n.d.)].* https://austhrutime.com/sydney_basin.htm

Morford, Scott & Houlton, Benjamin & Dahlgren, Randy. (2016). *Geochemical and tectonic uplift controls on rock nitrogen inputs across terrestrial ecosystems. Global Biogeochemical Cycles.* 30. n/a-n/a. 10.1002/2015GB005283.

Murray, C.G. (1994). *Basement cores from the Tasman Fold Belt System beneath the Great Artesian Basin in Queensland.* Geological record, Queensland Department of Minerals And Energy, 1994/10.

O'Neill, C., & Danis C. (2013). *Background paper on Coal Seam Gas: the geological characteristics and history of NSW with a focus on coal seam gas (CSG) resources.* ARC Centre for Core to Crust Fluid Systems.

Offler, Robin. (1984). *Geology and ore genesis of silver-lead-zinc-copper sulphide deposits, Sunny Corner, NSW..* Australasian Institute of Mining and Metallurgy, proceedings. 51-57.

Offler, R. & Gamble, J. (2002). *Evolution of an intraoceanic island arc during the Late Silurian to Late Devonian, New England Fold Belt.* Australian Journal of Earth Sciences, 49, 349-366.

Olympus NDT (2012). *DELTA Family Handheld XRF Analyzers User's Manual*. International edition, Revision B. 48 Woerd Avenue, Waltham, MA 02453, USA. 103201-01EN.

Pickett, J. & Adler, J. (1997). *Layers of Time:the Blue Mountains and their Geology. 1st ed. Sydney:* New South Wales Department of Mineral Resources.

Powell, C.M. (1984). (h) *Late Devonian and early Carboniferous: continental magmatic arc along the eastern edge of the Lachlan Fold belt*. In: Veevers, J.J. (ed.) *Phanerozoic Earth History of Australia*. Oxford Science Publications, Oxford, 329-240.

Prothero, D.R. & Schwab, F. (2013). *Sedimentary Geology*. 3rd ed. New York: W. H. Freeman and Company, pp.9-12, 549.

Raymond, O.L. (1996). *The Dulladerry Volcanics Middle Devonian A-type volcanics from central-west New South Wales*. Abstracts of the Geological Society of Australia, 41, 359.

Reinhard, Christopher & Planavsky, Noah & Olson, Stephanie & Lyons, Timothy & Erwin, Douglas. (2016). *Earth's oxygen cycle and the evolution of animal life.* Proceedings of the National Academy of Sciences. 113. 201521544. 10.1073/pnas.1521544113.

Richardson, J.B., Dr. (2018). *Why should we care about quartz?:* National Critical Zone Observatory. Retrieved February 15, 2021, from https://czo-archive.criticalzone.org/national/blogs/post/why-should-we-care-about-quartz/

Rietra, Rene & Heinen, Marius & Dimkpa, Christian & Bindraban, P.S.. (2017). *Effects of Nutrient Antagonism and Synergism on Yield and Fertilizer Use Efficiency*. Communications in Soil Science and Plant Analysis. 48. 1895-1920. 10.1080/00103624.2017.1407429.

Rutland, R.W.R. (1976). *Orogenic evolution of Australia.* Earth Science Reviews, 12, 161-196.

Sadofsky, S.J. & Bebout, G.E. (2003). *Record of forearc devolatilization in low-T, high-P/T metasedimentary suites: Significance for models of convergent margin chemical cycling.* Geochem. Geophys. Geosyst., 4(4), 9003, doi:10.1029/2002GC000412.

Scheibner, E. (1973). *A plate tectonic model of the Palaeozoic tectonic history of New South Wales*. Journal of the Geological Society of Australia, 20, 405-426.

Scheibner, E. & Veevers, J.J. (2000). *Tasman Fold Belt System. Billion-year earth history of Australia and neighbours in Gondwanaland*. In: Veevers, J.J. (ed.) *Billion-year earth history of Australia and neighbours in Gondwanaland*. GEMOC Press, Sydney, 154-234.

Singh, B. & Schulze, D.G. (2015). *Soil Minerals and Plant Nutrition*. Nature Education Knowledge, 6, 1-10.

Slansky, E. (1973). *Clay mineral identification in Ashfield shale from the Maroota area*. Rep. Geological Survey of New South Wales, GS 1973/396 (unpubl.).

Sparks, D.L.. (2001). *Dynamics of K in soil and their role in management of K nutrition.* Proceeding international symposium on role of potassium in nutrient management for sustainable crop production. 79-101.

Stevenson, F.J. (1962). *Chemical state of nitrogen in rocks*. Geochimica et Cosmochimica Acta. 26. 797-809. 10.1016/0016-7037(62)90040-6.

Stevenson, F.J. & Cole, M.A. (1999). *Cycles of Soil (Carbon, Nitrogen Phosphorus Sulfur, Micronutrients).* John Wiley and Sons Publishers, Hoboken, 427 p.

Stewart, I.R. & Glen, R.A. (1991). *New Cambrian and Early Ordovician ages from the New South Wales south coast.* Quarterly Notes of the Geological Survey of New South Wales, 85, 1-8.

Thomas, O.D., Johnston, A.J., Scott, M.M., Pogson, D.J., Sherwin, T. & MacRae, G.P. (2002). *Goulburn 1:100 000 Geological Sheet 8828, First Edition.* Geological Survey of New South Wales, Orange and Sydney.

Thummanatsakun, V. & Yampracha, S. (2018). *Effects of interaction between nitrogen and potassium on the growth and yield of cassava*. International Journal of Agricultural Technology. 14. 2137-2150.

Turner, N.J., Bottrill, R.S., Crawford, A.J. & Villa, I. (1992). *Geology and prospectivity of the Arthur Mobile Belt*. Bulletin of the Geological Survey of Tasmania, 70, 227-233.

Turner, N.J., Black, L.R. & Kamperman, M. (1998). *Dating of Neoproterozoic and Cambrian orogenies in Tasmania.* Australian Journal of Earth Sciences, 45, 789-806.

Van der Beek, Peter & Pulford, Anna & Braun, Jean. (2001). *Cenozoic Landscape Development in the Blue Mountains (SE Australia): Lithological and Tectonic Controls on Rifted Margin Morphology*. Journal of Geology - J GEOL. 109. 35-56. 10.1086/317963.

VandenBerg, A.H.M. (1981). *A complete Ordovician graptolitic sequence at Mountain Creek near Deddick, eastern Victoria*. Geological Survey of Victoria, Melbourne. Report 1981/81.

VandenBerg, A.H.M., Nott, R.J. & Glen, R.A. (1992). *Bendoc 1:100 000 map geological report.* Geological Survey of Victoria, Melbourne, Report 90.

VandenBerg, A.H.M. & Stewart, I.R. (1992). *Ordovician terranes of southeastern Lachlan Fold Belt: stratigraphy, structure and palaeogeographic reconstruction.* Tectonophysics, 214, 177-192.

VandenBerg, A.H.M., Willman, C.E. & Maher, S.E.A. (2000). *The Tasman Fold Belt System in Victoria. Geology and Mineralisation of Proterozoic to Carboniferous rocks.* Geological Survey of Victoria, Melbourne, Special Publication.

Veevers, J.J., Conaghan, P.J. & Powell, C. McA. (1994). *Eastern Australia*. In: Veevers, J.J. & Powell, C. McA. (eds) *Permian-Triassic Basins and Foldbelts Along the Panthalassan Margin of Gondwanaland.* Memoir of the Geological Society of America, 184, 11-171.

Williams, L.B., Wilcoxon, B.R., Ferrell, R.E. & Sassen, R. (1992). *Diagenesis of ammonium during hydrocarbon maturation and migration.* Wilcox-Group, Louisiana, Appl. Geochem., 7(2), 123-134.

Williams, I.S. & Chappell, B.W. (1998). *Crustal evolution in southeastern Australia: a zircon viewpoint. The Bruce Chappell Symposium: granites, island arcs, the Mantle and ore deposits.* Record of the Australian Geological Survey Organisation, 1998/33, 44.

Wyborn, D. & Owen, M. (1986). *Araluen New South Wales. 1:100000 Geological map commentary.* Bureau of Mineral Resources, Canberra.

Zhang, Qing & Buckman, Solomon & Bennett, V.C. & Nutman, Allen & Song, Y.. (2019). *Lachlan Orogen, Eastern Australia: Triangle Formation Records the Late Ordovician Arrival of the Macquarie Arc Terrane at the Margin of Eastern Gondwana*. Tectonics. 38. 10.1029/2019TC005480.

8. Appendix

Appendix A

Locations mapped out using coordinate tool in ArcMap GIS − listed in alphabetical order:

Australian Botanical Garden	-34.068726, 150.771943
Bilpin	-33.434324, 150.593335
Bradbury	-34.088452, 150.805719
Kurrajong Heights	-33.541091, 150.632800
Leumeah Road	-34.051973, 150.848549
Lithgow (50)*	-33.446875, 150.061355
Lithgow (55, 59)*	-33.446634, 150.057518
Mount Banks	-33.586825, 150.369706
Mount Wilson	-33.501734, 150.367896
Mulgoa National Park	-33.795283, 150.662388
Narrabeen	-33.702277, 151.309136
Sunny Corner (66)*	-33.240320, 149.553210
Sunny Corner (69)*	-33.244830, 149.512080

**Samples are apart from each other.*

Appendix B

Table 3. *List of collected samples from Triassic to Silurian.*

Sample (#)	Age (Ma)	Location	Rock Type	Texture
22	251,9 - 237 Triassic	Narrabeen	Devonian Shale *(0,3 - 0,4 m)	Thinner and thicker layers (black and grey colored), medium hard, sorted and silty, no cracks or weathering. Color: Black, gray.
17	251,9 - 237 Triassic	Narrabeen	Shale *(1,2 m)	Layers, fissility, smooth surface, angular edges, shallow cracks and weathering, very sorted. Color: Dark brown, black, black-gray, red.
21 (1)	251,9 - 237 Triassic	Narrabeen	Shale *(1,7 m)	Layers, fissility, smooth surface, angular edges, shallow cracks and weathering, very sorted. Color: Dark brown, black, black-gray, red.
21 (2)	251,9 - 237 Triassic	Narrabeen	Shale *(1,7 m)	Layers, fissility, smooth surface, angular edges, shallow cracks and weathering, very sorted. Color: Dark brown, black, black-gray, red.
25	251,9 - 237 Triassic	Narrabeen	Devonian Shale *(3 m)	Laminated, smooth surface, no cracks, little to no weathering, siltstone, medium hard. Color: Black, gray, dark red/purple, brown.
23	251,9 - 237 Triassic	Narrabeen	Sandstone/ Siltstone *(6 m)	Laminated, silty, angular, micas, soft surface, sand streak inside (red-pink colored - K-feldspar), poorly sorted. Color: White, gray, beige.
27	251,9 - 237 Triassic	Narrabeen	Sandstone *(7-8 m)	Sandy, medium sand, subangular grains, some quartz, silty, poorly sorted, cracks (red/brown - Fe), spots and streaks of black sand grains. Color: White/beige
36-45 (1-5) Black	251,9 - 237 Triassic	Leumeah Road	Ashfield Shale/ Wiannamatta Shale	Thick, solid, smooth surface, hard, shallow weathering, no cracks. Color: Black, white/ gray spots.
36-45 (1-5) Brown	251,9 - 237 Triassic	Leumeah Road	Ashfield Shale/ Wiannamatta Shale	Laminated, smooth surface, silty texture, weathered, surface can be scratched, some cracks (minimal), sorted. Color: Brown, black, orange, pale.
30-32 (1)	251,9 - 237 Triassic	Bradbury	Ashfield Shale/ Wiannamatta Shale	Smooth surface, laminated, minor cracks, siltstone (shale), sorted, little to no weathering, medium hard, pale color. Color: Brown, black, red-purple.
30-32 (2)	251,9 - 237 Triassic	Bradbury	Ashfield Shale/ Wiannamatta Shale	Smooth surface, laminated, minor cracks, siltstone (shale), sorted, little to no weathering, medium hard, pale color. Color: Brown, black, red-purple.
30-32 (3)	251,9 - 237 Triassic	Bradbury	Ashfield Shale/ Wiannamatta Shale	Smooth surface, laminated, minor cracks, siltstone (shale),sorted, little to no weathering, medium hard, pale color. Color: Brown, black, red-purple.
30-32 (4)	251,9 - 237 Triassic	Bradbury	Ashfield Shale/ Wiannamatta Shale	Smooth surface, laminated, minor cracks, siltstone (shale), sorted, little to no weathering, medium hard, pale color. Color: Brown, black, red-purple.
33	251,9 - 237 Triassic	Australian Botanical Garden	Claystone/Ash-field Shale/ Minchinbury Sandstone	No particular shape, asymmetrical, clay, silt, ooid shapes inside (inside ooid; beige/yellow - followed by an enclosing thick line; brown - outside line; reddish/brown - all around the rock), mostly clay (moderately sorted), some cracks. Color: Yellow, white, orange, gray, red, brown, black
5	251,9 - 237 Triassic	Mulgoa National Park	Schist	Laminated, subangular, medium sorted, siltstone, few cracks, shallow weathering. Color: Black, gray, dark red/purple.
12	251,9 - 237 Triassic	Kurrajong Heights	Hawkesbury Sandstone	Smooth surface, laminated, angular, black micas, wavy ripples, sandy, sorted, few cracks, surface weathering. Divided in two layers of color: White/beige (4,5 mm) - Red, white (10,5 mm).
29	251,9 - 237 Triassic	Kurrajong Heights	Sandstone	Cracks, coarse sand, easily scratched and easy to crumble. Color: White, gray, some black sand grains.

** = Height in the Narrabeen stratigraphy*

Table 3 (cont.). *List of collected samples from Triassic to Silurian.*

Sample (#)	Age (Ma)	Location	Rock Type	Texture
71	251,9 - 237 Triassic	Bilpin	Trias Shale	Laminated, smooth surface, fine sand, white-beige area contains P/K, dark brown area contain only K, well sorted, sharp edges, dark and light lamination. Color: White, beige, brown, light yellow.
72	251,9 - 237 Triassic	Bilpin	Trias Shale	Laminated, smooth surface, silty texture, cracks, sharp edges, some layers are sticking out, well sorted, ripples (in the white area). Color: White, red, brown.
73	251,9 - 237 Triassic	Bilpin	Trias Shale	Laminated, easily cracked, sandy/silty texture, hard, minerals, poorly sorted, shallow weathering. Color: Brown, gray, beige, pale.
1	358,9 - 298,9 Carboniferous	Mt Wilson	Basalt	Angular, smooth on surface, sharp edges, weathered surface (brown/reddish hue), hard, thin cracks. Color: Gray, brown-red, black, blue.
10	358,9 - 298,9 Carboniferous	Mt Banks	Basalt	Opaque minerals (few), angular, sandy, shallow and thin/fine cracks, hard, weathered (chemically) in cracks, sorted. Color: Brown, blue, black-gray.
50	382,7 - 346,7 Devonian	Lithgow	Devonian Shale	Some epidote, sharp edges, medium hard, shallow weathering, sorted, soft surface, minor/thin cracks. Color: Black, gray.
55	382,7 - 346,7 Devonian	Lithgow	Devonian Shale	Medium sand, subrounded, sandstone, poorly sorted, weathered, cracks, laminated. Color: White, beige, orange, pale.
59	382,7 - 346,7 Devonian	Lithgow	Devonian Shale	Orientation of cracks (2 different orientations), fine sand texture, surface weathering. Color: Red, yellow.
66	427,4 - 419,2 Silurian	Sunny Corner	Silurian Shale	Different cuts, mixed, smooth surface, poorly sorted, clay/silt - mixed, deep cracks, weathered. Color: Yellow, red, brown.
69	427,4 - 419,2 Silurian	Sunny Corner	Silurian Shale/ Sandstone	Similar to calcite/marble, fine/medium sand, sandy surface, well sorted, minor cracks, well sorted, sandstone. Color: White, beige, brown, light yellow.

Appendix C

Table 4. *Wash procedures for the rocks.*

Sample	Rock Type	Location	Wash Procedure
1	Basalt	Mount Wilson	Hydrogen-peroxide boiling
5	Schist	Mulgoa National Park	Distilled water wash
10	Basalt	Mount Banks	Distilled water wash
12	Sandstone	Kurrajong Heights	Distilled water wash
17	Shale	Narrabeen	Hydrogen-peroxide boiling
21 (1-2)	Shale	Narrabeen	Hydrogen-peroxide boiling
22	Devonian Shale	Narrabeen	Distilled water wash
23	Siltstone	Narrabeen	Distilled water wash
25	Devonian Shale	Narrabeen	Distilled water wash
27	Sandstone	Narrabeen	Distilled water wash
29	Sandstone	Kurrajong Heights	Distilled water wash
30-32 (1-4)	Ashfield Shale	Bradbury	Hydrogen-peroxide boiling
33	Claystone	Australian Botanical Garden	Distilled water wash
36-45 (Brown)	Ashfield Shale	Leumeah Road	Hydrogen-peroxide boiling
36-45 (Black)	Ashfield Shale	Leumeah Road	Hydrogen-peroxide boiling
50	Devonian Shale	Lithgow	Distilled water wash
55	Devonian Shale	Lithgow	Distilled water wash
59	Devonian Shale	Lithgow	Distilled water wash
66	Silurian Shale	Sunny Corner	Distilled water wash
69	Silurian Shale	Sunny Corner	Distilled water wash
71	Triassic Shale	Bilpin	Distilled water wash
72	Triassic Shale	Bilpin	Distilled water wash
73	Triassic Shale	Bilpin	Distilled water wash

Appendix D

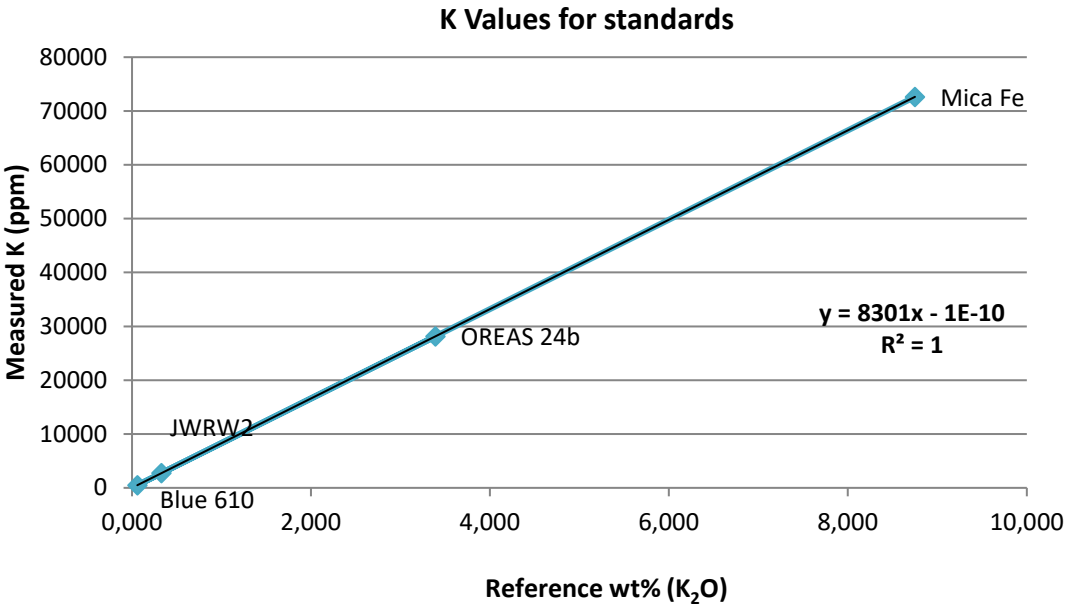

Figure 39. Reference values of potassium (K), using standards from GeoReM (Jochum, K.P., et al., 2007).

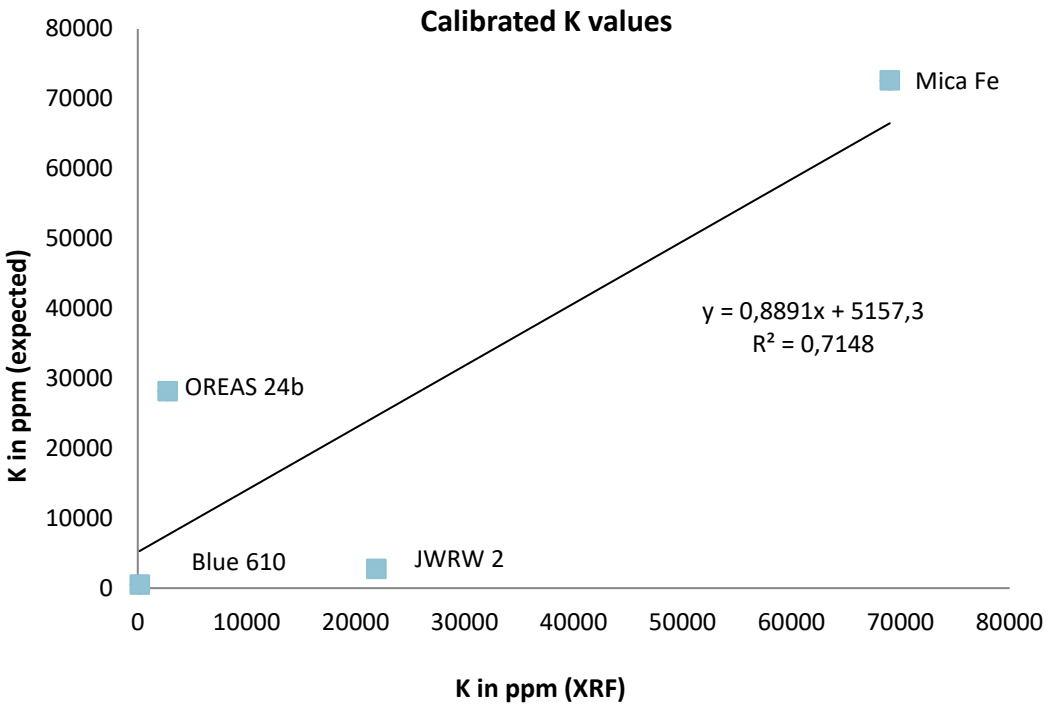

Figure 40. Calibration curve for potassium (K), using standards from GeoReM (Jochum, K.P., et al., 2007).

Table 5. *Reference values for K in different standards.*

Measured samples	Reference (K_2O Wt %)	Reference (K in ppm)	wt%	ppm
Mica Fe A2	8,750		8,750	72634
Blue 610	0,059		0,059	490
JWRW 2	-	-	-	-
OREAS 24 b	3,390		3,390	28140

Table 6. *Reference, measured and calibrated values of potassium (K).*

	Ref. - ppm	Meas. - ppm	Calibrated ppm	Difference
Mica Fe	72634	68998	73119	-0,7%
Blue 610	490	166	12953	-96,2%
JWRW 2		2731	15195	-82,0%
OREAS 24b	28140	21865	31920	-11,8%

Appendix E

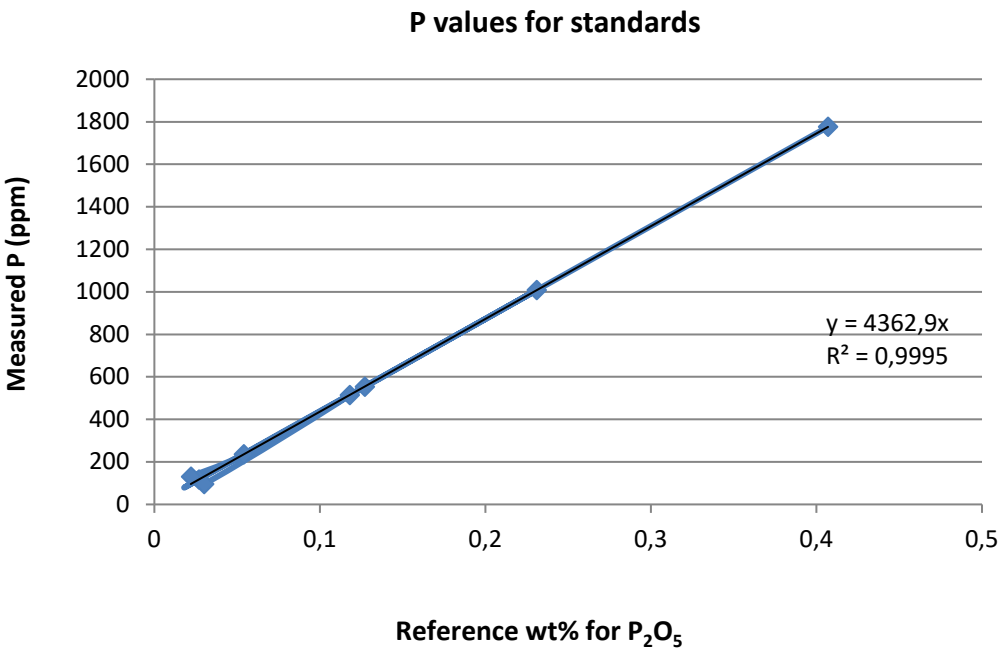

Figure 41. Reference values of phosphorus (P), using standards from GeoReM (Jochum, K.P., et al., 2007).

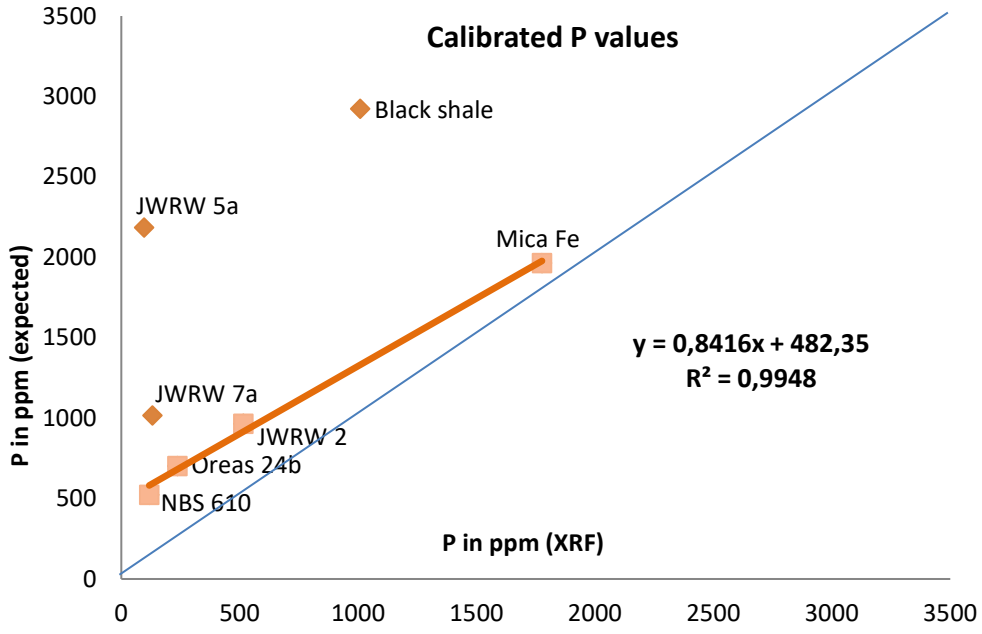

Figure 42. Calibration curve for phosphorus (P), using standards from GeoReM (Jochum, K.P., et al., 2007).

Table 7. *Reference values for P in different standards.*

Sample (References)	Reference (P_2O_5 Wt %)	Reference (P in ppm)	wt%	ppm
Mica Fe A2	0,450		0,450	1964
Blue 610	0,120	~400	0,120	524
Transparent 612	0,01-0,02	~50	0,010	44
FK-N A3	0,024		0,024	105
JWRW 2		965	0,221	965
JWRW 5a		2186	0,501	2186
JWRW 7a		1016	0,233	1016
OREAS 24 b	0,161		0,161	703
Black shale	0,670		0,670	2924

Table 8. *Reference, measured and calibrated values of phosphorus (P).*

	Ref. - ppm	Meas. - ppm	Calibrated ppm	Difference
Mica Fe	1964	1776	1977	-0,7%
Blue 610	524	118	582	-9,9%
JWRW 2	965	515	916	5,4%
OREAS 24b	703	236	681	3,2%

Appendix F

Table 9. *All samples and their nutrient content (alphabetical order), as shown in results (see figures 21 - 23).*

Region/Site	ppm (P)	ppm (K)	N (%)	C (%)
ABG-Clay	7948	9185	0,065	0,45
BB-Ash	566	17290	0,068	0,797
BPTri-Sh	1290	10272	0,032	0,331
KJHSa	0	9803	0,018	0,062
LG-DevSh	0	17684	0,007	0,032
LMR-AshBl	29195	12864	0,039	0,615
LMR-AshR	385	18395	0,072	0,712
MNP-Sch	2469	11140	0,031	5,494
MtB-Ba	2681	12304	0,002	0,092
MtW-Ba	3294	10997	0,002	0,078
NB22	0	20907	0,047	1,703
NBSa7-8	0	1848	0,002	0,028
NBSh-1-2	667	21701	0,048	1,601
NBSh3	0	9341	0,026	0,287
NBSi-6	0	20520	0,044	0,216
SC-sh	0	12514	0,005	0,028

Table 10. *Phosphorus (P) and potassium (K) measured by XRF and calibrated to a standard for samples, excluding Narrabeen.*

Rock sample	K (ppm) Calibrated	P (ppm) Calibrated
ABG-Clay	20288,837	7759,891
	21340,943	6871,311
	20346,884	7080,605
	21369,967	6974,122
BB-Ash*	27298,040	924,192
	27201,295	702,659
	29095,086	869,115
	28088,934	1336,659
BPTri-Sh*	25629,183	1811,548
	20896,519	2137,421
	15301,612	1293,821
	25317,179	1029,451
KJHSa*	21491,503	ND
	21261,128	
LG-DevSh*	37349,886	ND
	19181,102	
LMR-AshBl	17110,751	40622,650
	25701,742	20614,921
	29344,205	13921,199
LMR-AshR	27660,836	930,312
	31368,603	654,925
	27631,812	834,844

Table 10 (cont.). *Phosphorus (P) and potassium (K) measured by XRF and calibrated to a standard for samples, excluding Narrabeen.*

Rock sample	K (ppm) Calibrated	P (ppm) Calibrated
MNP-Sch	21304,664	2006,154
	25135,781	1870,297
	21776,297	2127,324
	22588,959	5872,577
	21921,416	922,968
MtB-Ba	23053,337	2457,787
	22668,774	2659,737
	26180,631	3137,073
	22349,514	2700,127
MtW-Ba	23038,825	3287,618
	22465,608	3232,541
	21964,951	3104,027
	22211,652	3394,101
SC-sh*	28424,520	ND
	19068,031	

** = More than one sample analyzed; this means that their results are based on the 'mean value' of each rock in that group, instead of measured content per rock. Note the difference in the results in these groups.*

Table 11. *Carbon (C) and nitrogen (N) content measured by IRMS, excluding Narrabeen.*

Sample	C (%)	N (%)
ABG-Clay	0,4485	0,06456
	0,4514	0,06536
	0,4492	0,06482
BB-Ash	0,8237	0,06755
	0,8335	0,06841
	0,8488	0,06919
	0,7814	0,07083
	0,7704	0,07028
	0,7702	0,06937
	0,8282	0,06788
	0,819	0,06827
	0,8135	0,0682
	0,7569	0,06649
	0,7556	0,06744
	0,7648	0,06704
BPTri-Sh	0,2739	0,03607
	0,2936	0,03805
	0,2732	0,03601
	0,2608	0,02301
	0,2793	0,02282
	0,2795	0,02262
	0,4462	0,03588
	0,4406	0,03584
	0,4353	0,03582
KJHSa	0,0815	0,01768
	0,0793	0,0175
	0,0781	0,0173
	0,0443	0,01817
	0,0432	0,01837
	0,0447	0,0189

Sample	C (%)	N (%)
LG-DevSh	0,0217	0,007
	0,0188	0,00602
	0,0159	0,00555
	0,0332	0,01175
	0,031	0,01064
	0,0273	0,01034
	0,0452	0,00315
	0,0499	0,00301
	0,046	0,00276
LMR-AshBl	0,6028	0,03857
	0,6186	0,03843
	0,624	0,03838
LMR-AshR	0,7157	0,07154
	0,7071	0,07185
	0,7121	0,07166
MNP-Sch	5,5097	0,0318
	5,5016	0,03115
	5,4714	0,03135
MtB-Ba	0,0904	0,00163
	0,0953	0,00174
	0,0903	0,00166
MtW-Ba	0,0786	0,00218
	0,0748	0,00229
	0,0792	0,00198
SC-Sh	0,0321	0,00213
	0,034	0,00276
	0,035	0,00275
	0,0217	0,0069
	0,0212	0,00733
	0,0254	0,00759

Appendix G

Table 12. *Narrabeen sequence; phosphorus (P) and potassium (K) measured by XRF and calibrated to a standard.*

Height (rock type #*)	K (ppm) Calibrated	P (ppm) Calibrated
30-40 cm (Devonian Shale 1*)	31608,048	No detection
	32297,358	
	30316,497	
30-40 cm (Devonian Shale 2*)	33784,819	No detection
	28829,036	
	33632,445	
30-40 cm (Devonian Shale 3*)	30098,819	No detection
1,2 m (Shale)	33944,449	1011,092
	33879,146	750,393
	33922,681	1088,200
	34575,712	779,767
1,7 m (Devonian Shale 1*)	31738,654	1058,825
	32210,288	970,702
	29387,741	996,404
	28952,387	878,906
1,7 (Devonian Shale 2*)	30969,528	1337,883
	30265,705	1488,428
	30795,386	915,624
3 m (Shale)	25643,694	No detection
	26391,052	
	15064,586	
	16791,491	
6 m (Devonian Shale)	34902,228	No detection
	31078,367	
	25745,277	
	31252,508	
7-8 m (Sandstone)	16515,767	No detection
	13352,193	
	13402,984	

Table 13. *Narrabeen sequence analysis of nitrogen (N%) and carbon (C%) measured by IRMS elemental analyser, standard material was used and 3 replicates per sample.*

Height (rock #*)	N (%)	C (%)
30-40 cm (Devonian Shale)	0,04592	1,6962
	0,04685	1,7115
	0,04692	1,7027
1,2 m (Shale)	0,04634	1,7396
	0,04628	1,7373
	0,04733	1,7358
1,7 m (Devonian Shale 1*)	0,04774	1,5550
	0,04775	1,5558
	0,04742	1,5504
1,7 (Devonian Shale 2*)	0,04843	1,5163
	0,04901	1,5215
	0,04836	1,4945
3 m (Shale)	0,02537	0,2843
	0,02605	0,2963
	0,02548	0,2815
6 m (Devonian Shale)	0,04289	0,2157
	0,04461	0,2165
	0,04367	0,2154
7-8 m (Sandstone)	0,00130	0,0278
	0,00179	0,0302
	0,00177	0,0274

Appendix H

Table 14. *Total N (mg/kg) and K_2O (%) in various sedimentary and mafic rock types according to their geological age.*

Rock Type	Total Nitrogen (mg/kg)	K_2O (%)
Mafic igneous	115	0,36
Sandstone	141	1,13
Argillite	174	1,65
Silicaceous	181	1,26
Mafic igneous	185	0,36
Sandstone	204	0,32
Argillite	322	3,58
Slate	357	2,03
Slate	359	2,64
Slate	401	1,21
Slate	405	0,97
Sandstone	412	3,84
Argillite	424	2,57
Argillite	432	1,69
Argillite	436	0,98
Slate	447	4,22
Sandstone	471	4,04
Argillite	489	5,15
Argillite	542	1,73
Slate	547	1,76
Mudstone	571	3,52
Slate	612	4,93
Argillite	667	3,13
Slate	702	2,2
Slate	723	3,05
Slate	725	3,17
Mudstone	769	2,4
Shale	771	3,34
Mudstone	783	2,06
Slate	812	3,65
Slate	834	3,48
Slate	860	3,81
Slate	893	2,62
Slate	919	4,13

1st group - red: Sandstone, mafic igneous, argillite, silicaceous (2500 - 65,5 Ma for sandstone and silicaceous). The rest is between 542 - 145 Ma.

2nd group - blue: Argillite, slate, sandstone (542 - 145 Ma).

3rd group - green: Argillite, slate, mudstone (488 - 145 Ma).

4th group - orange: Argillite, slate, mudstone, shale (298,9 - 145 Ma).

This data belongs to the data base of Morford et al., (2016). Geological ages, rock types and nutrient content; nitrogen (N) and potassium (K).